UC San Diego

UC San Diego Electronic Theses and Dissertations

Title

Development of a dual joystick-controlled optical trapping and cutting system for optical micro-manipulation of cells

Permalink

https://escholarship.org/uc/item/3t97p293

Author

Harsono, Marcellinus Stevie

Publication Date

2011

Peer reviewed|Thesis/dissertation

eScholarship.org Powered by the California Digital Library
University of California

UNIVERSITY OF CALIFORNIA, SAN DIEGO

Development of a Dual Joystick-Controlled Optical Trapping and Cutting System for Optical Micro-manipulation of Cells

A thesis submitted in partial satisfaction of the requirements for the degree Master of Science

in

Bioengineering

by

Marcellinus Stevie Harsono

Committee in charge:

Professor Michael W. Berns, Chair
Professor Michael Heller
Professor Yu-Hwa Lo
Professor Jeffrey H. Omens

2011

Copyright

Marcellinus Stevie Harsono, 2011

All rights reserved.

The Thesis of Marcellinus Stevie Harsono is approved and it is acceptable in quality and form for publication on microfilm and electronically:

_____

_____

_____

_____
Chair

University of California, San Diego

2011

For my mother, Maria, my father, Adrianus, and my sister, Stella and her fiancé, Glenn, as well as for all of my friends.

TABLE OF CONTENTS

LIST OF TABLES

LIST OF FIGURES

ABBREVIATIONS AND SYMBOLS

Abbreviations

BrdU: bromodeoxyuridine

CCD: charge-coupled device

CW: continuous wave

DAQ: data acquisition

DC: Direct current

DPDT: double-pole, double throw

fs: femtosecond

FSM: fast-steering mirror

HWP: half-wave plate

IBA: inverse Bremsstrahlung absorption

I/O: input and output

IR: infrared

MC: motion controller

MHz: megahertz

micron: micrometer

NA: numerical aperture

Nd:YVO4 - neodymium doped yttrium orthvanadate

nm: nanometers

NI: national instruments

P Trap: P polarization of trapping beam

PBS: polarizing beam-splitter

ROI: region of interest

S Trap: S polarization of trapping beam

TS: time series

V: volts

W: watts

Symbols

a: one of the rays in figures 1.2 and 1.3

α: polarizability

b: one of the rays in figures 1.2 and 1.3

c: speed of light

f: represents focal point in figure 1.3

F: resultant force of F_a and F_b

F_a: force due to refraction of ray a in figure 1.3

F_b: force due to refraction of ray b in figure 1.3

F_D^i: force due to reflection of incoming ray

F_R^i: force due to refraction of incoming ray

F_D^o: force due to reflection of outgoing ray

F_R^o: force due to refraction of outgoing ray

h: planck's constant

λ: wavelength of light

v: frequency of light

Q: dimensionless trapping efficiency

P: trapping power

p: momentum

ACKNOWLEDGMENTS

I would like to especially acknowledge Professor Michael Berns for the opportunity to develop and learn about biophotonics, and for being one of the most gentle and humorous advisors I know.

I would also like to deeply thank Dr. Linda Shi for her mentorship and support during the entire time I've worked in Dr. Berns' biophotonics lab.

I would also like to give special thanks to Angela Tsay and Michelle Duquette-Huber , without whom I would not have amazing cell preparations on which to perform experiments. In addition, I also want to thank Dr. Qingyuan Zhu, who I owe for designing the optics of the system.

I also want to thank both Charlie Chandsawangbhuwana and Norman Baker for their advice and guidance during my project.

Lastly, I also want to acknowledge Professor Jeffrey Omens, who not only has given me great advice and tutelage during my project, but has also been one of the greatest professors I've ever had the during my undergraduate years.

VITA

2010 Bachelor of Science, *summa cum laude*, University of California, San Diego

2011 Master of Science, University of California, San Diego

PUBLICATIONS

Conference Proceedings:

1. Qingyuan Zhu, Shahab Parsa, Linda Z. Shi, Marcellinus Harsono, Nicole M. Wakida, and Michael W. Berns, "A combined double-tweezers and wavelength-tunable laser nanosurgery microscope" Proc. SPIE 7400, 74000B (2009), DOI:10.1117/12.825813

FIELDS OF STUDY

Major Field: Bioengineering

Studies in Biophotonics
Professor Michael Berns

ABSTRACT OF THE THESIS

Development of a Dual Joystick-Controlled Optical Trapping and Cutting System for Optical Micro-manipulation of Cells

by

Marcellinus Stevie Harsono

Master of Science in Bioengineering

University of California, San Diego, 2011

Professor Michael W. Berns, Chair

In many situations there is a need to physically manipulate microscopic objects with as much dexterity as our own hands provide in the macroscopic world. An example would be applying stresses onto cells in order to determine their mechanical properties. Our existing microscope-laser experimental system is capable of manipulating microscopic objects using two optical tweezers and one optical scissors to move and cut these objects, respectively. Despite these capabilities, however, the point-and-

click user interface for optical trapping and cutting was cumbersome and hard to use, limiting the system's potential for micro-manipulation. In order to resolve this limitation, a new, more intuitive and hands-on user interface using two joysticks was designed and developed from the ground up in order to provide responsive, real-time control of the optical tweezers and scissors for microscopic manipulation. This new joystick user interface was then used to verify whether or not forces other than those due to microtubule dynamics act upon chromosomes during mitosis, tested in mitotic PtK2 and Indian Muntjac cells by 1) depolymerizing microtubules using nocodazole, and 2) disrupting microtubules using laser ablation with optical scissors, and subsequently attempting to freely manipulate chromosomes using joystick-controlled optical trapping.

I. Introduction and Background

1.1. Optical Tweezers Theory

The phenomenon of optical tweezers is based on the fact that photons carry momentum and create optical forces when light is incident on an object, as shown in Figure 1.1 below (Ashkin, 1970).

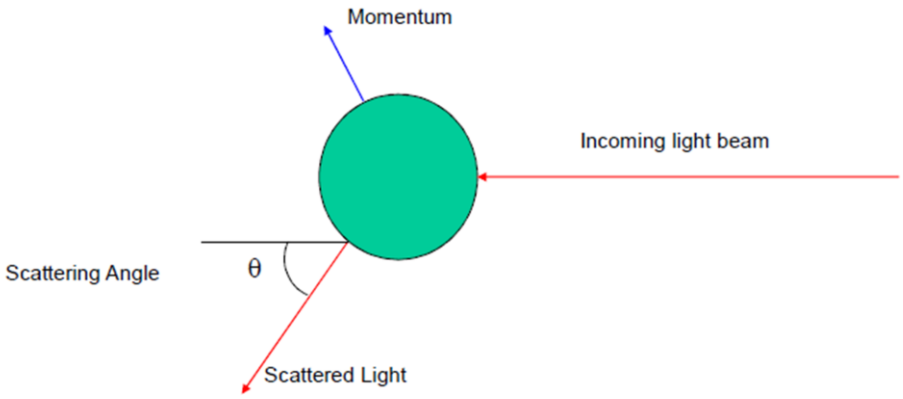

Figure 1.1. Photon transferring momentum and creating optical forces (Ashkin, 1970).

The momentum imparted on the object due to incident photons can be expressed as

$$p = \frac{hv}{c}$$

where h is Planck's constant, ν is the frequency of the incident light, and c is the speed of light. Because the speed of light is very large, the momentum imparted is usually very small, and thus the effect of the momentum (motion due to optical forces) is usually only visible and practical for objects on the order of microns (Ashkin, 1970).

Optical tweezers theory is divided into three regimes based on the size of the object that is trapped (Ashkin, 1986). The Rayleigh regime includes particles whose characteristic length is much less than the wavelength of the incident light, usually around 100 nm or smaller. The particle is then considered an induced dipole with polarizability α, with a Lorentz force acting on this dipole due to an electric field gradient. Optical tweezers in this range exhibit two forces on the trapped object: a scattering force which pushes the object away and a gradient force which pulls it into the trap. Trapping in this regime is based on the balance of these two forces (Harada et al, 1996).

The Mie regime includes particles whose characteristic length is much greater than the wavelength of incident light, usually around 5 microns or larger. Here, optical tweezers are considered using ray optics, where the incident beam can be divided into rays traced through the trapped object with infinite reflections and then summed. If the particle's characteristic length is approximate with the wavelength of light, then rigorous wave analysis would be required to analyze the mechanism through which optical tweezers occurs (Ashkin, 1986).

The Mie regime will be discussed in more detail since the particles trapped in this project fall into this regime. Ray optics suggests that momentum transfer due to incident photons occurs when the rays of light change direction due to a change in refractive index as light passes through the interface of the object and the medium in which it is surrounded. Most biological objects act as lenses in which light is refracted, usually having a refractive index larger than that of the buffer solution in which they are suspended. Thus, light rays are bent toward the surface normal and transfer momentum. Due to the Gaussian distribution of intensity of a light beam, the different forces generated by each ray sum to a resultant force directed towards the optical axis, as shown in Figure 1.2 below (Ashkin, 1970).

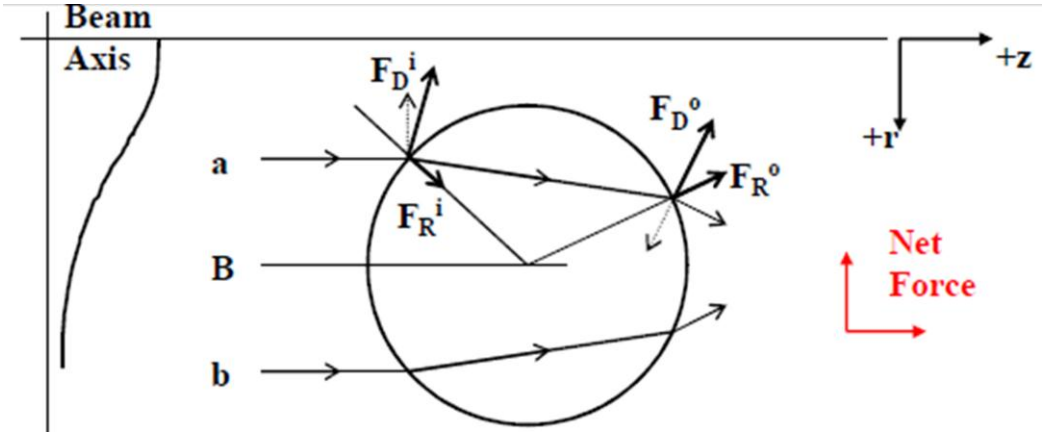

Figure 1.2. Lateral forces for Mie regime of optical trapping (Ashkin, 1970).

The Gaussian distribution of intensity of light can be seen towards the left of the figure. Thus, ray "a" has a higher intensity than ray "b". As the rays are refracted and reflected, forces due to each interaction (forces due to refraction have the subscript "R" while forces due to reflection have the subscript "D") develop from the momentum transfer, with the force due to reflection being greater than that due to

refraction (Ashkin, 1970). For ray “a”, this momentum transfer creates forces pushing the object towards the center of the beam, while the forces from ray “b” (not shown) would push the object away from the beam center. However, because the intensity of ray “a” is greater than ray “b”, forces from ray “a” are greater than from ray “b” and thus the object is pushed towards the center (Ashkin, 1970).

Although these forces pull the object towards the center of the beam, the radiation pressure (momentum transfer due to incoming photons, see Figure 1.1) pushes the object towards the positive direction of the z-axis (towards the right in Figure 1.2). Figure 1.3 below shows the forces that prevent light pressure from scattering the trapped object.

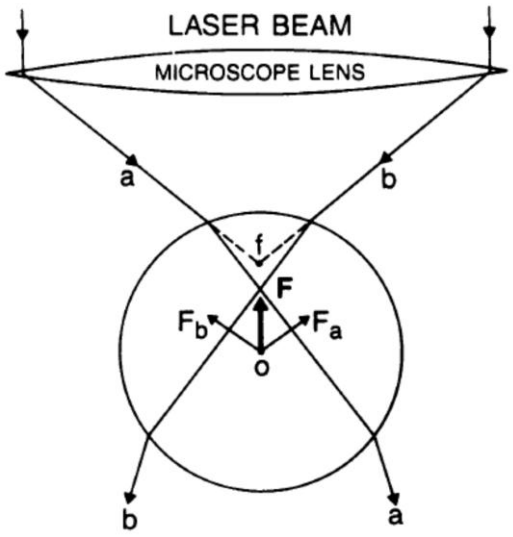

Figure 1.3. Forces acting against light pressure in Mie regime of optical trapping (Ashkin 1992).

The small “f” represents the focal point of the light source, which is closer to the source than the center of the sphere. Rays “a” and “b” are bent toward the surface normal because the refractive index of the particle is greater than that of the media. This change in direction again imparts momentum that results in reaction forces F_a and F_b due to the two incident rays, which sum to the resultant force F. This resultant force is responsible for pulling the object towards the light source, and the object will be trapped as long as this force is greater than the light pressure. This is usually only possible with focused light, since the resultant force will be weaker for less focused light and forces due to radiation pressure will be stronger than this resultant force. Focused light ensures that the rate of change of electric field

with respect to the z-axis (downwards in the figure above)—which causes the lateral forces—is greater than the magnitude of the light pressure, which is most efficient when the light is focused with a high numerical aperture (Ashkin 1992).

1.2. Optical Scissors Theory

The mechanism of cutting and ablating chromosomes or other objects using optical scissors is not yet fully understood, although several mechanisms of interaction depending on irradiance and exposure time are known and shown in Figure 1.4 below.

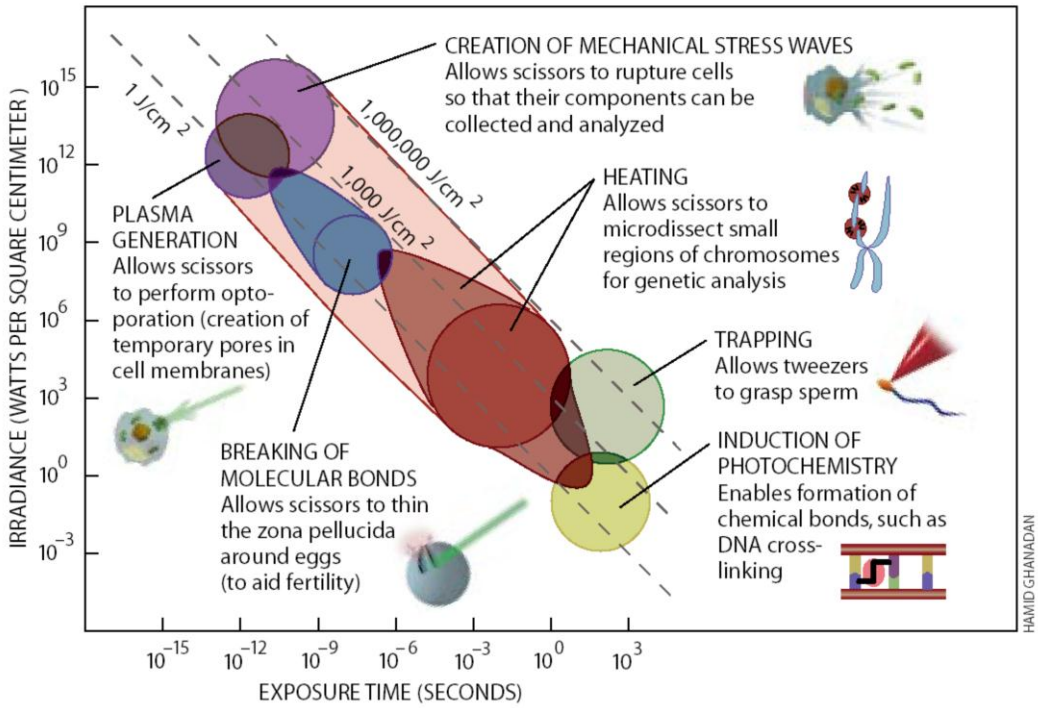

Figure 1.4. Mechanisms of laser interaction, depending on irradiance and exposure time (Berns, 1998).

It is possible that during laser ablation, heating, breaking of molecular bonds, creation of mechanical stress waves, and plasma generation can all occur to some degree, resulting in the severing of chromosomes. The intense electric field created at the focused spot may also contribute to damaging the sample (Berns, 2007).

Also important for characterizing and understanding optical scissors is the size of the focused spot, which can be expressed with the formula below:

$$Focused\ spot\ size = \frac{1.22\lambda}{NA}$$

where λ is the wavelength of incident light and NA is the numerical aperture of the microscope objective. Usually, focused spot sizes range from 0.26 – 1.22 microns (Quinto-Su et al, 2007). In fact, due to the Gaussian distribution of intensity, a very high intensity "hot-spot" in the center of the focused beam can also produce a lesion smaller than the focused spot size, as seen in Figure 1.5 below.

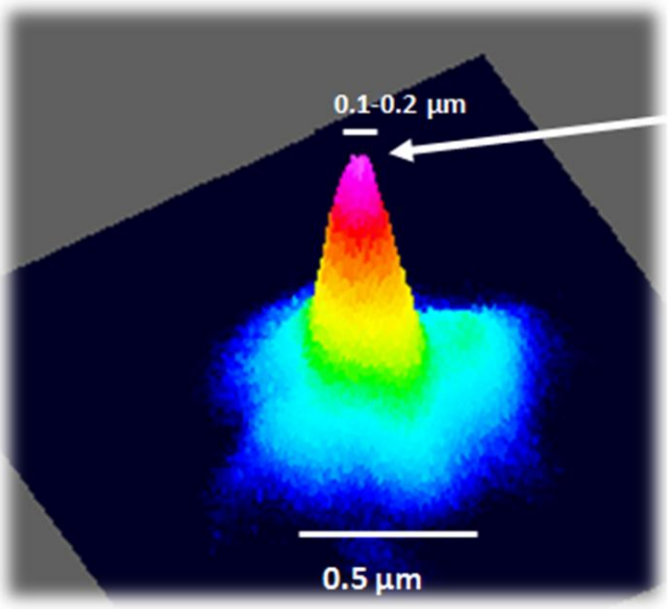

Figure 1.5. "Hot-spot" due to Gaussian distribution of intensity of beam (Vogel et al, 2007).

Since a femtosecond laser is being used to perform optical cutting in our system, it is likely that plasma generation is the mechanism creating damage at the microscopic level, which is caused by avalanche ionization, which is itself due to multiphoton ionization, a phenomenon that occurs on a timescale of femtoseconds. Essentially, electrons already excited by a single photon may absorb the energy of other photons through a nonresonant process called inverse Bremsstrahlung absorption (IBA) as the electron collides with other charged particles (impact ionization). Absorption of this energy increases the kinetic energy of the original excited electron, which may excite other electrons due to impact ionization. The repetition of IBA events and impact ionization with many electrons leads to a

rapid growth in the number of excited free electrons if the laser irradiance is sufficient to overcome energy losses through diffusion of electrons out of the focal volume and recombination (rejoining of electrons with electron holes). This process can be referred to as avalanche or cascade ionization, which contributes to plasma generation after a large density of free electrons has been produced due to multiphoton ionization. Figure 1.6 below shows a diagram of how avalanche ionization occurs (Vogel, et al, 2003).

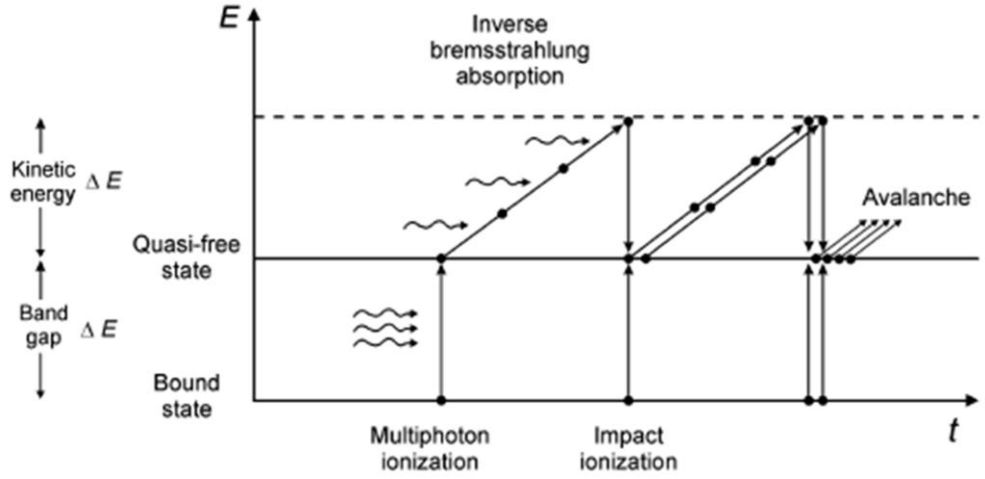

Figure 1.6. Avalanche ionization due to inverse Bremsstrahlung absorption and impact ionization. (Vogel et al, 2003).

Avalanche ionization allows the irradiance threshold to be exceeded, which results in laser-induced plasma-mediated ablation, also known as laser-induced breakdown, a phenomena dependent on nonlinear absorption in the target material (Vogel, et al, 2003).

1.3. Existing System Setup

Zhu et al designed and built a system that has both optical tweezers and optical scissors (Zhu et al, 2009). The optical tweezers are split into two beams using a polarizing beam splitter, which creates two “hands” that can trap or “hold” microscopic objects. After these objects are trapped, the individual positions of the S polarized trap and the P polarized trap (referred to from now on as S Trap and P Trap) can be controlled and thus the held microscopic objects can be moved anywhere the user desires. At the same time, the optical scissors, whose position can also be controlled individually, can perform optical

cutting in any shape and location within the field of view. Thus, the simultaneous optical trapping and cutting make possible optical micro-manipulation of microscopic objects. This capability can be analogized to having a set of two microscopic hands and one pair of microscopic scissors which can be used to manipulate objects viewed under a microscope.

1.3.1. Hardware Setup

This system, called Robolase IV, is a microscope-laser system capable of simultaneous optical trapping and cutting as well as automated imaging. The microscope used is a non-automated Zeiss Axio Observer A1 usually used with a plan-Apochromat, 63x, 1.4 NA, phase 3 oil objective (Carl Zeiss International, Germany). The camera used for image acquisition is a Hamamatsu Orca-R^2 Digital Camera C10600 that uses a charge-coupled device (CCD) sensor (Hamamatsu Photonics, Japan). The trapping laser is a Spectra Physics Millennia infrared (IR) laser (Newport Corporation, Irvine, CA). This laser uses a neodymium doped yttrium orthvanadate ($Nd:YVO_4$) crystal capable of 1064 nm continuous wave (CW) with a maximum power of 10 W. A polarizing beam splitter (PBS) splits this trapping laser into two beams, creating two, individually controlled optical tweezers. The cutting laser is a tunable (710 – 990 nm), 76 MHz, 200 fs Spectra Physics Mai Tai laser also developed by Newport, which uses a titanium-sapphire crystal. Also from Newport Corporation are three fast-steering mirrors, model FSM-CD300, as well as a Newport ESP300 motion controller for controlling three rotating motorized stages containing half-wave plates. The fast-steering mirrors are the devices that control the positions of the optical traps and scissors, and are thus a very important element for developing the new user interface. The mirror positions are adjusted by applying x- and y-voltages from the computer from a range of –10 V to +10 V. In addition, the system uses a LUDL Electronic Products (Hawthorne, NY) nano-positioning stage for precise stage automation and a Uniblitz VMM-D3 (Uniblitz, Rochester, NY) shutter controller to control three mechanical, millisecond shutters to turn “on” and “off” the lasers as well as arc lamp light sources. The system also uses several devices from National Instruments (Austin, TX), including a NI-USB 6229 Data Acquisition (DAQ) Board and a CA-1000 Configurable Connector Accessory Enclosure, each of which contains arrays of analog and digital inputs and outputs. The arc

lamp light source used for fluorescence imaging is an X-CITE Series 120 model with a 120 W lamp (Lumen Dynamics, Canada). Lastly, the computer used to control the entire system is a Dell Precision T3500 desktop computer (Dell, Round Rock, TX). The configuration and connections between each piece of hardware are shown below in Figure 1.7.

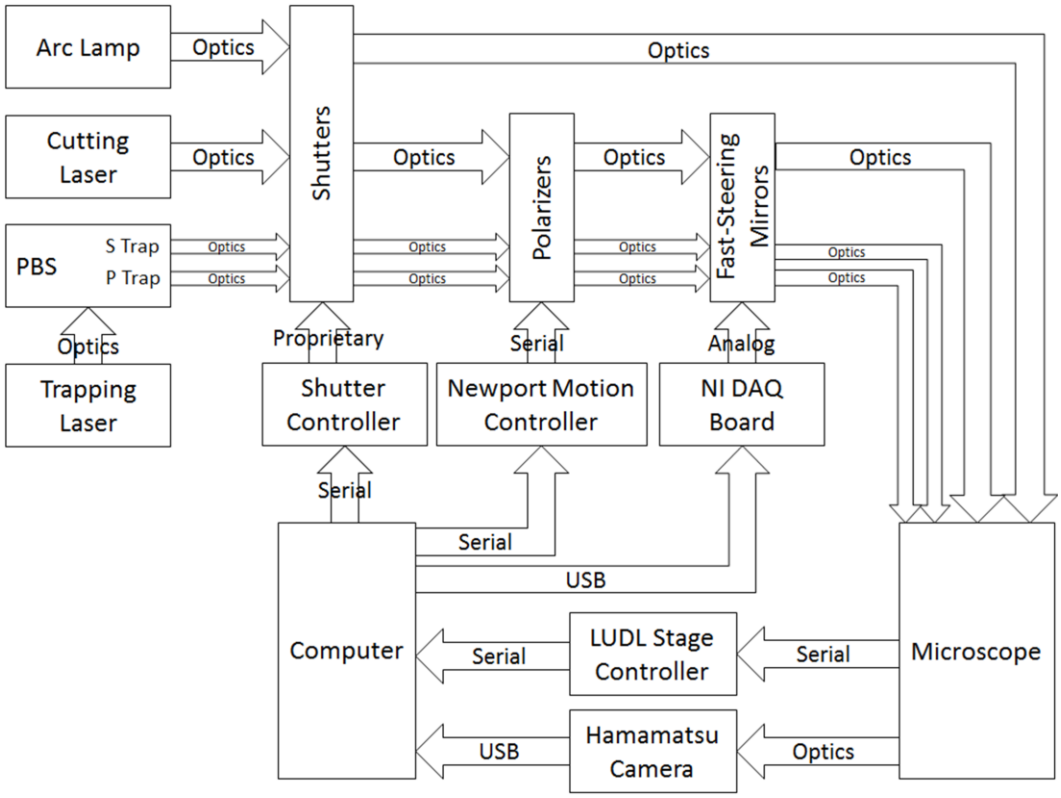

Figure 1.7. Hardware Setup of Robolase IV System. This figure shows how each piece of hardware is connected and through what type of interface the connections occur.

1.3.2. Optical Setup

Figure 1.8 below shows the optical setup of the Robolase IV system.

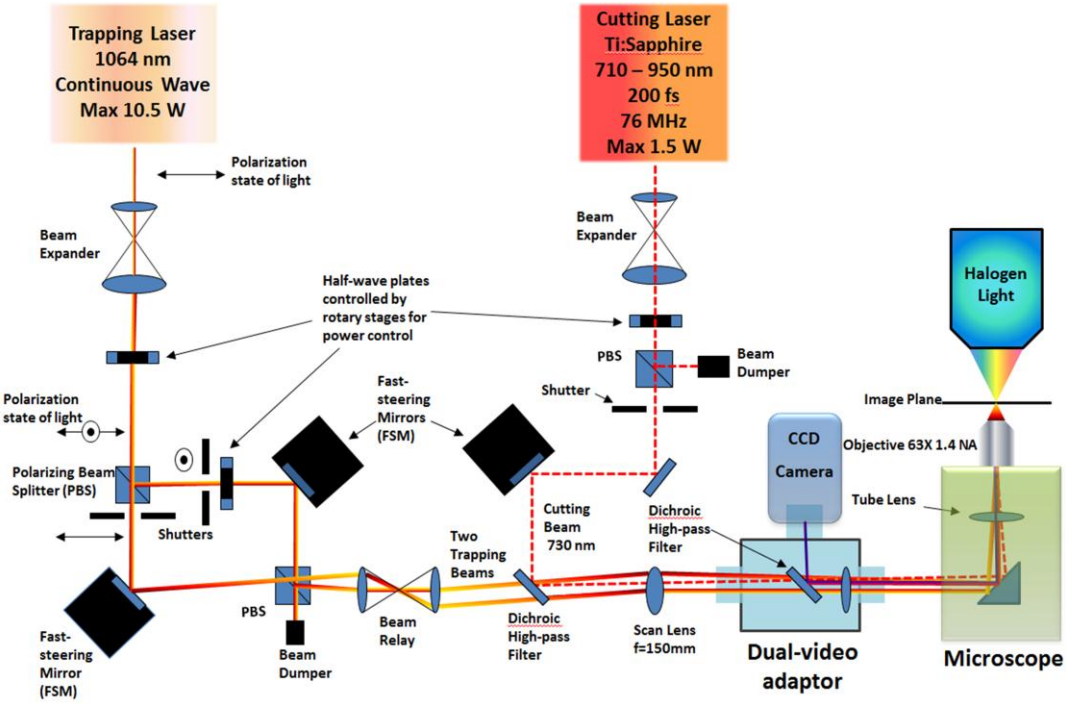

Figure 1.8. Optical Setup of Robolase IV System (Parsa, 2010). This figure shows the path of the trapping and cutting lasers into the microscope as well as the image path from the microscope to the camera (see text for explanation of components).

The beam expanders are used to make the trapping and cutting lasers more efficient when entering the microscope. The half-wave plates (HWP) are placed inside rotating motorized stages controlled by the computer and are used to adjust the power of each laser. Half-wave plates can rotate the polarization of a beam by an amount depending on the angle between the incoming beam polarization and the inherent angle of the half-wave plate. Thus, rotating the half-wave plate determines how much of the laser beam will pass through to the microscope, and thus the power of the cutting or trapping beams. The polarizing beam splitters (PBS) split the trapping laser into two beams of perpendicular polarizations and directions or join two beams with perpendicular polarizations into one direction. As mentioned before, the PBSs are used to split the trapping laser into two separate beams, an S polarization trap (S Trap) and P polarization trap (P Trap) which can be manipulated independently. The shutters in the diagram refer to the mechanical, millisecond Uniblitz shutters that allow turning “on” and “off” the laser by opening and closing the shutter. Beam dumps are used to block stray laser light reflected from the polarizing beam splitters. The dichroic high-pass filters allow certain wavelengths of light through while reflecting

others. Dichroic high-pass filter #1 allows laser light from the trapping lasers at 1064 nm to pass through, while reflecting the cutting laser, which emits at smaller wavelengths. Dichroic high-pass filter #2 allows the trapping and cutting lasers through while reflecting light representing the image returning from the image plane of the microscope and going into the Hamamatsu camera. The scan lens and the lenses within the microscope are used such that at the surface of the back-aperture (the aperture at the back of the objective) is a mirror image of the surface of dichroic high-pass filter #1. However, the surfaces of the fast-steering mirrors (FSM) must also be mirror images of the back-aperture of the objective; thus, beam relays are used to achieve this effect. As a result of this optical design, the beam does not move at the back-aperture when the FSM is rotated and the beam is directed. Otherwise, without mirroring these images, the beam would move partially out of the back-aperture when the FSM is rotated, resulting in a different laser power delivered compared to laser power measured before the objective (Parsa, 2010).

The transmission of laser power through the 63x oil objective is 26% at 1064 nm (trapping wavelength), for the 170 micron-thick cover glass used in our experiments (Parsa, 2010).

1.3.3. Software: Robolase IV

The entire system is controlled and integrated using a custom-designed LabVIEW program called Robolase IV. Figure 1.9 below shows the front panel of Robolase IV, which consists of many tabs, not all of which are shown. When the LabVIEW program is run on the computer, the system initializes all the hardware mentioned above and then waits in a timeout stage in a while-loop, constantly checking for the user's button presses made by the user which initiate events.

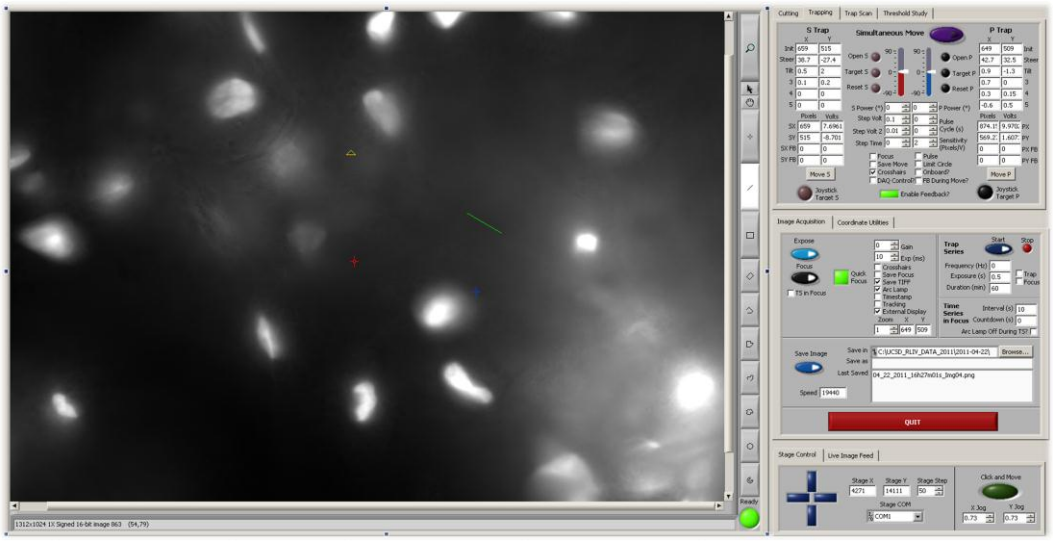

Figure 1.9. Front Panel of Robolase IV. The user interacts with the buttons and controls on this panel to control the hardware in the Robolase IV system.

The large rectangle on the left represents the Main Image Control, while the right side consists of tabs that consist of various Boolean, numeric, and other types of controls that are used to interface with the system. The user interacts with the system by pressing buttons in order to initiate events, such as "Expose" to acquire images from the camera or "CutROI" to cut a shape drawn on the main image. From this front panel, all the hardware mentioned above can be controlled. A more detailed explanation of some of the controls relevant to this project can be found in Appendix A.

1.4 Objectives

In addition to the functions mentioned above, the Robolase IV LabVIEW program also controls the optical trapping and cutting used for optical micro-manipulation. However, the two optical tweezers and one optical scissors are controlled using a point-and-click method; that is, the user selects a point on the image and then presses a button in the front panel to actually move the trap. This type of control is very cumbersome and frustrating, since only one of the three optical tools can be moved at a time, and the movement of one optical tool has to be finished before another move can be performed. This is especially problematic in certain experiments where time is critical and an inability to respond quickly to a changing situation may drastically affect the results of the experiment. Thus, while the

potential for optical micro-manipulation exists with Robolase IV's two optical tweezers and optical scissors, the ability to actually manipulate microscopic objects is limited by the difficult user interface used to control the movement and positions of these optical tools. Therefore, developing a more responsive, real-time user interface is of high priority in order to unlock this system's full potential with respect to optical micro-manipulation. To develop a better user interface, an engineering design process involving assessment of needs and evaluation of different design alternatives will be used, and is thoroughly documented in Chapter 2.

Once this new user interface has been developed, it will be used to determine whether or not there are forces other than those due to attached microtubules acting upon chromosomes during mitosis. If only microtubules are bound to chromosomes during mitosis and are responsible for their movement, then disrupting these microtubules should release the chromosomes from any attachments and eliminate any forces acting upon the chromosome. Microtubules are disrupted using two methods, which can be used together. The first method is to depolymerize microtubules by treating mitotic cells with nocodazole. The second method is to perform laser ablation using optical scissors in the area around chromosomes. Once free, it should be possible to manipulate this chromosome or fragment using the optical tweezers controlled by the new user interface. However, if it remains impossible to freely move chromosomes or chromosome fragments cut using the optical scissors, then there may be unknown obstacles or forces acting on the chromosomes during mitosis other than those due to microtubule attachments.

References

Ashkin, A. "Acceleration and Trapping of Particles by Radiation Pressure." *Physical Review Letters* 24.4 (1970): 156-59. Print.

Ashkin, A. "Forces of a Single-beam Gradient Laser Trap on a Dielectric Sphere in the Ray Optics Regime." *Biophysical Journal* 61.2 (1992): 569-82. Print.

Ashkin, A., J. M. Dziedzic, J. E. Bjorkholm, and Steven Chu. "Observation of a Single-beam Gradient Force Optical Trap for Dielectric Particles." *Optics Letters* 11.5 (1986): 288-90. Print.

Berns, Michael W. "Laser Scissors and Tweezers." *Scientific American* Apr. 1998: 62-67. Print.

Berns, Michael W., Tadir, Yona, Hong Liang, and Bruce Tomberg. "Laser Scissors and Tweezers." *Laser Manipulation of Cells and Tissues*. By Michael W. Berns. Ed. Karl Otto Greulich. Amsterdam: Elsevier Academic, 2007. 71-98. Print.

Harada, Yasuhiro, and Toshimitsu Asakura. "Radiation Forces on a Dielectric Sphere in the Rayleigh Scattering Regime." *Optics Communications* 124.5-6 (1996): 529-41. Print.

National Instruments. "What Is NI LabVIEW?" *National Instruments: Test, Measurement, and Embedded Systems*. National Instruments. Web. 16 Feb. 2011. <http://www.ni.com/labview/whatis/>.

Parsa, Shahab. *A Double Tweezers and Laser Scissors Microscope for Biological Studies*. Thesis. University of California, San Diego, 2010. Print.

Quinto-Su, Pedro A., and Vasan Venugopalan. "Mechanisms of Laser Cellular Microsurgery."*Laser Manipulation of Cells and Tissues*. Ed. Michael W. Berns and Karl Otto Greulich. Vol. 82. Amsterdam: Elsevier Academic, 2007. 113-51. Print.

Vogel, Alfred, and Vasan Venugopalan. "Mechanisms of Pulsed Laser Ablation of Biological Tissues (577−644. Published on the Web 02/12/03.)." *Chemical Reviews* 103.5 (2003): 577-644. Print.

Vogel, Alfred, Verena Horneffer, Kathrin Lorenz, Norbert Lins, Gereon Huttmann, and Andreas Gebert. "Principles of Laser Microdissection and Catapulting of Histologic Specimens and Live Cells." *Laser Manipulation of Cells and Tissues*. Ed. Michael W. Berns and Karl Otto Greulich. Vol. 82. Amsterdam: Elsevier Academic, 2007. 153-205. Print.

Zhu, Qingyuan, Shahab Parsa, Linda Z. Shi, Marcellinus Harsono, Nicole M. Wakida, and Michael W. Berns. "A Combined Double-tweezers and Wavelength-tunable Laser Nanosurgery Microscope." *Optical Trapping and Optical Micromanipulation VI*. Proc. of SPIE Optics + Photonics, San Diego Convention Center, San Diego, California, USA. Vol. 7400, 74000B, DOI:10.1117/12.825813. *SPIE Optics + Photonics*. SPIE, 20 Aug. 2009. Web.

II. Development of the Joystick User Interface

2.1. Needs Assessment and Problem Formulation

The Robolase IV system is unique in that it can perform both optical cutting and dual-beam trapping for optical micro-manipulation. As mentioned previously, however, both optical cutting and trapping are controlled using a point-and-click interface through the Robolase IV LabVIEW program. For cutting, different ROIs are drawn and the CutROI control is pressed to initiate the cutting sequence. For trapping, point ROIs are selected anywhere on the image and the traps can be moved in steps or targeted to those coordinates by pressing the correct control button in the LabVIEW program. Since there is only one mouse pointer, it is impossible to control all three tools (two optical traps and one optical scissors) at the same time. Although a program has been written to move the two traps simultaneously, they can still only be moved to one point, and the algorithm is not very flexible. For example, once the Move S/P control is clicked, the move must be canceled and a new point selected in order to change direction. Thus, with respect to controlling the optical traps and scissors the system is not very intuitive or user-friendly and there is a learning curve to being able to manipulate the optical traps and scissors. Even when the user has learned how to use the system well, controlling the optical tools is very slow and sometimes even frustrating.

It is obvious that there is a need to improve the method for controlling the two optical traps and optical scissors in order to perform optical micro-manipulation, since the original method of control—using the mouse in a point-and-click fashion—is very cumbersome and inflexible. Therefore, a significant part of this project is to develop a responsive, intuitive, and user-friendly method to simultaneously control two optical traps and one optical scissors.

2.2. Design Alternatives

2.2.1. Design Goals and Specifications

The design alternatives will be considered based on several design goals, which will be ranked in importance with respect to how significantly each affects the overall objective of this design

problem. Then, the design alternatives will be evaluated on how well each alternative fulfills each design goal using a decision matrix in section 2.2.6.

The design goals for the solution will be ease-of-use, ease-of-design, customizability, performance, and cost. Ease-of-use refers to how easy the design solution will be to use. The final design should be very easy to use since the objective calls for a method of controlling the two optical traps and scissors that is very user-friendly and intuitive, something that a new user can pick up almost instantly. Ease-of-design refers to the degree of complexity that is required to install the final design and to write programs in order to integrate the solution with the current Robolase IV software. Customizability will consider how easily and to what degree the design solution in terms of hardware and software can be modified to suit future needs. The performance design goal will assess how responsive control of the two optical tweezers and scissors actually is, what sacrifices, if any, are made to existing functions in Robolase IV, and what frequent problems may occur. Cost takes into account both the actual monetary cost of the hardware as well as cost of resources such as the time and effort it takes to install the solution. These design goals are rank-ordered in Table 2.1 below:

Table 2.1. Rank-order of Design Goals. This table shows which design goals prioritize over others. The outcome is used in the decision matrix for the design alternatives below.

	Ease-of-use	Ease-of-design	Customizability	Performance	Cost	**Total**
Ease-of-use	---	1	1	0.5	1	**3.5**
Ease-of-design	0	---	0	0	1	**1**
Customizability	0	1	---	0.5	1	**2.5**
Performance	0.5	1	1	---	1	**3.5**
Cost	0	0	0	0	---	**0**

From the rank-ordering of the design goals, it seems that ease-of-use and performance are the most prioritized. This makes sense because the Robolase IV system already has a method of controlling the two optical traps and scissors. However, the main objective is to improve this design to make it more responsive and easier to use. Thus, the overall goal is to improve the design but not lose any functionality that the system already has, i.e., the proposed solution still has to be able to control the

optical tweezers and scissors as precisely as before but with a better user interface. A solution with an easy-to-use and responsive user interface but limited functionality would be an unacceptable tradeoff. The second most important design goal is customizability. Because the experimental systems are always changing to suit different needs and goals for different research projects and experiments, the design solution must be capable of being modified to suit other needs instead of serving just a single purpose. Ease-of-design is not as important a factor in considering the design alternatives because the priority is to make the control method user-friendly and functional, despite how complex the solution is as long as it is possible to develop. Lastly, cost is not a major issue because only one of these designs will be produced for the Robolase IV system. Therefore, the resources necessary in terms of money, time, and effort will all be dedicated to improving this system's user interface with respect to controlling the optical traps and scissors.

There are also certain specifications that the final design must fulfill. The most important is that the solution must interface with the Newport Fast-steering Mirror CD300. Three of these motorized mirrors control each of the positions of the two optical traps and the scissors. By interfacing with these fast-steering mirrors, the design solution will not affect the current optics of the system. Instead, only the method of controlling these fast-steering mirrors will be improved upon. The angles of rotation of these fast-steering mirrors and thus the positions of the optical traps and scissors are controlled by applied x- and y-voltages which range from ±10 V. Thus, the design solution must output voltages in the same range in order to interface correctly with the fast-steering mirrors.

Another design specification, as previously mentioned, is that the current method of control for the optical traps and scissors—the point-and-click method using the mouse implemented in the LabVIEW software—must not be changed. Thus, after the final design is developed, the old method of choosing ROIs and cutting or moving the lasers must still work. This is necessary because—while the old method is very cumbersome to use—it is also very precise, which is useful for measuring laser dosage on samples during experiments (for example, when cutting using the point-and-click method, the exact number of times the shutter is opened to let laser through and the time that the shutter is opened every time is monitored such that energy delivered with each cut can be calculated).

2.2.2. Design Alternative #1: Simple Two-Axis Joysticks

The first design alternative is to use a simple joystick such as those used for computer games or to control microscope stages. Because joysticks are very ubiquitous, most users, even new ones, will be familiar with how to use the joystick. The horizontal position of the joystick would represent the position in the x-axis of the fast-steering mirror, while vertical position would represent position in the y-axis. Thus, the joystick would output two ±10V signals to control the x- and y-axes of the fast-steering mirror and thereby control the positions of the optical traps and scissors. However, since each optical trap and the scissors require two axes each, three of these joysticks would be required. Since users would only have two hands to operate the system, however, this design alternative will use only two joysticks, each to control one of the two traps. The cutting will be "controlled" using predetermined cutting ROIs. For example, code can be written such that when a button is pressed, the software can initiate a "CutROI" LabVIEW event using the two positions of the traps as end points for a line cut; that is, a line would be cut between the two positions of the traps. Other shapes can be cut as well, such as a rectangle, where the two points represent the upper left and bottom right corners, or an ellipse that is bounded by a rectangle defined by the two points in the same way. In this way, the two optical traps can be controlled while the cutting is controlled in a limited fashion.

The disadvantage of this design alternative, of course, is the fact that cutting control is not particularly flexible. The movement of the traps is easy and user-friendly, but the cutting control scheme would require some getting used to. Also, it would be impossible cut free shapes using the joysticks, so this would have to be done using the already-existing point-and-click method. In addition, extra programming would be necessary in order to create these predetermined cutting ROIs based on the positions of the joysticks. Fortunately, the point-and-click method is also based on end points for lines and rectangles as described, so only minor modifications to the existing code would be needed to implement the predetermined cutting ROI. An advantage of this alternative is the fact that joysticks such as this are very cheap and commercially available.

2.2.3. Design Alternative #2: Three-Axis Joysticks with Buttons

The second design alternative uses industrial joysticks that are much more complex than in the first design alternative and can be custom-built to suit the purposes of this project. Once again, two of these joysticks will be used to control each trap. However, these industrial joysticks will have a third axis which outputs a ±10 V range which is controlled by rotation. Each of the two joysticks controlling each trap will thus output a third voltage signal which together can be used to control the fast-steering mirror for the cutting laser. That is, one of the rotation axes on one of the joysticks will control the x-axis of the cutting fast-steering mirror and the other rotation axis will control the y-axis of the mirror. Thus, with these joysticks simultaneous control of all three fast-steering mirrors and, by extension, all three optical tools, would be possible. In addition, these joysticks can be customized to have several pushbuttons, which can be used for opening the shutters for the traps and scissors or other options, allowing greater customizability.

One of the disadvantages for this alternative, however, is that these industrial joysticks will have to be custom-ordered and manufactured. This means that it will cost significantly more than the simple two-axis joysticks and are not readily available since they must be ordered and built to our specifications. In addition, even though we do have more control for cutting using the rotation of the joystick, this control may be somewhat difficult, and can be likened to that of an Etch-a-Sketch, which uses two knobs to control horizontal and vertical movement. Thus, the only ROIs that would be easy to cut using this control would be horizontal or vertical lines. Diagonal lines and ellipses would be difficult to make. Another option would be to write code that allows the rotation axes and a pushbutton to select end points of a cut, and use the same predetermined cutting ROI from the first design alternative as the means to determining the shape of the cut. Thus, the difficult "Etch-a-Sketch" control can be avoided as well as the restriction from the first alternative that cutting ROI must be determined by the positions of the two traps. However, this would again limit the flexibility of cutting control by limiting the types of ROI that can be cut.

2.2.4. Design Alternative #3: Touchscreen Interface

The third design alternative would be to use a touchscreen interface capable of multitouch gestures. The display on the touchscreen will show the image coming from the Hamamatsu camera overlaid with three sets of ROI crosshairs denoting the current positions of the optical traps and scissors. The user would use his fingers to drag these crosshairs (simultaneously if desired) in order to control the positions of the two optical traps and optical scissors. For example, if the blue crosshairs represents one of the optical traps, the user would put his finger on the blue crosshairs and then drag it to a new position to move the optical trap. The position of the finger as it moves would be detected by the capacitive touchscreen, which outputs this position information in pixels to the Robolase LabVIEW program, which in turn performs calculations to convert the movement in pixels to voltages which are then outputted to the fast-steering mirror controlling that optical trap. Instead of dragging, the user can also move a trap instantaneously to a specific point or targeted. The user would tap on one of the crosshairs so Robolase knows that that specific optical tool is being targeted. The user can then tap anywhere else on the image on the touchscreen, and Robolase would convert this position in pixels to voltage and move the fast-steering mirror by applying the voltages.

The optical scissors can be used in two ways. The first way is similar to the current method of cutting using the optical scissors, where ROI such as lines, rectangles, or ellipses can be drawn and the CutROI button pressed to initiate cutting. Using the touchscreen would make drawing these ROI much easier when curved shapes are required. The second method would switch the system to “Cutting Mode” and any line or shape drawn on the image by the user’s fingers would cut the sample in real-time. Thus, after switching to Cutting Mode, the user can simply draw a line on a cell and Robolase will move the scissors fast-steering mirror in real-time to the position of the user’s finger and cut as the user’s fingers move.

In addition to these actions, many other “controls” are available to use because many gestures would be possible on this touchscreen. Robolase can be programmed to recognize these gestures, which makes this interface very customizable. For example, the user can tap on a crosshairs and then continuously rotate his finger in a clockwise direction to increase the power of that optical trap or counterclockwise to decrease the power. Or, the user can do a pinch action (moving to fingers closer

together) to close the shutter of one of the optical tools, or move his fingers farther apart to open the shutter. Furthermore, since users would have more than one finger and multitouch capabilities allow the recognition of more than one finger at one time, the two optical traps and scissors could be controlled simultaneously using different fingers.

The main disadvantage of this alternative is the fact that control of the optical traps and scissors would have to go through the Robolase software, which means the computer would act as an intermediary between the touchscreen and the fast-steering mirrors, unlike the second alternative which can output voltages directly to the mirrors. Because the information coming from the touchscreen would have to be processed by Robolase, this may affect the performance of this control method in terms of speed or responsiveness. In addition, it is likely that far more programming would be necessary for this design alternative compared to the other two because control is based on gestures instead of simply moving a joystick. In addition, although touchscreen monitors or tablets are readily available on the market, these touchscreens are not typically used in the way we would like to use them for this project. Instead, the touchscreen would likely be used only for mouse pointer control and may also have some pre-programmed gestures. It would thus take some time to be able to learn how to extract the position information from these touchscreens, which is necessary for programming in Robolase, implying that developing this alternative would take more resources than the first two in terms of time and human effort. Another option would be to order a special, custom-ordered touchscreen that outputs this data, but then this would probably cost much more than commercial ones already available. Lastly, interfacing with a touchscreen is not as hands-on as with joysticks, which provide tactile feedback.

2.2.5. Mouse “Point-and-Click” Interface

The fourth “design alternative” is actually the current user interface used to control the optical traps and scissors on the Robolase IV system, and is included in order to provide perspective as well as a comparison with the new design alternatives. This interface is similar conceptually to the touchscreen interface, in that the user interacts directly with the image acquired by the camera. However, instead of using a touchscreen and fingers to control the trap position, the user would control the mouse cursor on

the normal computer monitor. To move the traps, the user designates the desired final destination of the trap by placing the point ROI tool anywhere on the image. The user then can choose to Target or Move either the S or P trap. As before, targeting moves the trap directly to the desired position, whereas moving moves the trap in steps toward the desired position. Because the user points to a position and clicks Move or Target, this alternative is called the "point-and-click" interface. As with the touchscreen interface, Robolase converts the pixel position information to voltages and applies the voltages to the fast-steering mirrors. For the optical scissors, other ROI tools such as the line tool are selected and an ROI is drawn on the image. Clicking on the CutROI button will then initiate the cutting sequence.

Just like the touchscreen interface, many controls are also possible, since new Boolean button or numeric controls can be placed on the front panel of Robolase IV to control any imaginable task. However, in addition to being limited by the finite number of different types of controls provided by LabVIEW, this interface would be limited in the fact that each control can only be used one at a time, since there is only one mouse cursor. For example, you cannot cut an ROI and move the trap at the same time, since different sub-programs govern cutting and moving the trap and the second event (e.g. moving the trap) will occur after the first event (cutting) has completed. This is analogous to having only one hand to handle many tasks and is unlike the touchscreen interface where different actions can be performed simultaneously because of its multitouch capabilities. Thus, this lack of flexibility makes the point-and-click alternative very cumbersome and in dire need of improvement.

The only advantage provided by this alternative is its precision, which is important especially for the optical scissors where laser dosage must always be monitored during experiments. Using the "point-and-click" method, cutting is not done in real-time and images can be saved recording the position of the cut. In contrast, using the joysticks or the latter method of controlling cutting with the touchscreen described above, the location and dosage of each cut would be more difficult to determine since cutting occurs in real time as the cursor moves (controlled either by the joystick or a finger on the touchscreen) and is subject to the lack of precision of the user's movements. This alternative's precision is one of the reasons the new and improved user interface must not interfere with functions that are currently possible on the system.

2.2.6. Decision Matrix

The weighing factors for each design goal were chosen based loosely on the rank-order of design goals. Since Ease-of-use and Performance were ranked the highest, they were both given maximum weighing factor values of 100 points. Thus, each individual "point" can be considered as worth 0.035 units from the rank-order, since the aforementioned design goals both had rankings of 3.5. Customizability, which had a ranking of 2.5, would have a weighing factor of about 2.5 units divided by 0.035 points, or an approximate weighing factor of 70. The weighing factor for Ease-of-design was found in a similar fashion. Although the Cost design goal had a ranking of zero, it is still given a very small weighing factor of 5. With these weighing factors, the qualitative features of the design alternatives are scored quantitatively with respect to each design goal. The weighing factors and results of the decision are shown in the decision matrix in Table 2.2 below, where the number to the left of the slash represents the score out of 10 and the number to the right of the slash is the left number multiplied by the weighing factor.

Table 2.2. Decision Matrix. This matrix lists the scores for each design alternative with respect to individual design goals. The highest-scoring alternative is highlighted in yellow.

	Goals					
	Ease-of-use	Ease-of-design	Customizability	Performance	Cost	
	Weighing Factors					
Design Alternatives	**100**	**30**	**70**	**100**	**5**	**Total**
Simple Joysticks	10/1000	7/210	3/210	3/300	8/40	**1760**
3-Axis Joysticks	8/800	5/150	6/420	8/800	2/10	**2180**
Touchscreen Interface	7/700	4/120	10/700	6/600	3/15	**2135**
Mouse Interface	5/400	10/300	8/560	1/100	10/50	**1410**

The simple joystick alternative was given the highest score (10/10) for Ease-of-use because these types of joysticks are familiar to most people and thus even new users would be able to intuitively

pick up this method of control. The three-axis joysticks with a score of 8/10 would also be easy to use, but the addition of a third axis and the "Etch-a-Sketch" control of cutting would make it slightly more difficult to use this control method. The touchscreen interface was given a slightly lower score of 7/10 than the three-axis joysticks because capacitive multitouch touchscreens are newer and a bit less familiar to use than joysticks, and the many gesture controls that may be implemented on the touchscreen may cause some confusion. The mouse interface was given a score of 5/10 because, while almost everyone knows how to use a mouse on a computer, the limited capabilities of the "point-and-click" methods of control make this option very cumbersome, as discussed previously.

For Ease-of-design, the mouse interface was given the highest score because no extra hardware or hardware/software interface would be needed for this alternative. The only "hardware" necessary would be to create buttons on the front panel of Robolase. Although programming would be required to designate these as events as well as determine their actions, just as much or maybe even more programming would similarly be necessary for each of the other alternatives. Even though the simple joysticks could be easily plugged in to the computer like a mouse, it received a score of 7/10 because extra programming would be necessary to configure the communication between Robolase and the joysticks, since the purpose of these joysticks would be very specialized and the way the joysticks control the fast-steering mirrors would have to be programmed specifically, especially for the predetermined cutting ROI. Both the three-axis joysticks and the touchscreen were given relatively low scores of 5/10 and 4/10, respectively, because it would be especially difficult to implement and program these alternatives. For example, the custom industrial three-axis joysticks cannot simply be "plugged in" to the computer and would probably communicate with the computer and the mirrors via the data acquisition board with wires that carry the voltages denoting the x- and y-positions of the joysticks. After connecting the hardware, programming would also be necessary to determine how Robolase interprets these voltages (for example, it would have to convert voltages to pixels to show the movement of crosshairs on the image and also must constantly monitor the joysticks' positions). The touchscreen may either be plugged in or configured by wires, depending on the type that is purchased, but this alternative would require even more programming than the three-axis joysticks since custom

gesture controls and multitouch functionality must be programmed so Robolase can handle the input appropriately. This requires more than the simple voltage reading and outputting that is necessary with the three-axis joysticks.

However, this complexity of design goes along with the increased potential for Customizability with the touchscreens, giving it a score of 10/10 for this design goal. Because so many controls can be made using multitouch gestures and other features of the touchscreen, the possibilities for customizing how the touchscreen actually controls the traps and scissors are virtually limitless. Although the mouse interface does not have multitouch gesture controls, it follows with a score of 8/10 because it also has potential for customizability because of the variety of LabVIEW controls and events and the many ways in which control of the traps and scissors can be programmed. On the other hand, the three-axis joysticks are slightly limited in their customizability, with a score of 6/10, since input from the joysticks is limited to changing voltages and possibly digital input from a limited number of buttons. The simple joysticks are even more limited with a score of 3/10 since it only has two axes and possibly limited forms of communication with the computer, i.e., only certain types of data can be sent from the joystick's proprietary (possibly USB or serial) connection. The three-axis joysticks suffer less from this since the raw analog voltage or digital input data can be manipulated by the programmer, whereas the simple joystick may only tell Robolase if it has moved, by how much, and in what direction, depending on proprietary software drivers.

With respect to Performance, however, the three-axis joysticks scored the highest because it can directly control the fast-steering mirrors without having to rely on the computer as an intermediary, which would slow down responsiveness. Because these joysticks can also send raw data to Robolase, it can be programmed at a much lower level, which implies that optimizing performance will probably be easier using this alternative. Also, the three-axis joysticks would allow direct simultaneous control of all three optical tools and would not have to rely on the predetermined cutting methods that would be necessary using the simple joysticks. Because the simple joysticks would have this type of limited functionality and would also lack the ability to send low-level data, this alternative was given a low score of 3/10. Even if the simple joysticks were not plugged into the computer and configured with

wires and voltages like the three-axis joysticks, the build quality would not be as good as the custom-ordered three-axis industrial joysticks, and it would likely also not meet the design specification of requiring ±10 V output. This might necessitate a software or hardware (e.g. electrical circuit) solution that would hinder performance by adding noise. The performance of the touchscreen interface, with a score of 6/10, may also be hindered because it requires the computer as an intermediary to process the data it outputs, which may slow communications and make control more difficult than the three-axis joysticks. Lastly, the performance of the mouse interface was given a score of 2/10 because it can only perform at the bare minimum, just able to move the mirrors and cut or trap using the "point-and-click" method and can control only one of the optical tools at a time.

Despite the mouse interface's poor performance, it does exceed with respect to the design goal of Cost, with the highest score out of the different alternatives. With respect to both monetary cost and cost of time and effort to develop this alternative, the mouse interface is very cost-effective since computer mice are widely available for relatively low prices and the only programming necessary would be the controls and the actions (cutting or moving traps) those controls govern. Since the other three alternatives would need even more programming in addition to this, this alternative is the "cheapest" with respect to cost of time and effort. The simple joysticks are the second least costly alternative, since computer joysticks are also widely available for low prices (but not as low as a mouse) and less programming would be necessary than the remaining alternatives. These alternatives were given low scores of 2/10 for the three-axis joysticks and 3/10 for the touchscreen because each would cost relatively more money to purchase. The joysticks would have to be custom-ordered and would probably be more expensive than a touchscreen, although touchscreens are still considerably more expensive than a computer joystick or mouse. Also, there would be much more programming necessary to implement these control methods in Robolase, which means much more time and effort would be necessary to develop these alternatives when compared to the simple joysticks or mouse interface.

However, since Cost is the lowest-prioritized design goals, it does not significantly affect the final decision. The winning alternative by a small margin is the three-axis joysticks, with a total score of

2180, just slightly above the total score of 2135 for the touchscreen interface. While both alternatives are very good solutions to solving the design problem of cumbersome control of the optical tools for the Robolase IV system, the three-axis joysticks provide a good middle-ground solution that is capable of meeting all the design goals and fulfilling the needs of the system outlined in the introduction.

2.3. Proposed Solution

2.3.1. Hardware: Custom Industrial Joysticks

Several companies that make joysticks were researched, but CH Products was chosen to supply them, who was able build a joystick within the aforementioned design specifications (e.g. 3-axis, ±10 V output). The line of joysticks that was suggested by the company was the HFX Series III, a heavy duty Hall effect controller meant for industrial purposes (CH Products, 2011). A schematic of the specific joystick ordered is shown in Figure 2.1. The joystick would be built with ±10 V output and would require a 12 V DC power source and cost approximately $400 each.

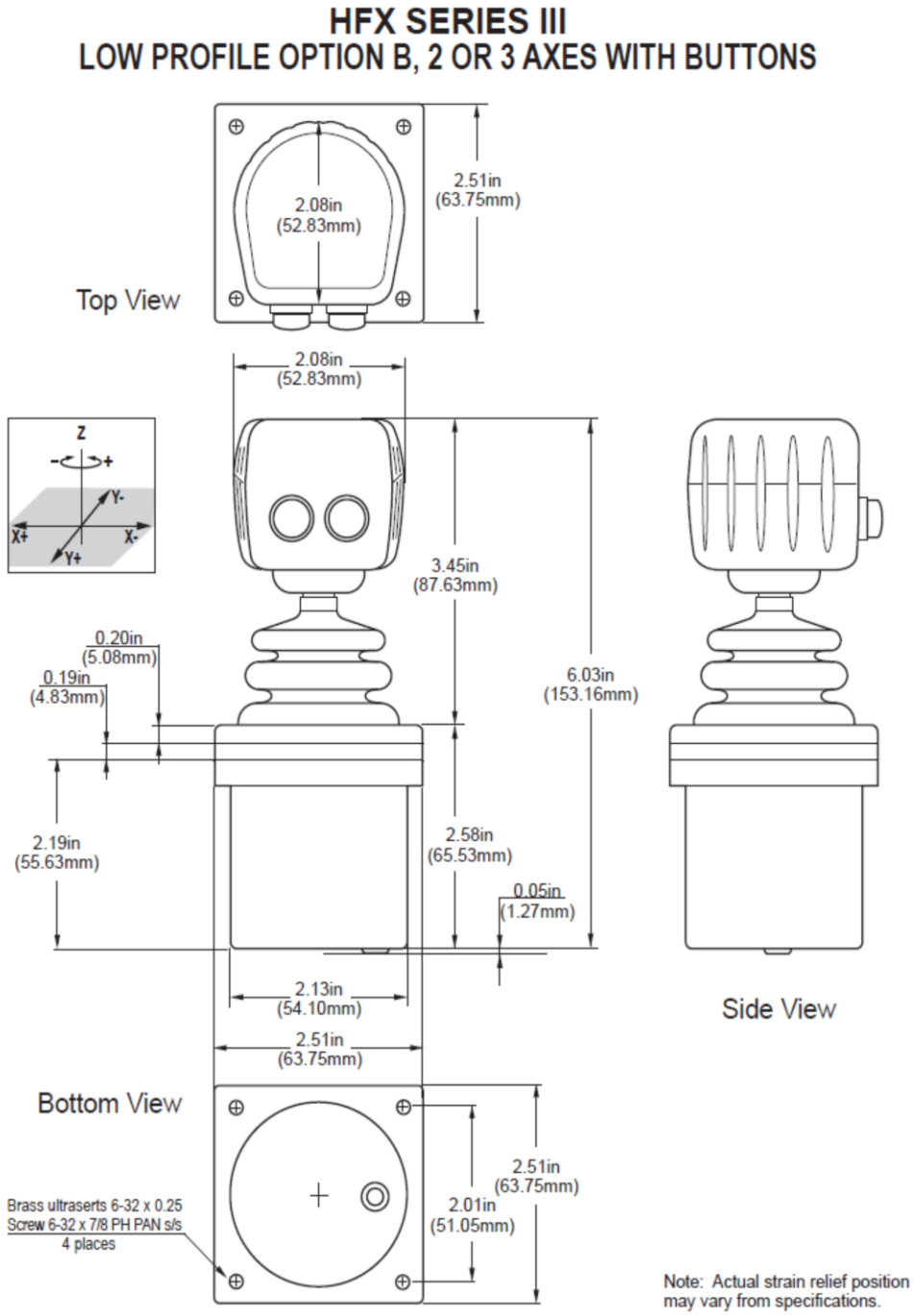

Figure 2.1. Schematic of HFX Series III joystick from CH Products. This industrial joystick uses the Hall effect and provides 3-axis support with buttons (CH Products, 2011).

2.3.2. Earlier Control Schemes

The different control schemes describe how the joysticks were integrated into the existing Robolase IV system (e.g. hardware connections) and in what manner the joysticks actually controlled

the two optical tweezers and scissors (e.g. programming in Robolase IV LabVIEW program). Three different control schemes were developed, each one an improved version of the previous version to better fulfill the needs for a responsive and intuitive, user-friendly control method. The two earlier control schemes, Positional and Velocity control, will be described briefly with respect to how they work conceptually and why certain limitations of these control schemes necessitated the evolution of the third control scheme. This newest Onboard/Simultaneous control scheme, which is being currently used, will be described in detail thereafter. Detailed descriptions of the two earlier control schemes can be found in Appendix B.

2.3.2.1. Positional Control

This control scheme was the original, intended control interface on which the decision matrix is based. However, serious flaws became apparent as it was being developed, which led to the need for better control schemes as discussed later. The hardware setup and software developed for the Positional control scheme can be found in Appendix B.

With the Positional control scheme, the voltages outputted by the joysticks (which depend on the position of the joystick) directly represent the voltages applied to the fast-steering mirrors. For example, if the joystick was moved in the x-axis to a position corresponding to 5 V, the fast-steering mirror connected to the joystick would rotate in the x-axis at 5 V. Thus, the user would be able to move the two optical traps to any location as fast as the user can move the joysticks, since the output voltages of the joystick would be directly connected to the input voltages of the fast-steering mirrors.

However, because the joysticks are designed to revert back to their neutral position (i.e. 0 V on both axes) once the user releases the joystick, the hardware setup and software had to be designed to be able to physically switch control (using relays) of the position of the mirror back to Robolase IV on the computer after the user moved the traps to their desired positions. Thus, the user would move the joysticks to move the traps to their desired positions and then switch control to the computer so the optical traps can be maintained at those positions even after the joysticks are allowed to revert to their neutral, zero voltage position.

With respect to controlling cutting, moving the third axis (i.e. rotation) of the joysticks, does not directly control the scissors fast-steering mirrors unlike trapping. Instead, the rotation axes control a feedback triangle ROI on the main image, which is used to designate the start point and end point of a cut using the buttons on the joystick. The shape of the cut between these start and end points can be chosen on the Robolase IV front panel by the user.

Because of the switching of control of the traps and the general manner in which the scissors are controlled, however, both trapping and cutting using the joysticks each require a different 6-step procedure that the user must learn and perform every time an object needs to be trapped or cut (detailed explanations of these procedure for trapping and cutting can be found in Appendix B, section B.1.2.1). Thus, the joysticks themselves are easy to use and intuitive for new users, but in order to use them correctly the user must also learn the two different 6-step procedures involved with cutting and trapping with the joysticks. Therefore, with this control scheme there is still a learning curve in order to be able to use the joysticks, even though the joysticks themselves are easy to use. This was one of most significant problems that made it necessary to develop a newer, better control scheme.

Furthermore, since only the start point and end point of a cut can be designated by the user, and the shapes that can be cut between these points are predetermined by the Robolase IV program, the control of cutting using the joysticks is limited to only these shapes. In addition, it would be very difficult and frustrating to control the movement of the feedback triangle ROI to designate these points using the “Etch-a-Sketch” control that results from using the rotation axes of the joysticks. It would also be very difficult to simultaneously control joystick cutting and trapping, since the user would have to simultaneously rotate and move both joysticks to control both the tweezers and the scissors at the same time.

Another issue is that feedback must be enabled in Robolase IV in order to read the voltages from the joysticks, which causes the program to be very slow, since the computer has to read the analog voltages from each of the six channels (x, y, and z for both joysticks) one at a time. This causes the algorithm that reads the feedback to iterate very slowly and the positions of the traps to update slowly as well. Lastly, a back-calculation is necessary to convert the joystick positions in voltages to trap ROI

positions on the main image in pixels. However, this back-calculation is not always in agreement with the forward conversion from pixels to voltage used in the point-and-click method, which worsens the more the trap is misaligned. Although these factors do not prevent the trapping from working, they may cause some frustration during use, which further makes this design less attractive for users, both new and familiar.

2.3.2.2. Velocity Control

Obviously, the issues that arose with the positional control scheme—such as the complicated multi-step processes required to control joystick trapping and the limited control of cutting using the joysticks—led to a need for developing a better control scheme that was as easy to use and intuitive as the joysticks themselves. Thus, the next control scheme that was developed was based on velocity control, for which a detailed description can again be found in Appendix B.

In many applications where joysticks are used, the joysticks themselves control the movement of an instrument or a cursor on a computer screen. Applying this to the Robolase IV system, moving the joysticks would control the velocity of the optical traps and scissors. Moving the joystick to the left, for example, would cause the trap to the left at a certain velocity. If the user moves the joystick to its furthest position to the left, then the trap will move at maximum velocity. Since even new users would be familiar with using a joystick in this manner, learning to use optical trapping and cutting on Robolase would be much more intuitive and would have less of a learning curve, which would help fulfill the design goal of being easy to use.

Because the joysticks would control the velocity of the optical traps (and thus the fast-steering mirrors), connecting their output voltages directly to the input voltages of the fast-steering mirror would not fulfill this purpose without a signal conditioning circuit. Instead of using a circuit to convert the output voltages of the joystick into velocities for the fast-steering mirrors, software—specifically LabVIEW programming—was used instead. This means that the output voltages of the joysticks are sent directly to the computer, where the signals are read and translated into movement for the fast-steering mirrors.

Although it would have been possible to use the z-axis (rotation) of each joystick to also control the movement of the optical scissors, the difficult "Etch-a-Sketch" control would make this more difficult than using the joystick in the x and y directions. Thus, instead of using the z-axes, the LabVIEW VI instead switches the target of control of one of the joysticks from an optical trap to the optical scissors using software. This is triggered again by one of the joystick pushbuttons. When switched to this cutting mode, the joystick controlling the S trap is switched to control the cutting fast-steering mirror instead of the S trap fast-steering mirror. The S trap itself maintains its position immediately before the switch and cannot be moved while in cutting mode, while the joystick controlling the P trap can still move the P trap fast-steering mirror.

This control scheme drastically improves upon the Positional control scheme, since those multi-step processes for controlling cutting and trapping have been made unnecessary. Now, the control scheme using the joysticks is as simple and easy-to-use as the joysticks themselves. After enabling feedback in Robolase IV, the user can move the joysticks and intuitively move the traps wherever the user desires. By using the joysticks to control how much the fast-steering mirrors are displaced with each iteration, the user can control how much the optical traps move, and the position of the trap does not revert back to a default position whenever the joysticks revert back to their default, 0 V position, since 0 V sent to the computer in this case implies that the optical trap has no movement.

Furthermore, joystick control of cutting has been improved significantly as well. Because we do not use the rotation (z-axis) of the joysticks for controlling the cutting beam, the user no longer has to deal with the difficult, "Etch-a-Sketch" type of control. Simply by pressing one of the pushbuttons, one of the joysticks controls the cutting beam instead of a trap, so that cutting and trapping with one optical trap can be performed simultaneously and very easily. Cutting with the joystick is now no longer limited to a line, rectangle, or ellipse, and cutting complicated shapes such as circles or curves is much easier than using CutROI in Robolase IV. However, since this type of control resembles a "manual" setting for cutting, the laser ablation during joystick cutting is not as precise, which may sometimes be necessary when exact laser dosage must be known during an experiment. Also, it is not possible to control all three optical tools—two traps and one scissors—at the same time. Adding another joystick

would make this possible, but unless two people are working on the system it would be difficult to control all three joysticks at once regardless. However, it is possible to control two traps using the joystick and control the optical scissors using Robolase IV, which is more precise than manual joystick cutting. For example, at the end of this chapter the two joysticks are used to apply tension on a red blood cell in suspension, a line is then across the center on the main image in Robolase IV, and then CutROI is initiated from the program. This situation efficiently employs all three tools in a very cooperative way.

The only limitation that makes control difficult is the noticeable amount of time it takes for the LabVIEW VI to iterate in order to read the joystick voltages and update the trap positions. Since this VI is built into Robolase IV and checks the voltages as Robolase IV checks for events, the speed at which the VI can update the voltages depends on how fast Robolase IV is iterating, which is not slow, but slow enough that the user will notice a delay while moving the joysticks. That is, when the user moves the joystick, the crosshairs and the fast-steering mirror controlling the optical trap "jump" from one location to the next, such that the movement is not smooth. If the sensitivity is set low enough such that these jumps are not large, then most likely the trap will not lose whatever it is holding during a jump. However, if the sensitivity is too high or the movement too large, then the trap may move too far and whatever it is holding may be lost or scattered. Thus, while control of the optical tweezers using this control scheme is very intuitive, it lacks the responsiveness necessary for dynamic experiments and can be somewhat frustrating since the user must patiently wait for the trap to move to the desired position.

In order to resolve this limitation, a double-while loop structure was experimented with, where the LabVIEW VI that checks the joystick voltages runs in a separate while-loop than the main Robolase IV while-loop that checks for events. Although this helped to speed up the movement slightly, it was still slow enough that the above problems could still occur. The main problem was that the program used to monitor the joysticks had to be built into Robolase IV, which meant that the joysticks had to use the computer as an intermediary to communicate with the fast-steering mirrors. Since Robolase IV is such a heavy program that consumes a significant amount of the computer's resources, slowing of the code is inevitable. While it would have been possible to write and run a separate LabVIEW VI

concurrently with Robolase IV, many issues would have occurred, such as how to pass values from one program to the other without lag, as well as how to control the same hardware (such as the DAQ board) from two different VIs.

2.3.3. Current Control Scheme: Onboard/Simultaneous Control

The newest control scheme was developed in two parts. In the first part, the control scheme is designed around an onboard program running on a motion controller to monitor joystick voltages and displace trap positions in response. Thus, the hardware setup and software were designed with this original intention. The second part of the development of this control scheme represents a slight revision to the first, replacing the onboard program with a simultaneous program running on the same computer as but separately from Robolase IV. This was done because of the limitations of using the onboard program that will be discussed in section 2.3.3.5 and also because of the discovery of new methods to solve the problems that occur when using two simultaneous LabVIEW programs mentioned above. Because both the Onboard and Simlutaneous control schemes share the same hardware setup, however, the development of both parts will be described.

2.3.3.1. Onboard Control Scheme

In light of the problems that occurred in the Velocity control scheme, a solution based on using new hardware—the NI motion controller 7344, capable of onboard programming—was considered and developed. This control scheme would use the motion controller's onboard programming capabilities to run a program independent and physically separate from Robolase IV that could monitor the joystick voltages and move the fast-steering mirrors accordingly, all without the need to communicate with Robolase IV on the computer. Because the onboard program would not depend on Robolase IV, the code would run very quickly and the slow-down experienced in Velocity control would not occur to such an extent. In addition, the NI motion controller is designed to communicate with LabVIEW programs as well, which means that passing voltage values from the onboard program running in the motion controller to Robolase IV running on the computer would be very easy. Thus, while this

onboard program runs separately, monitoring the joysticks and moving the mirrors, Robolase IV can communicate with the motion controller simultaneously to monitor the positions of the fast-steering mirrors as well and update the crosshairs representing the traps on its main image.

Since new hardware is required, the hardware setup is much more complicated than in Velocity control, where all voltage signals simply went to the computer and were processed by the Robolase IV program. In addition, the motion controller has only four analog output and four analog input channels, enough for only two mirrors (x- and y-voltages for each mirror). This meant that a hardware workaround had to be developed in order to be able to switch from trapping mode to cutting mode as in Velocity control (switching modes in this Velocity control was a simple software matter, since all voltage signals went through the computer). To develop a method for hardware switching, the same relays used in Positional control described in Appendix B were again employed in order to carry out this switching.

2.3.3.2. Hardware Setup

In order to be able to physically switch the target of control of the S Trap joystick between the S Trap fast-steering mirror and the scissors fast-steering mirror, the hardware setup was built around relays, or electrically controlled switches, that would perform the switching. The relay used in this setup was the Omron G2R-24 5VDC, shown in Figure 2.2 below.

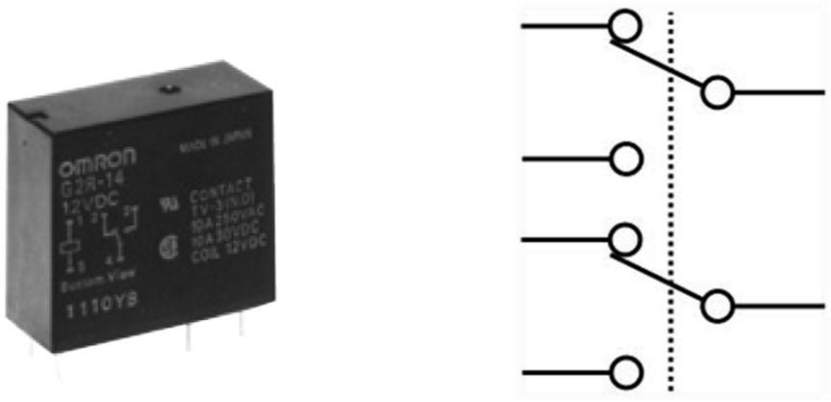

(a) (b)

Figure 2.2. (a) Omron G2R DPDT relay (Omron, 2011) (b) Diagram of a double-pole, double-throw (DPDT) switch.

These relays are double-pole, double throw (DPDT) in order to handle switching of two sets of voltages per relay. The relay is triggered by a 5 V signal (i.e. a digital input) called the coil voltage, which toggles the relay between the two positions. Two relays were needed in order to accomplish the switching of the S Trap joystick target, working together in order to enable the switching between trapping mode and cutting mode for the S joystick.

Because each relay requires many electrical connections with the computer, motion controller, joysticks, and the fast-steering mirrors, for the sake of organization and customizability all the wires from each of these devices were connected to a solderless breadboard that would act as the central hub of all the signals, appropriately called the Joystick Hub. It is unlikely that permanent connections (i.e. soldered) will be made between the electrical connections on the breadboard in order to preserve the ability to customize the hardware setup (which already occurred as this control scheme was developed after two earlier ones, requiring the modification of the electrical connections in these early control schemes).

Besides the addition of the Joystick Hub to the hardware setup, the NI motion controller is also added as well as an NI MID stepper motor drive, which communicates with the motion controller and actually houses the analog input and output terminals used for receiving the joystick voltages and outputting the fast-steering mirror voltages. In order to understand all the connections between the hardware, the hardware setup will be discussed first, which is shown in Figure 2.3 below.

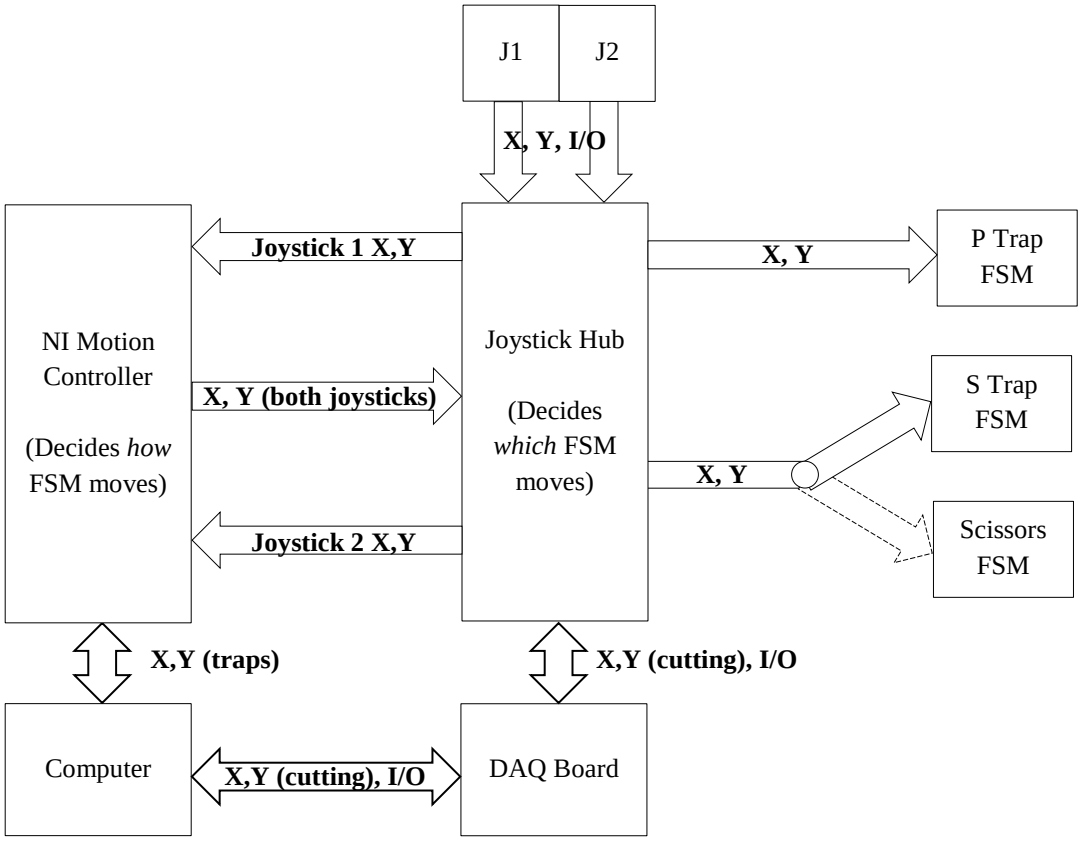

Figure 2.3. Hardware setup for Onboard/Simultaneous control scheme. The computer communicates via an NI DAQ board. Not shown is the MID stepper motor drive, through which the motion controller communicates with the joysticks and Joystick Hub.

The Joystick Hub communicates with the fast-steering mirrors, and the relays inside—controlled by the computer communicating via the DAQ board—decide whether the cutting or S trap fast-steering mirror is controlled by the S joystick. Thus, digital signals pass between the Joystick Hub and the computer to turn the relays on and off. Digital signals from the joysticks' pushbuttons also pass through the Joystick Hub and on to the computer via the DAQ board so Robolase knows when to turn on these relays, determining whether or not the scissors FSM is controlled by the S joystick as well as when to open the shutters for each trap and the scissors. The analog x- and y-voltages for the cutting fast-steering mirror also are passed from the DAQ board to the Joystick Hub when not in joystick cutting mode.

Unlike Velocity control—where a program running within Robolase IV in the computer decides how the fast-steering mirrors move in response to joystick movement—the movement of the

traps in response to movement of the joysticks by the user is decided in this control scheme by the onboard program running on the NI motion controller. Thus, the output voltages of the joysticks, communicated again via the Joystick Hub, are read by the onboard program on the motion controller, the onboard program calculates a displacement for the fast-steering mirrors just like in Velocity control, and these new displaced voltages are sent back to the Joystick Hub, where the Joystick Hub passes the new voltages to the S Trap and the P Trap FSMs or the P Trap and the Scissors FSM, depending on whether the system is in trapping mode or cutting mode. Meanwhile, Robolase IV on the computer is also monitoring where the onboard program is sending the fast-steering mirrors and moving the crosshairs on the main image accordingly. The computer communicates with the motion controller through an NI PXI interface, which connects to a PCI card in the computer. The PXI interface itself and the MID stepper motor drive that actually houses the analog input and output ports are not shown. Robolase IV can also send commands to the motion controller in order to move the fast-steering mirrors. Thus, the point-and-click method remains functional in this control scheme, despite the fact that the method of communication with the fast-steering mirrors (motion controller instead of DAQ board) is different.

The complete hardware diagram is shown in Figure 2.4 below.

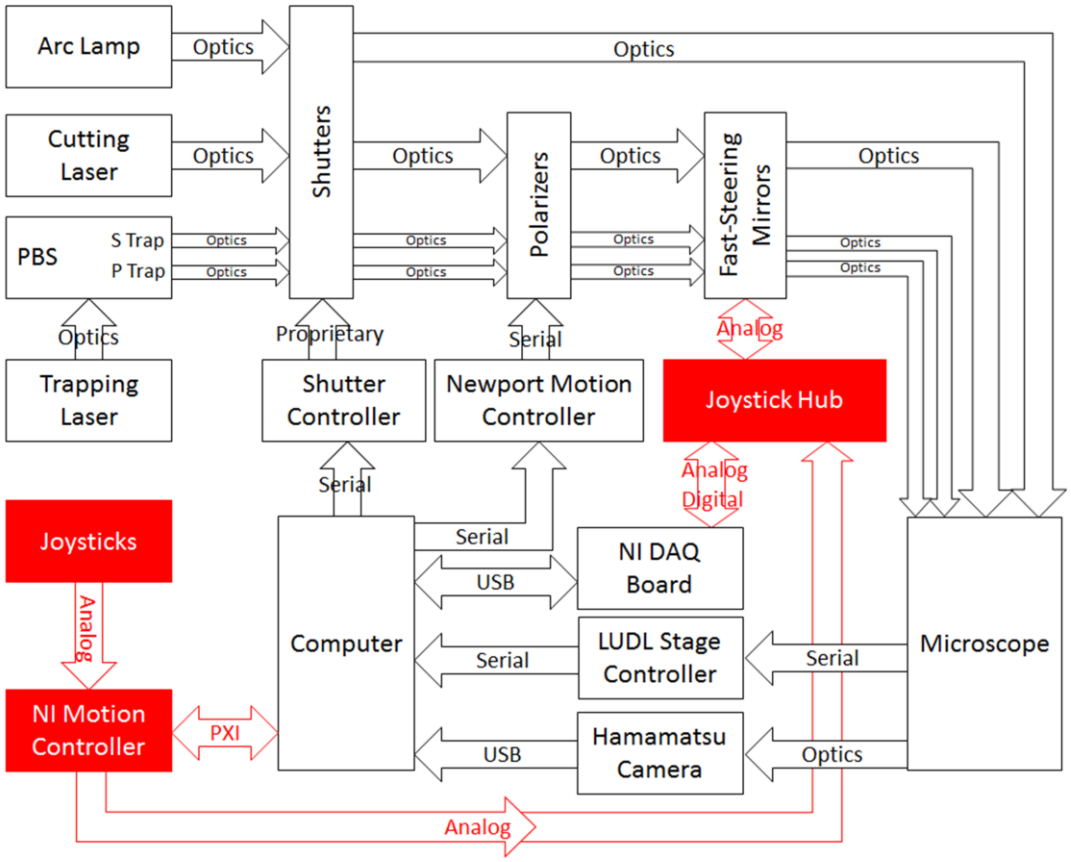

Figure 2.4. Complete hardware diagram for the Onboard/Simultaneous control scheme. The joysticks actually communicate with the motion controller via the Joystick Hub, but this is omitted in order to simplify the diagram.

The DAQ board has a much more limited purpose in this hardware setup compared to the original in Figure 1.7, since it only passes along the digital signals from the joystick and computer to turn on and off the relays as well as the analog voltages from the cutting fast-steering mirror. It does not, however, handle the analog voltages of the joysticks and their corresponding fast-steering mirrors. With the exception of the digital signals and the analog cutting signals, the motion controller has essentially replaced the DAQ board with respect to communicating the analog signals for the traps. In addition, the motion controller also processes these analog signals remotely (i.e. not requiring the computer), reading the output voltages of the joystick (via the Joystick Hub, whose purpose as an intermediary is not shown in the figure above) and calculating appropriate displacements for the fast-steering mirrors as well as forwarding commands from the computer when the point-and-click method is used.

The circuit diagram of part of the Joystick Hub in Figure 2.5 below illustrates exactly how switching of the target of control of the S joystick is achieved using two relays working in conjunction.

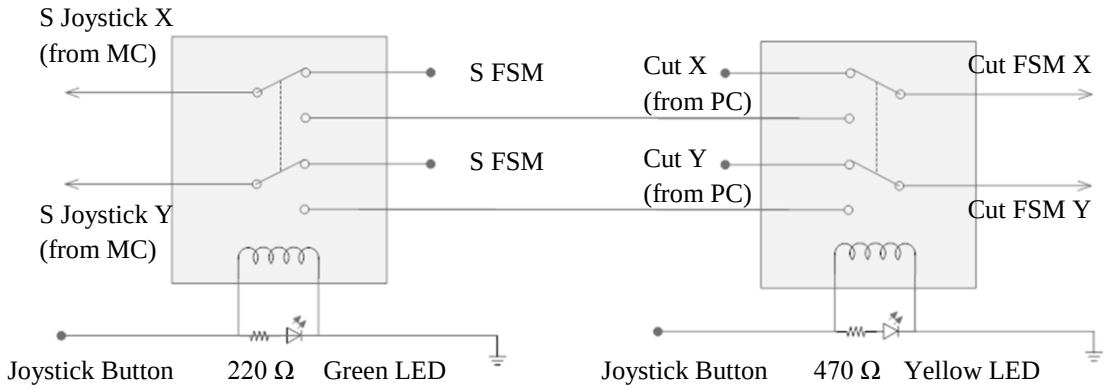

Figure 2.5. Switching circuit diagram of Joystick Hub for the Onboard/Simultaneous control scheme. MC refers to motion controller, while Cut refers to the signals for the scissors.

The relays are triggered by a 5 VDC coil. The signal comes from the DAQ board, which is triggered by Robolase IV whenever the appropriate joystick pushbutton is pressed (one button triggers both). The triggering coils are in parallel with LEDs and current limiting resistors in order to visually indicate the status of each relay. Robolase IV turns always turns on both relays when activated, rather than just one at a time. The incoming voltages, labeled "S Joystick X" and "S Joystick Y" are actually the new, displaced voltages outputted by the motion controller (MC) calculated by the onboard program. Thus, when the relays are off and the system is in trapping mode, these output voltages are sent to the S trap fast-steering mirror, so that moving the S joystick will cause the onboard program to calculate new displaced voltages and the S trap fast-steering mirror will move accordingly. In this relay-off state, the x- and y-voltages for the cutting beam are also passed from Robolase IV (via the DAQ board) to the cutting fast-steering mirror.

When the relays are on, the system is in joystick cutting mode. At the first relay, the new displaced voltages from the motion controller are no longer connected to the S trap fast-steering mirror, so the S trap no longer moves in response to S joystick movement. The outputs of the first relay are now connected to the second relay. Since both relays are on, this means the new displaced voltages from the motion controller (controlled by the S joystick) are now connected to the cutting fast-steering mirror.

Thus, moving the S joystick now moves the cutting fast-steering mirror, and the system has been switched from joystick trapping mode to joystick cutting mode.

The P trap, meanwhile is always controlled by the P joystick. This is shown in the next figure, which shows the rest of the electrical connections made in the Joystick Hub for the Onboard/Simultaneous control scheme.

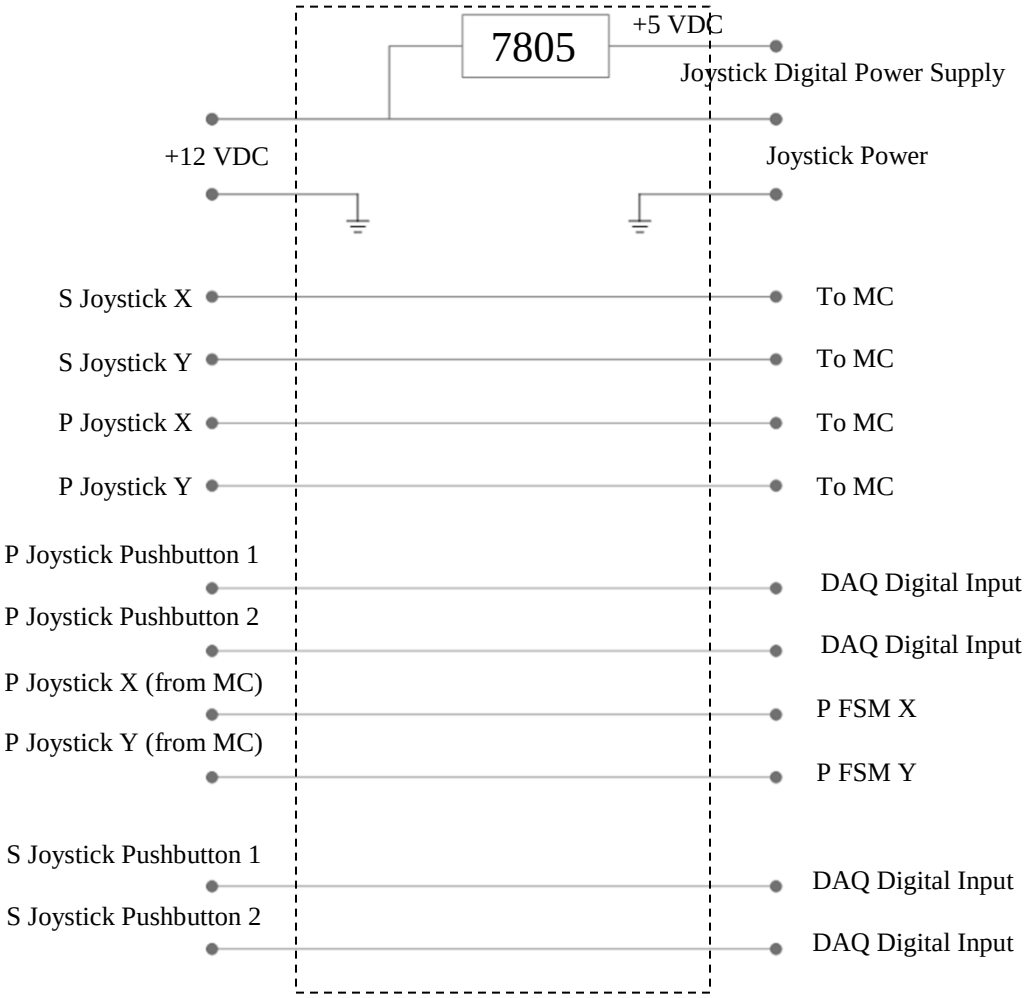

Figure 2.6. Circuit diagram (non-switching portion) of Joystick Hub for the Onboard/Simultaneous control scheme. MC is the abbreviation for motion controller.

The connections near the top provide power to the joysticks as well as the buttons using a 5 VDC regulator. The next set of four inputs and outputs represent the joystick voltages, which are sent to the motion controller where the onboard program reads these voltages to calculate the new displaced voltages. In the next set of four inputs and outputs, the second two represent the displaced voltages for

the P trap from the motion controller, which are sent to the P trap fast-steering mirror. The first two are the digital inputs and outputs for the pushbuttons on the P joystick, while the last set are for the pushbuttons on the S joystick.

2.3.3.3. Control by User

To control the position of the traps, the user moves the joystick in any direction and the trap correspondingly pans in the same direction, similar to how joysticks are used in most applications as in Velocity control. One of the buttons on each joystick controls the shutters for the S and P traps. When a shutter is open, the trap is considered "on." Thus, the user can move the trap by moving the joysticks with the shutter closed to a bead, for example, turn on the trap by pressing the pushbutton, then move the trap with the joysticks with the bead held by the trap, and then close the trap to let go. In addition, this can be done simultaneously with both traps at once.

In order to cut using the joystick, the user presses the other button on the P trap joystick (the one not dedicated for the shutter). A subVI within Robolase IV—discussed in the next section—"sees" the button press and switches the target of control for the S joystick by sending a signal to the relays in the Joystick Hub described in the previous section. After this switch, moving the S joystick now moves the cutting fast-steering mirror. The second button on the S joystick opens the cutting beam shutter. Thus, the user can move the joystick to control the cutting beam, and press the button whenever he or she wants to cut. The P joystick still controls the P trap, so one trap and one joystick can be controlled simultaneously, while the S trap remains stationary.

2.3.3.4. Software

In this control scheme, there are two programs worth discussing: the LabVIEW VI in Robolase IV monitoring the fast-steering mirrors and the onboard program on the motion controller itself, responsible for reading the voltages from the joysticks and calculating and outputting the new displaced voltages.

The LabVIEW VI running as a subVI within Robolase IV is essentially the same as the one for Velocity control with the omission of communication with the joysticks and the fast-steering mirrors for the traps. Instead, this VI communicates only with the motion controller, which in turn communicates with the joysticks and fast-steering mirrors. The flow chart for the pseudo-code is shown below in Figure 2.7.

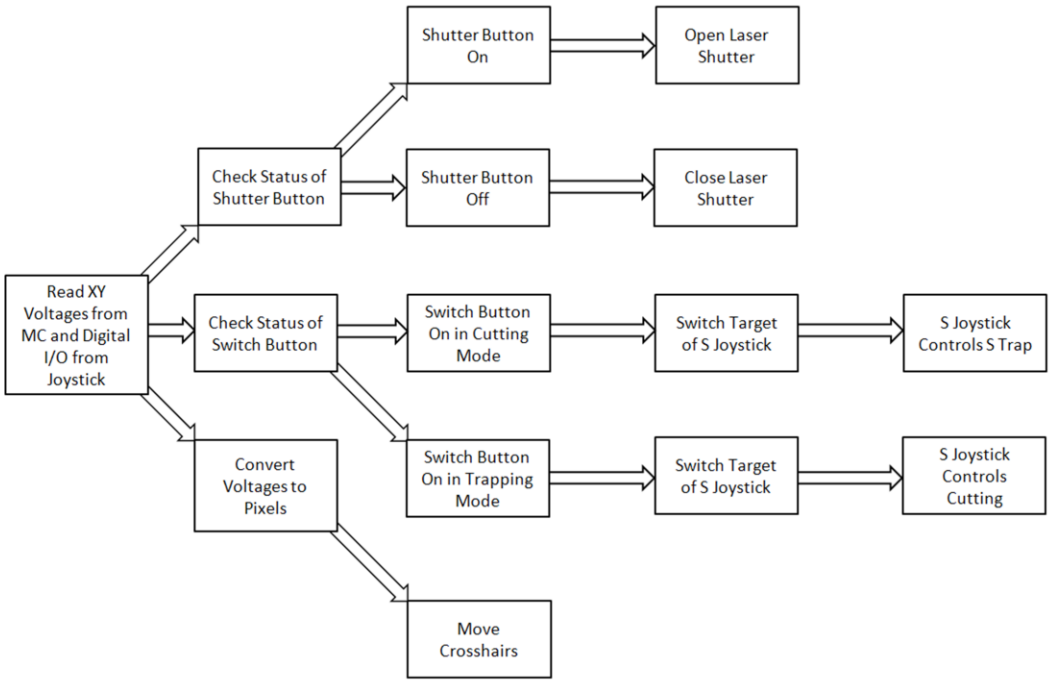

Figure 2.7. Flow chart of pseudo-code for LabVIEW subVI within Robolase IV for the Onboard control scheme.

This VI reads the digital input and output signals coming to and from the joystick. One of these digital signals is used for checking the status of whether the system is in joystick trapping (S and P trap) mode or cutting (P trap and scissors) mode. The other three digital signals are used for opening and closing the shutters for the traps (not shown) and scissors. Again, the shutter for the scissors remains open as long as the button is pressed, while the trap shutters stay open even if the button has been released, closing the next time the button is pushed. The main difference between this VI and the one in Velocity control shown in Appendix B is the bottom path. Here, the x- and y-voltages—which are read from the motion controller (MC) instead of the joysticks—are not used to calculate the displaced voltages.

Instead, they are simply converted from voltage to pixels and the crosshairs on the main image of Robolase IV are moved accordingly. Note that here the voltages that are read are the actual positions of the fast-steering mirrors—since the computer only monitors the position of the fast-steering mirrors—not the output voltages of the joysticks as in the other two control schemes.

In this control scheme, the output voltages of the joysticks from are read by the onboard program running within the motion controller. From the joystick voltages, the displacements of the trap positions are calculated and the onboard program outputs these displaced voltages to the fast-steering mirrors. Thus, the onboard program moves the trap positions in response to movement of the joysticks. A pseudo-code flow chart of the onboard program is shown in Figure 2.8 below.

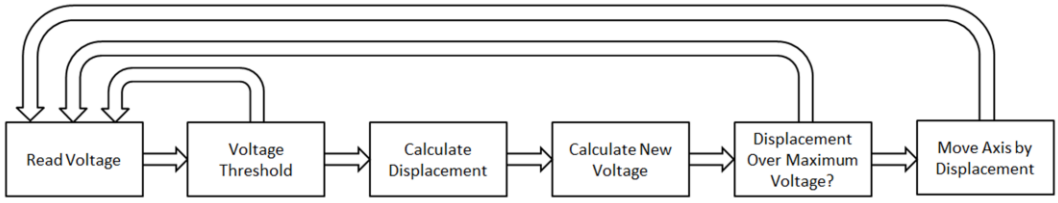

Figure 2.8. Flow chart of pseudo-code for onboard program running within the motion controller. This code is repeated for each axis.

The code in the figure above actually runs four times, one for each axis involved: SX, SY, PX and PY. The code first reads the voltage for the corresponding axis from the joystick. If the voltage is below the threshold for random noise, then the program loops back and reads the voltage again. If the user is not moving the joystick, then the code simply runs between these two boxes. If the user is moving the joysticks, then the code passes the voltage threshold and the onboard program calculates a displacement again based on a sensitivity value.

The program then checks whether the next movement based on the displacement value would result in a voltage outputted that is over the maximum possible range (-10 V to +10V). If the move is outside of the possible range, then the program sets the axis to the maximum possible voltage and returns back to the beginning of the program. Thus, if the fast-steering mirror is already at its limit for any axis, but the user is still moving the joystick for that axis towards the maximum direction, then the program will disregard this and not move the fast-steering mirror any further. Because this check is built-in to Robolase IV when outputting voltages to the fast-steering mirrors through the DAQ board,

the code was never explicitly shown in the figures for the LabVIEW VI in the Position and Velocity control schemes. If the move is not outside the possible range, however, the axis is moved by the displacement calculated and returns to the beginning to continue reading the voltage.

This onboard program is run when Robolase IV is first run. Thus, the fast-steering mirrors can be controlled as soon as the program starts (although feedback must be enabled in order to see the crosshairs on the main image move as the joysticks are used). After initializing values (such as sensitivity or maximum values) as well as the analog output and input channels, the code in the onboard program sequentially checks every axis and repeats.

2.3.3.5. Limitations

Using the onboard program on the motion controller essentially solves the slow-down problem with Velocity control. Unlike in the previous control scheme, the speed of the iteration (and thus the speed with which the position of the joystick can update) is not limited to how fast Robolase IV can iterate, since the onboard program runs in the motion controller instead of the computer, which is a completely different piece of hardware. In fact, the onboard program can even run without Robolase IV open, although this would be impractical since it would be impossible to know where the traps are moving without images from the camera. Thus, Robolase IV reads from the onboard program in order to synchronize the position of the crosshairs on the main image with the actual position of the fast-steering mirrors.

The Onboard control scheme therefore provides the most seamless integration of the joysticks into the existing Robolase IV system without sacrificing performance or ease-of-use, and thus best fulfills the design goals specified earlier. This control scheme does not require the multi-step processes involved with the Position control scheme, and does not suffer the slow-down that occurs with the Velocity control scheme.

However, this control scheme does share one limitation with the Velocity control scheme: the inability to simultaneously control all three optical tools. Although this would be possible by adding another joystick, another motion controller would also be needed because the motion controller is

limited to four sets of analog input and output channels. Also, the three joysticks would not be able to be simultaneously controlled by one user.

For most situations, however, simultaneous control of all three optical tools should not be necessary. In fact, in trapping mode simultaneous control is possible, since Robolase IV can control the scissors. This is usually the best configuration since precise cutting is necessary in order to measure laser dosage imparted onto the sample during experiments, as well as the fact that laser ablations are usually in small areas of the cell, which are harder to target when using the more "manual" control during joystick cutting.

Another limitation is the back-conversion from voltages to pixels for the trap positions. Because Robolase IV monitors the position of the traps by reading voltages from the motion controller, the program must back-calculate the pixel values of the traps from those voltages. Because of the complexity of the pixel-to-voltage calculation—which takes into account many correction factors in order to align the actual trap position with the crosshairs on the screen—the conversion from voltage-to pixel does not always correspond. For example, if the crosshairs on the main image are at position (500, 500) in pixels, the pixel-to-voltage calculation may yield voltages of (4.331 V, 2.168 V) for x- and y-axes of the fast-steering mirror. Converting that same voltage back to pixels may yield the coordinates (498, 501). This inaccuracy results from round-off error—which is significant since many of the alignment parameters such as steer (calibration of pixels/volt) are very small, on the order of 10^{-4} to 10^{-3}—as well as the fact that the motion controller can only work with 16-bit integer values at the most, which also causes rounding error when converting double-precision floating point variables to integers. Although this problem is minimized by working near the (0 V, 0 V) trap position such that the error is only 1 or 2 pixels, the discrepancy becomes increasingly larger the further from this zero-voltage position.

2.3.3.6. Simultaneous Program

In order to solve this problem, this control scheme was developed further in order to avoid the discrepancies that result from the back-conversion. This further development represents the second part

of the development of the Onboard/Simultaneous control scheme, where the onboard program is replaced by a LabVIEW program that runs on the computer simultaneously with but completely separate from Robolase IV. This simultaneous program basically performs the same code as the onboard program but runs on the computer instead of the motion controller. Although it was stated in the description of the Velocity control scheme that this would be difficult, the addition of motion controller to the hardware setup allowed two separate LabVIEW programs, Robolase IV and this simultaneous program, to both access and output to the voltages of the fast-steering mirrors connected to the motion controller. Furthermore, a new method was developed in order to share values between two LabVIEW programs on the same computer without the use of global variables or embedding the simultaneous program as a subVI within Robolase IV. This new method involved using the same strict type definition control that houses all the controls in Robolase IV in the simultaneous program and employing an Invoke Node to force the simultaneous program to read the values of the controls from the same place in memory as Robolase IV. Thus, the values between the two separately running LabVIEW programs are consistent even though the two programs are not physically wired to each other (i.e. one program's outputs are not connected to the other's inputs).

To avoid the inaccurate back-conversion, the simultaneous program calculates the displacement of the trap position in pixels from the joystick voltages. This is in contrast to the onboard program, which reads the voltages of the joystick and calculates a displacement in volts and moves the trap position accordingly. Because the simultaneous program displaces the trap position in pixels, it must then perform the same pixel-to-voltage calculation that Robolase IV also does when moving the traps using the point-and-click method. Thus, the position of the trap in volts always corresponds when moving the trap using either the joysticks via the simultaneous program or the point-and-click method via Robolase IV. Because this calculation has many steps and divisions, it would have been very difficult and inaccurate (due to round-off error) to perform the calculation within the onboard program, which cannot handle non-integer numeric data types. Figure 2.9 shows a pseudo-code of the simultaneous program, which is similar to the onboard program.

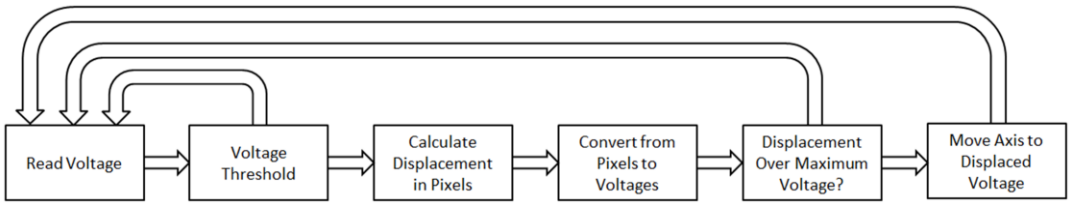

Figure 2.9. Flow chart of pseudo-code for simultaneous program running on the computer but separately from Robolase IV. This code is repeated for each axis.

This code also runs for each axis, but does so concurrently instead of sequentially like in the onboard program.

Because the overall architecture of this control scheme is the same as with the onboard program, the switching between trapping mode (S and P trap) and cutting mode (P trap and scissors) is still functional, since the LabVIEW VI described in section 2.3.2.3. and shown in Figure 2.7 still runs within Robolase, with the exception that this VI no longer reads the trap position voltages from the motion controller.

Thus, the development of a simultaneous program resolves the back-conversion problem that arose from using an onboard program without having to sacrifice any previous functionality. Since the simultaneous program runs completely separately from Robolase IV (other than the fact that the program is started the same time Robolase IV starts), the speed of its iterations and thus the responsiveness of the joysticks is not affected as they were in Velocity control. In fact, because the simultaneous program is a LabVIEW program, it would be easier to customize when necessary, since onboard programs are very inflexible and limited in functionality. Thus, this minor change has made the already-successful onboard control scheme even better.

It could have been possible to revert the hardware setup similar to that in the Velocity Control Scheme, since the main purpose for using the motion controller was to run the onboard program, but, as mentioned, reading the NI DAQ board is much slower (e.g. voltages cannot be read concurrently) and problems would arise if two LabVIEW programs tried to access the DAQ board at the same time (which is more likely to occur because of the slower communication).

2.4. Preliminary Demonstrations

The demonstrations in this section were performed in order to make sure the newly-developed joystick user interface works and to illustrate the dexterity and ease-of-use with which microscopic objects can be manipulated.

2.4.1. Demonstration of Joystick Trapping

In this demonstration 10 micron beads were used in order to demonstrate the ability to trap using the joystick. The trapping power before the objective was 0.539 W (irradiance of 7.26×10^7 W/cm^2) for the P trap (blue rectangle below) and 91 mW (irradiance of 1.29×10^7 W/cm^2) for the S trap (red rectangle). Figure 2.10 contains several frames showing two beads each being moved by one of the traps, both of which are controlled entirely by the joystick user interface.

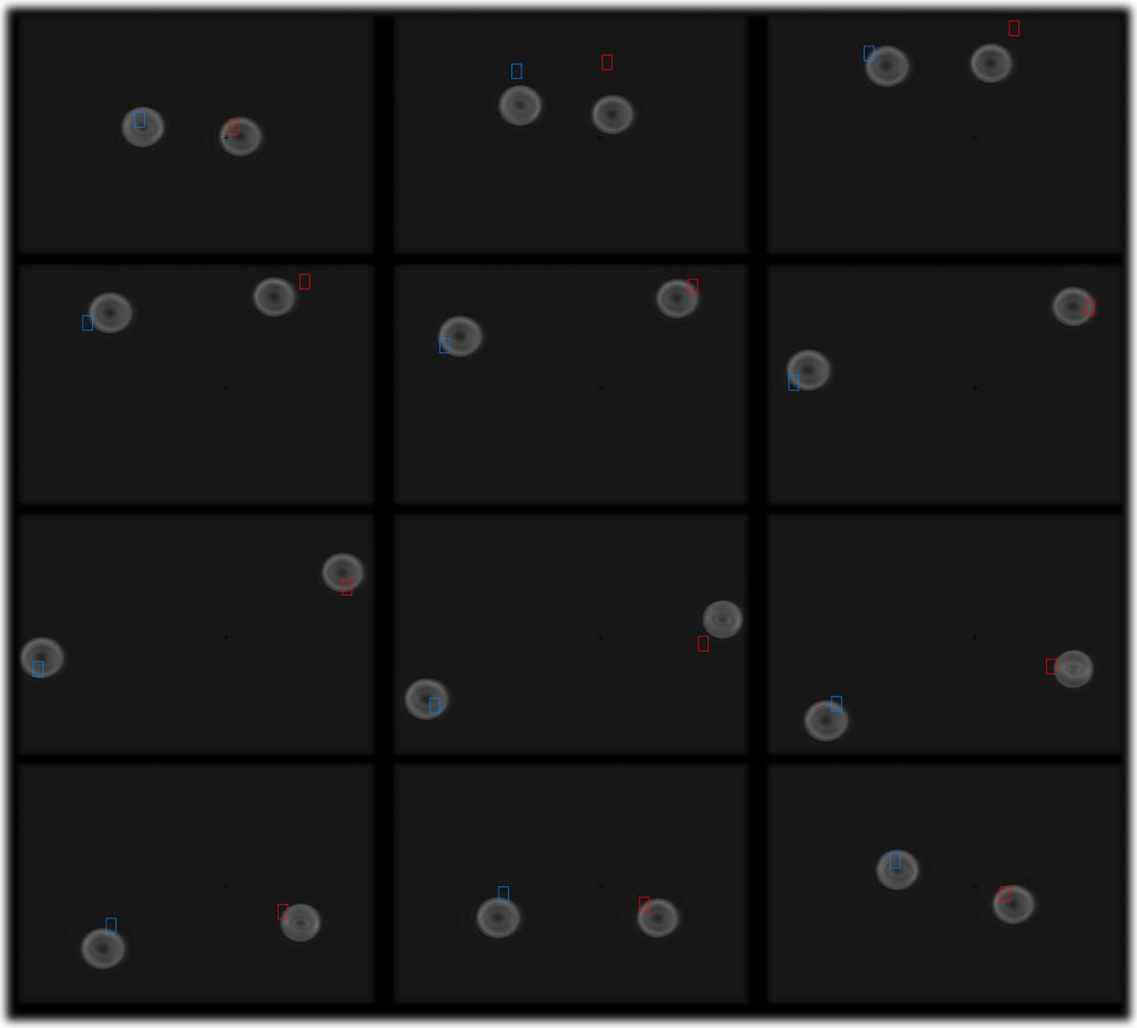

Figure 2.10. Demonstration of joystick trapping using two beads being moved in circular directions. The time between each frame is about 0.12 s.

Since the time between each frame is only about $1/8^{th}$ of a second, the movement of the traps using the joystick is very quick and responsive. However, the red and blue rectangular ROIs indicating the trap position on the main image update faster than do the positions of the fast-steering mirrors, which creates the effect that the ROIs lead the trap. Also worth mentioning is the semicircular motion of each bead, illustrating that using the joysticks to manipulate the traps is much easier, since a circular motion using the point-and-click method is not possible without many calculations and results in a very slow movement.

2.4.2. Demonstration of Joystick Cutting

In order to demonstrate cutting using the joystick, we used a smear of red blood cells, usually used to test cutting prior to experiments. Figure 2.11 shows several frames where "UCSD" was cut into the red blood cells using the titanium: sapphire femtosecond laser at 730 nm. The speed at which it is cut demonstrates the dexterity with which we can control the optical scissors using the joysticks. The laser power before the objective was 64.7 mW (irradiance of 1.94×10^7 W/cm^2).

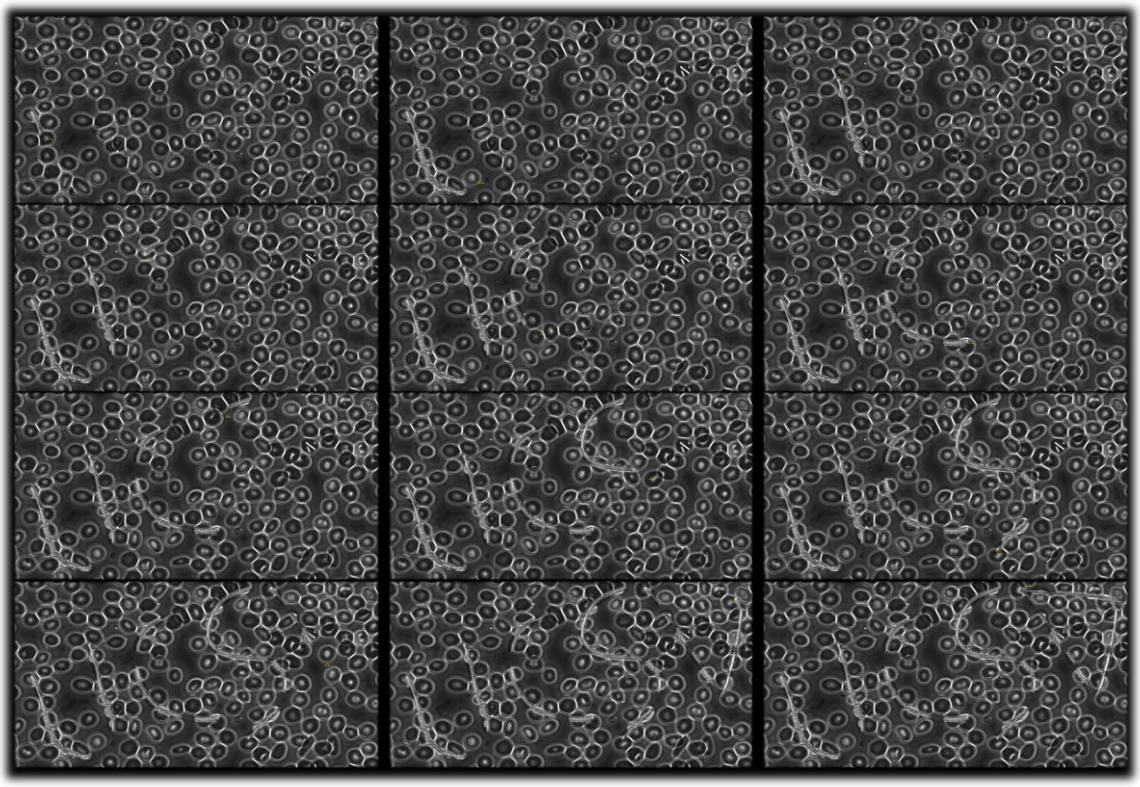

Figure 2.11. Demonstration of joystick cutting using red blood cells. The time between each frame is about 2-3 s.

Again, cutting curves using the point-and-click method would take many calculations in order to determine the points necessary to cut and the cutting itself would take much more time. Similar to trapping, the feedback triangle also "leads" the actual position of the beam. Due to alignment issues, the triangle is also not exactly on top of the beam when cutting near the edges of the field of view.

2.4.3. Combined Demonstration of Joystick Trapping and CutROI

In the last demonstration, joystick trapping and cutting using the Robolase IV LabVIEW program (a function called CutROI) are used simultaneously on red blood cells in suspension. In order to perform optical cutting with CutROI, the user draws a green ROI on the main image and presses the CutROI button on the Robolase IV LabVIEW program front panel (Figure 1.9 and also in Appendix A). Robolase IV then calculates the points that will be cut and moves the scissors fast-steering mirror automatically while opening the laser shutter.

The demonstration is done in a focal plane above the bottom surface of the dish, where red blood cells are still in suspension and in the process of settling down towards the bottom. Thus, the red blood cells are not partially adhered to the dish and can be freely manipulated. In this case, the two traps controlled by the joystick are used to stretch a cell and then cut down the center between the two traps.

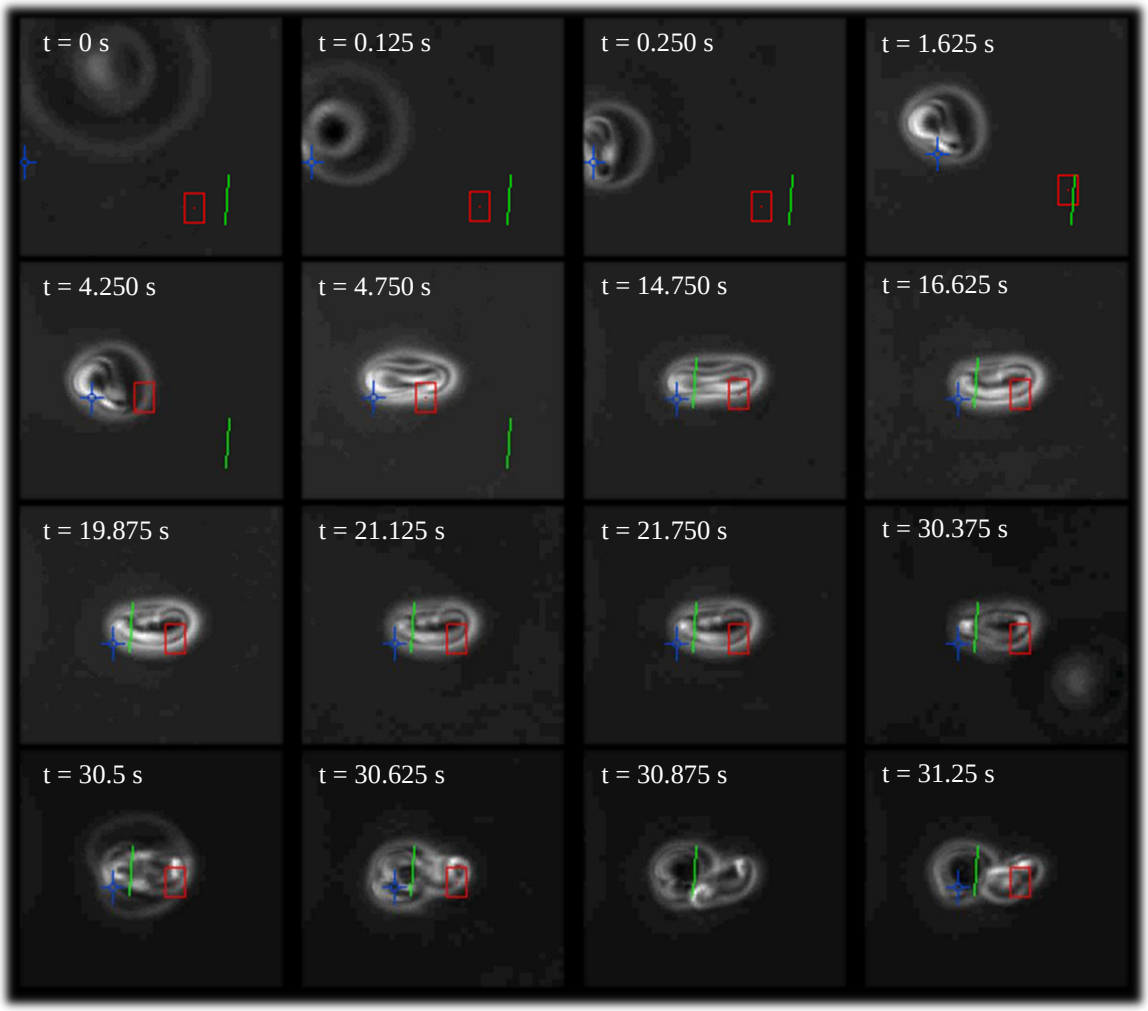

Figure 2.12. Mouse red blood cells stretched using two optical traps and cut using optical scissors above the bottom surface of a dish.

In these images, the power of both traps was approximately 0.81 W (irradiance of 1.15 x 10^7 W/cm^2), while the cutting power was again 13.47 mW (irradiance of 4.05 x 10^6 W/cm^2). In frame 1, the out-of-focus red blood cell in the upper left corner is attracted slowly to the P trap, represented by the blue crosshair. Frame 2 shows the red blood cell pulled in abruptly by the beam, settling into an equilibrium position in frame 3. In frame 4, the trap is moved using the joystick towards the center. In frame 5, the S trap is moved towards the right side of the cell, and its influence is seen in frame 6, where the red blood cell has become stretched. Frame 7 shows the positioning of the line for the CutROI sequence. Frame 8 shows the cell during the cut, while frame 9 shows the cell after the cut. Frame 10 shows the cell during a second cut, and frame 11 shows the results. Another cut was attempted in frame 12, but the trap acts

like a magnet and pulls in another nearby red blood cell in the bottom-right of the image. This second red blood cell also gets caught in the cutting, which is performed through the last four frames.

These images clearly demonstrate how easy it is to perform optical micro-manipulation using optical cutting and joystick trapping together. Since moving the trap positions using the joystick does not depend on the Robolase IV program, the traps can be moved dynamically and quickly to wherever the user desires. Cutting using CutROI can then be performed seamlessly after the tweezers have trapped the object to be cut. CutROI can even be done simultaneously as the traps are moved with the joystick, although this would not make much sense in this demonstration.

References

CH Products. "Industrial Joysticks and Trackballs." *Hand Grip HFX Series III Joysticks*. CH Products. Web. 24 Feb. 2011. <http://www.chproducts.com/oem/hg_series_III.html>.

Omron. "PCB Relay G2R-2 | OMRON Electronic Components Web." *OMRON Global*. Omron, 11 Apr. 2011. Web. 20 Apr. 2011. <http://www.omron.com/ecb/products/pry/121/g2r_2.html>.

III. Experimental Studies

3.1. Introduction and Hypothesis

We hypothesize that it is possible to freely move chromosomes or chromosome fragments in vivo in mitotic cells after interfering with microtubule dynamics. Since it is believed by many people that only microtubules are attached to chromosomes and that their dynamics are solely responsible for creating forces on chromosomes during mitosis, depolymerization of these microtubules due to the effects of nocodazole and laser ablation should free the chromosome from any attachments, making it possible to manipulate these chromosomes (or chromosome fragments cut using optical scissors) using our joystick-controlled optical tweezers. However, if the chromosomes cannot be moved even after treatment with nocodazole, it may be possible that there are other forces acting on chromosomes other than those due to microtubule attachments, possibly the result of the action of other cytoskeletal elements attached to or pushing on the chromosome or physical obstacles in the cytosolic environment. Thus, the experiments conducted will test whether or not it is possible to move chromosomes in vivo.

The cell lines used were PtK2—epithelial cells from the Tasmanian rat kangaroo (*Potorous tridactylus)*—suspended in DMEM containing pen-strep + glutamine, and fetal bovine serum (FBS), and Indian Muntjac (*Muntiacus muntjak*) fibroblasts, suspended in RPMI also containing pen-strep + glutamine, and FBS (Baker et al, 2010). PtK2 cells are well-suited for mitotic studies because they do not round up during mitosis and Indian Muntjac was used because of their large chromosome size and small ploidy (Green et al, 1975).

In the following section, the different types of experiments are outlined. Some of these experiments use certain drugs for different purposes, the chemical structures of which are shown in the figures below.

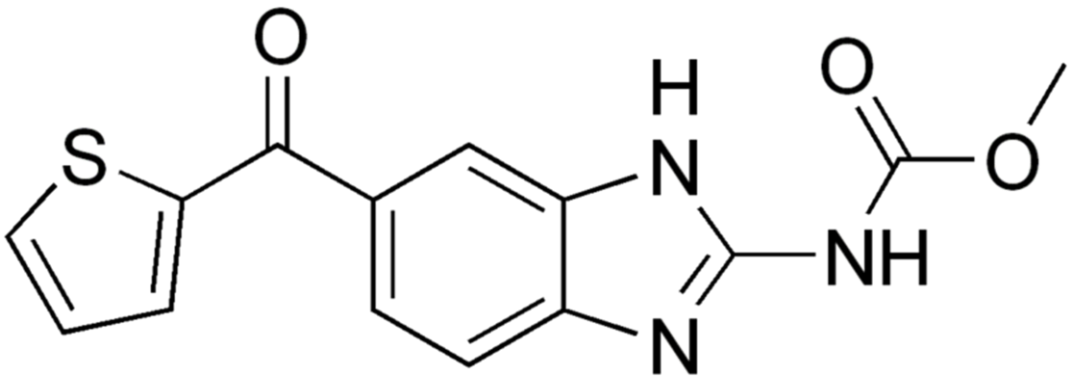

Figure 3.1. Chemical structure of nocodazole.

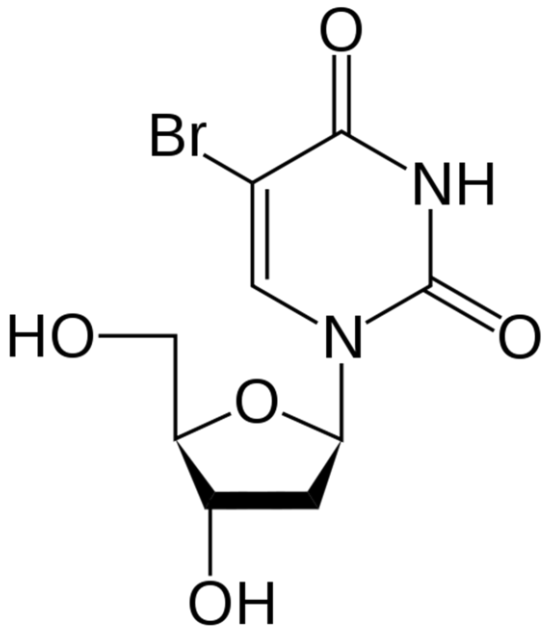

Figure 3.2. Chemical structure of bromodeoxyuridine.

Nocodazole binds microtubule subunits (tubulin) and prevents microtubule polymerization (Alberts, 2008). Upon treatment with nocodazole, the tubulin subunits are bound. Continuing dynamic instability of microtubules ultimately results in their shortening and depolymerization since the microtubules cannot elongate by adding free tubulin subunits because the tubulin subunits are sequestered by nocodazole. Bromodeoxyuridine (BrdU) is a synthetic analog of thymidine that can be incorporated into DNA during replication (Alberts, 2008). For our purposes, it acts as a sensitizer absorbing laser light by

two-photon absorption and thus increasing the damage due to laser ablation. This allows us to ablate with less power and thus decrease the chances of cell death due to excessive laser exposure (Rogakou et al, 1999). The results from these experiments—whether or not it was possible to move chromosomes—will be summarized in section 3.4.

All laser powers are reported with their power before the objective first in W, then with irradiance at the focal spot in parentheses following the power.

3.2. Methods

3.2.1. Indian Muntjac Isolated Chromosomes

The first set of experiments serve as positive controls in order to show that the movement and manipulation of isolated chromosomes using optical tweezers is possible outside of a cell in the absence of any interaction with the cytoplasm. Due to their relatively large size, Indian Muntjac chromosomes were used with the nucleic acid-binding fluorescent dye SYBR Green to distinguish chromosomes in the preparation from other cell matter. By demonstrating that it is possible to trap and cut chromosomes outside the cell, we eliminate the possibility that the optical tweezers or scissors are too weak to manipulate chromosomes when attempted within cells whose microtubules have been depolymerized.

The protocol for isolating chromosomes is as follows. Indian Muntjac cells were grown at 37° C under 5% CO_2 in alpha MEM supplemented with L-glutamine, 10% Fetal Bovine Serum, and Penicillin/Streptomycin. Cells were grown to 70% confluence in a 10 cm cell culture dish, then incubated 16 hours in 500 nM nocadazole (Vasquez et al, 1997). Cells were rinsed twice with PBS and incubated in 0.25% trypsin to lift the cells from the culture dish surface. 10 mL of alpha MEM media was added to the dish to quench the trypsin, and the cells were then pelleted by spinning in a clinical centrifuge for 5 minutes at 1500 rpm. The cell pellet was re-suspended gently in 500 µL of 0.075 M KCl and transferred to a microcentrifuge tube. Cells were pelleted in a table top microcentrifuge at 5000 rpm for 2 minutes and re-suspended again gently in 500 µL of 0.075 M KCl. The cells were heated in a 37° C water bath for 10 minutes to promote cell swelling. Cells were then passed 15 times through a 23 ½ gauge syringe to lyse the cells. Cells were monitored during the lysis procedure via light microscopy

(10 µL on a coverslip). Once the cells were efficiently lysed, protease inhibitors and EDTA were added (final concentration of 2 mM) to inhibit proteases as well as nucleases. To visualize condensed chromosomes, 0.5 µL of SYBR Green (Invitrogen, Carlsbad, CA) was added to the tube containing the ruptured cells.

3.2.2. PtK2 and Indian Muntjac Control

These experiments serve as negative controls, demonstrating that it is not possible to move chromosomes using optical tweezers in a control cell that is not treated with nocodazole. Thus, the microtubules in these cells are intact which should make it impossible to move chromosomes or chromosome fragments with the optical tweezers. More specifically, after cutting chromosomes with optical scissors, moving the cut fragments with joystick trapping should be difficult, if not impossible, because of the stiff/resistant microtubule cytoskeleton.

The power used to cut was generally ~48 mW before objective, which corresponds to an irradiance of 1.44×10^{7} W/cm^2 at the focal spot and 3.74×10^{-4} J of energy also at the focal spot for one 30 ms pulse of the laser. Typically, each laser ablation ranges from 100-200 pulses depending on the length of the line, or approximately 0.03744 – 0.07488 J of energy for each cut. The trapping power ranged from around 0.45 – 1.9 W before the objective (irradiance at the focal spot of 6.36×10^{7} – 2.69×10^{8} W/cm^2 and energy of 7.02 – 29.6 J at the focal spot for every minute the trap is on).

In order to flatten Indian Muntjac cells, the cells were grown overnight on 35 mm glass-bottom dishes in alpha MEM media. The media was aspirated from the dish and 15 µL of 10 mg/mL Fibrinogen in complete alpha MEM media was added to the glass coverslip containing cells. Then, 15 µL of thrombin was gently added and mixed with the pipette tip, after which a clot formed within a few seconds. A minute after the clot formed, 2 mL of alpha MEM media was added back to the dish (Forer et al, 2005).

3.2.3. PtK2 and Indian Muntjac with Nocodazole

As mentioned previously, nocodazole promotes depolymerization of microtubules. Upon treatment with nocodazole, it should be possible to freely move chromosomes or chromosome fragments using optical tweezers. Chromosomes fragments were again produced by severing whole chromosomes using optical scissors. Both the optical scissors and tweezers were used at the same powers as mentioned previously.

Two different concentrations of nocodazole were used: 0.01 µg/mL and 6 µg/mL (Jordan et al, 1999). The following protocol was used to prepare the nocodazole with a concentration of 10 ng/mL in the dish:

1. Dissolve 2 mg of nocodazole in 400 µL of DMSO for a 5 mg/mL solution.
2. Prepare twenty 20 µL aliquots and freeze. One aliquot is used for each experiment.
3. For experiment, put 2 µL of nocodazole melted from one aliquot in 5 mL of DMEM media.
4. Pipette 10 µL of this solution into the dish.

The protocol was used to create 6 µg/mL concentration was as follows:

1. Pipette 2.4 µL from the aliquots from the previous protocol into the dish.

3.2.4. PtK2 GFP-Tubulin Using Laser Ablation with Nocodazole and BrdU

Upon the discovery that it was still not possible to freely move chromosomes or chromosome fragments from experiments performed with nocodazole-treated mitotic cells (see raw images presented in the next section), it was hypothesized that there may be residual microtubule attachments that restricted free movement of the chromosomes or even that there may be forces other than those due to microtubules acting on the chromosomes/fragments. These other forces could be due to other cytoskeletal elements (non-microtubule) attached to the chromosome.

It is possible to physically destroy these remaining attachments using laser ablation (Baker et al, 2010). Therefore, laser scissors will be used to cut rectangular regions of interest (“box cut” ROIs) surrounding chromosome fragments in order to destroy any remaining cytoskeletal elements that may still be attached to the chromosome fragments. If it is then possible to move the fragments using optical

tweezers, these experiments may serve as evidence that depolymerizing microtubules using nocodazole is not enough to free the chromosomes and that there may be other cytoskeletal elements that exert forces on them.

These experiments utilized a PtK2 cell line (PtK2 P133) that expresses fluorescent GFP-tubulin. This allows us to visualize microtubules before and after the "box cut" ROI. Thus, the microtubules in these cells would emit green fluorescent light, which would show the state of the microtubules and the damage caused by laser ablation as well as the effects of nocodazole.

These box cuts, however, would result in more laser exposure, which would increase the chances and rate of cell necrosis. In order to perform more cuts on chromosomes but minimize damage to the entire cell, Bromodeoxyuridine (BrdU) was used as a sensitizer. Two µL of BrdU stock at 10 mmol/L was added to the dish for a concentration of 10 µM, 24 – 48 hours before the experiment (Rogakou et al, 1999). With BrdU, the chromosomes would absorb more energy from each ablation, making it possible to cut chromosomes with less laser power. The threshold laser power for cutting chromosomes due to the addition BrdU decreased by about 10 mW, so the threshold was roughly 38 mW before the objective (irradiance of 1.14×10^{7} W/cm^2 at the focal spot and energy of 2.96×10^{-4} J for each 30 ms pulse). Trapping power remained the same as with the controls.

3.2.5. New System Design and Stronger Trap

Experiments were also performed after redesign of the optical setup. The new optical design used a custom laser entry port that allowed the laser to enter the microscope just before it reaches the back aperture of the objective. Thus, the laser is not reflected through the internal mirrors within the microscope itself, which accounts for a significant loss in power. This custom laser entry port is situated above the reflector turret of the microscope and directly reflects incoming laser light into the objective, as shown in the figure below.

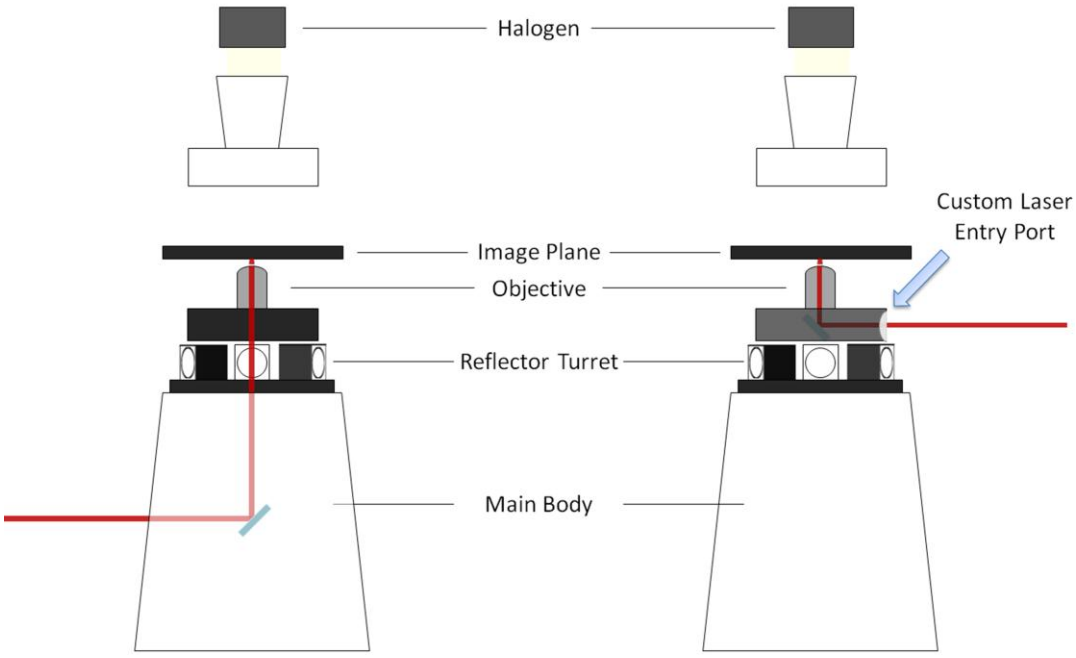

Figure 3.3. Diagram of custom laser entry port showing entry of laser into microscope before (left) and after (right) system redesign.

The mirror within the custom laser entry port has approximately 90% transmission over 380-675 nm and reflects 95% for 730 nm and 1064 nm. Thus, light from the sample and from the arc lamp for fluorescence is transmitted while both the trapping and cutting lasers are reflected. With this custom laser entry port, the maximum trapping power was increased from approximately 1.9 W to 5 W before the objective (irradiance of 7.07×10^8 W/cm^2 at the focal spot). This higher trapping power was used in subsequent experiments in an attempt to move chromosomes both in control cells and in cells treated with nocodazole.

An actual image of this custom laser entry port is shown below.

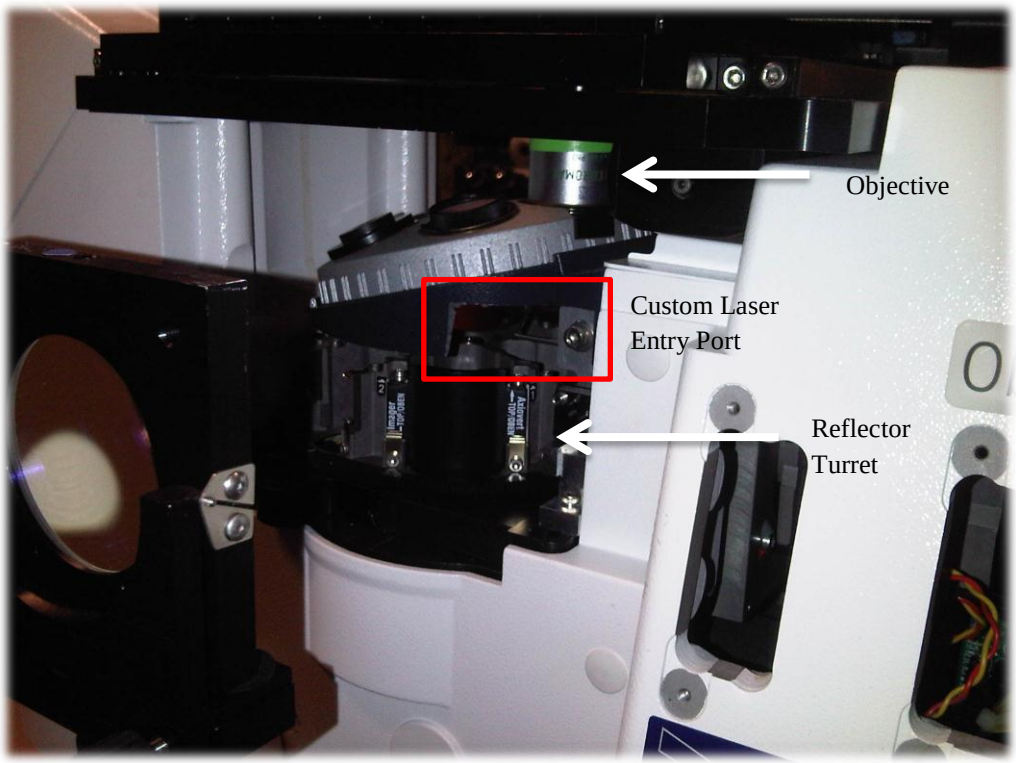

Figure 3.4. Actual photograph of custom laser entry port.

3.2.6. Expected Data and Statistics (Fisher Exact Test)

The data obtained from experiments consists of nominal data representing whether or not chromosome movement was possible in cells. That is, for each different test performed in the subsections of section 3.2 above, both the number of cells in which chromosome movement was possible and the number of cells in which chromosome movement was not possible were counted.

Whether there was a significant difference between different groups was then determined using Fisher exact tests. For example, to determine whether there was a significant difference between the control group and the nocodazole-treated group, a Fisher exact test was used to calculate the *P* value using a 2 x 2 contingency table for this data. If this *P* value was less than 0.05, then it was determined that there was a significant difference between the groups. This would confirm the hypothesis that chromosome movement using optical tweezers is possible due to the effects of nocodazole and laser ablation and the fact that there were no other forces than those due to microtubules acting on

chromosomes. If the *P* value is greater than 0.05, however, then there is no significant difference when interfering with microtubule dynamics. In our case, this would mean that movement was not possible in both groups, which could mean that either the drug did not work and/or there are forces other than those due to microtubules that prevented chromosome movement.

Fisher exact tests were used due to the small sample size of the data collected. A detailed explanation of how the *P* values were calculated using the Fisher exact test can be found in Appendix E, along with the contingency tables used to calculate these *P* values based on data from the actual experiments.

3.3. Imaging Data and Results

Several sets of images are shown in this section exemplifying cases both where it was possible and not possible to freely move chromosome fragments. Additional raw images are shown in Appendix D.

The first set of images shows an isolated Indian Muntjac chromosome using phase contrast and fluorescence microscopy (Figure 3.5). The bright SYBR Green fluorescence signal confirms that this is in fact an isolated chromosome.

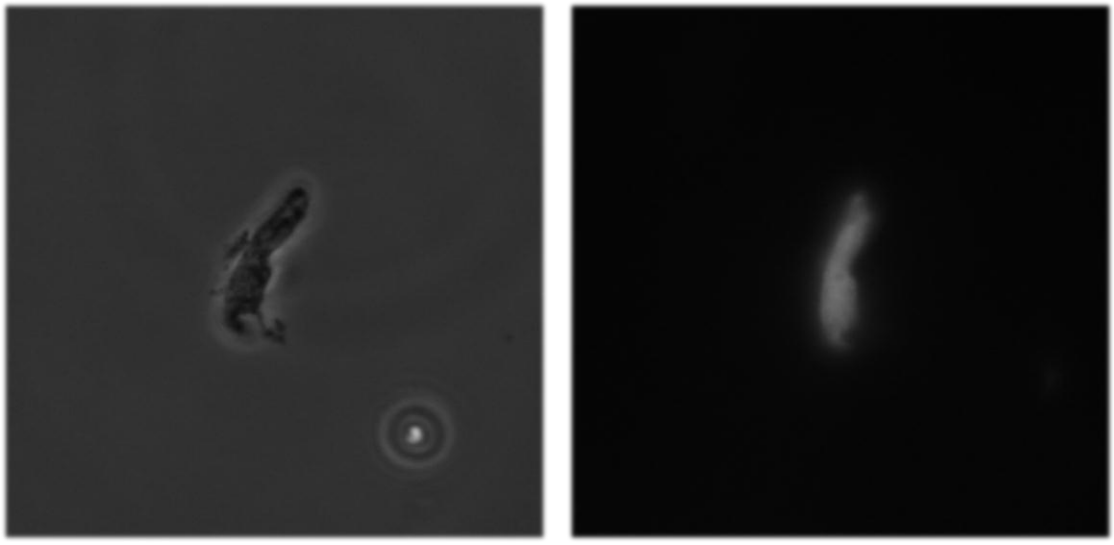

Figure 3.5. Isolated Indian Muntjac chromosome in phase contrast (left) and fluorescence (right). The SYBR Green signal confirms that this is a chromosome.

The successful movement of this isolated chromosome using optical tweezers is shown in Figure 3.6.

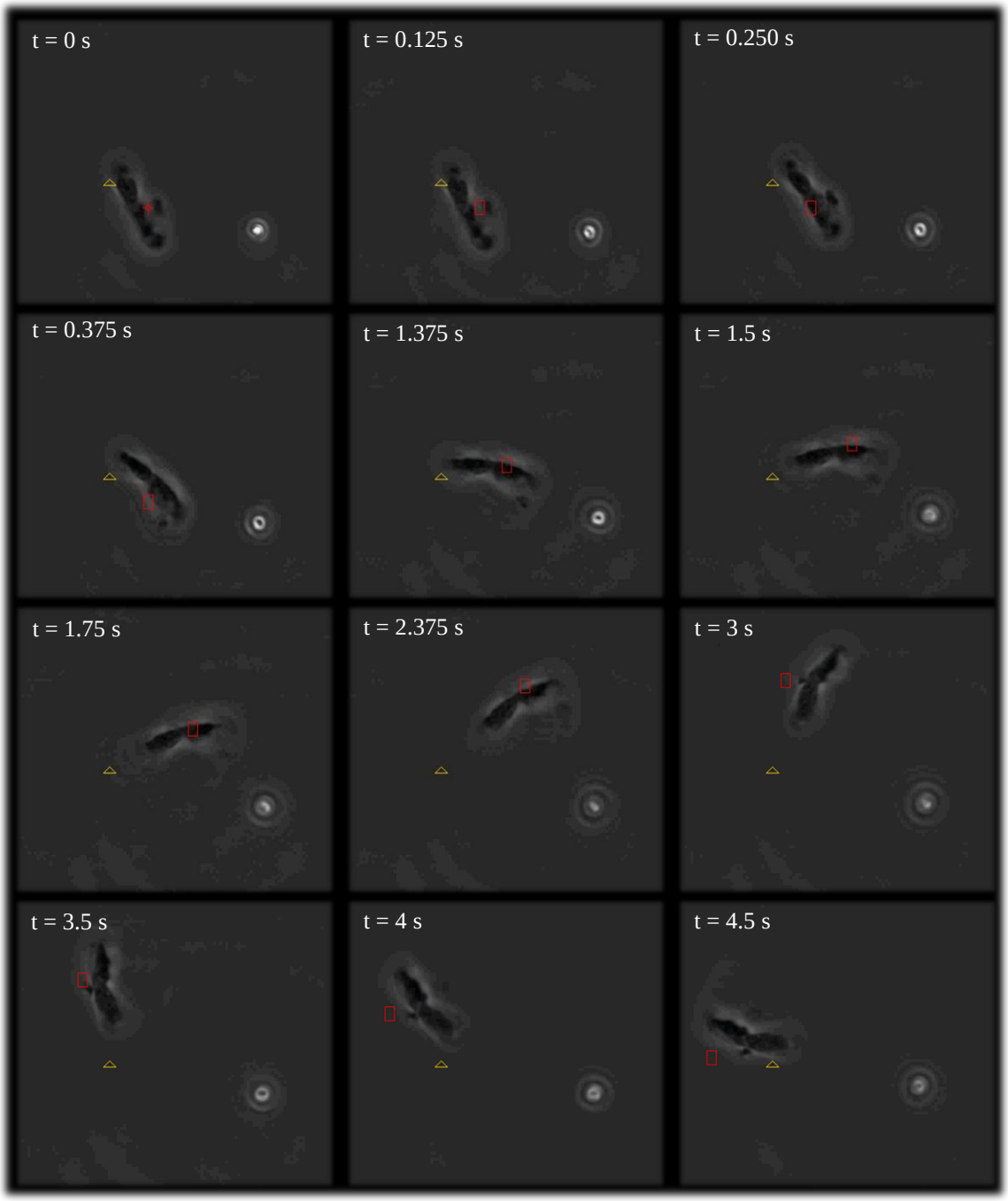

Figure 3.6. Time series of isolated Indian Muntjac chromosome being trapped and moved using the optical tweezers. The red crosshairs represents a closed trap, while the red rectangle represents the trap when it is on.

The trap power used during the experiment above was 0.2032 W (irradiance of 2.87 x 10^7 W/cm^2 at the focal spot). Referring to the images in the direction from the top left to the bottom right, frames 1-4 show what happens when the trap shutter is opened. The trap is closed in frame 1, where it is represented by a red crosshair. The trap is opened in frame 2, now represented by a small red rectangle. In frames 2-4, the isolated chromosome reacts to the forces created from the optical tweezers, and is caught stably in the trap by frame 4 (the trap is not being moved in these frames). From frame 5 and on, the trap is being moved in a counter-clockwise direction, and the chromosome clearly follows the movement of the red rectangle representing the trap. Thus, this experiment demonstrates that it is possible to trap and move isolated chromosomes using our optical tweezers outside of a cell using only 0.2032 W before the objective.

Despite the above result showing that chromosomes can be freely moved with a trap when isolated for the cell, it is not possible to move them with the laser power used when inside the cell. In Figure 3.7, it is not possible to move a chromosome in the PtK2 control cell, as expected.

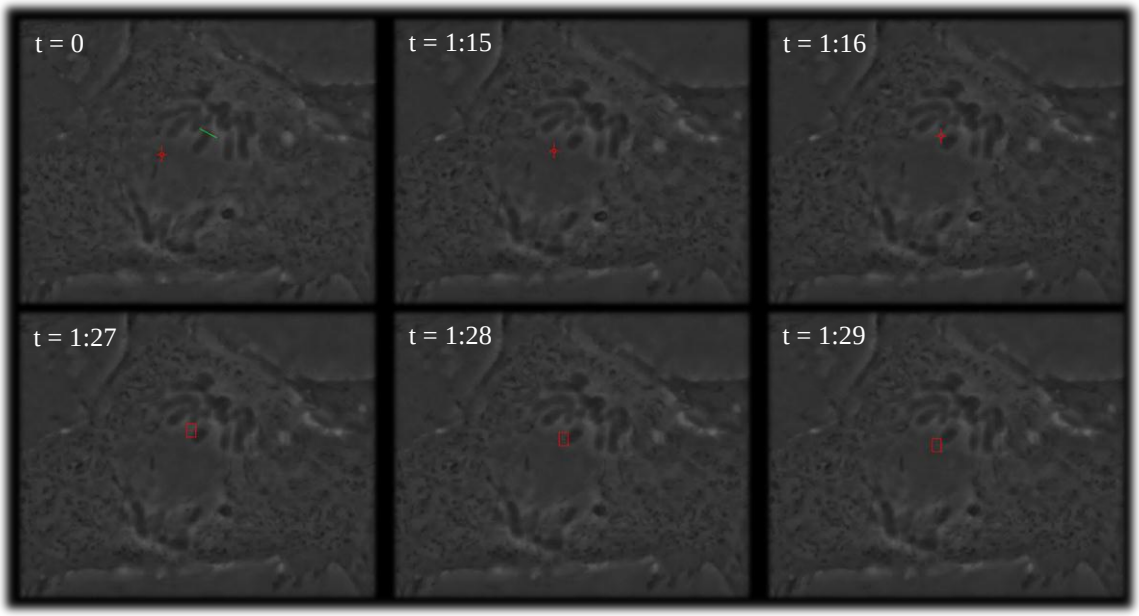

Figure 3.7. Unsuccessful attempt at moving chromosomes in a PtK2 control cell. The green line represents where the chromosome was cut, while the red rectangle and crosshair represent the optical tweezers.

In frame 1, five successive passes of the laser are performed over the green line at a cutting power of 18.4 mW. The trapping power was 0.512 W (irradiance of 7.24 x 10^7 W/cm^2 at the focal spot). After the laser scissors exposure in frame 1, frame 2 shows the post-cut image and the appearance of what looks like a clean severing of the chromosome. The trap position is then moved on top of this fragment in frame 3, and turned on in frame 4. However, in frames 5 and 6 it appears that the trap cannot move the chromosome fragment even though it has been severed. In fact, the trap does not seem to exert any influence on the chromosome fragment at all.

Surprisingly, however, when PtK2 cells were treated with nocodazole, it was also impossible to freely move chromosomes or chromosome fragments, as shown in Figure 3.8 below.

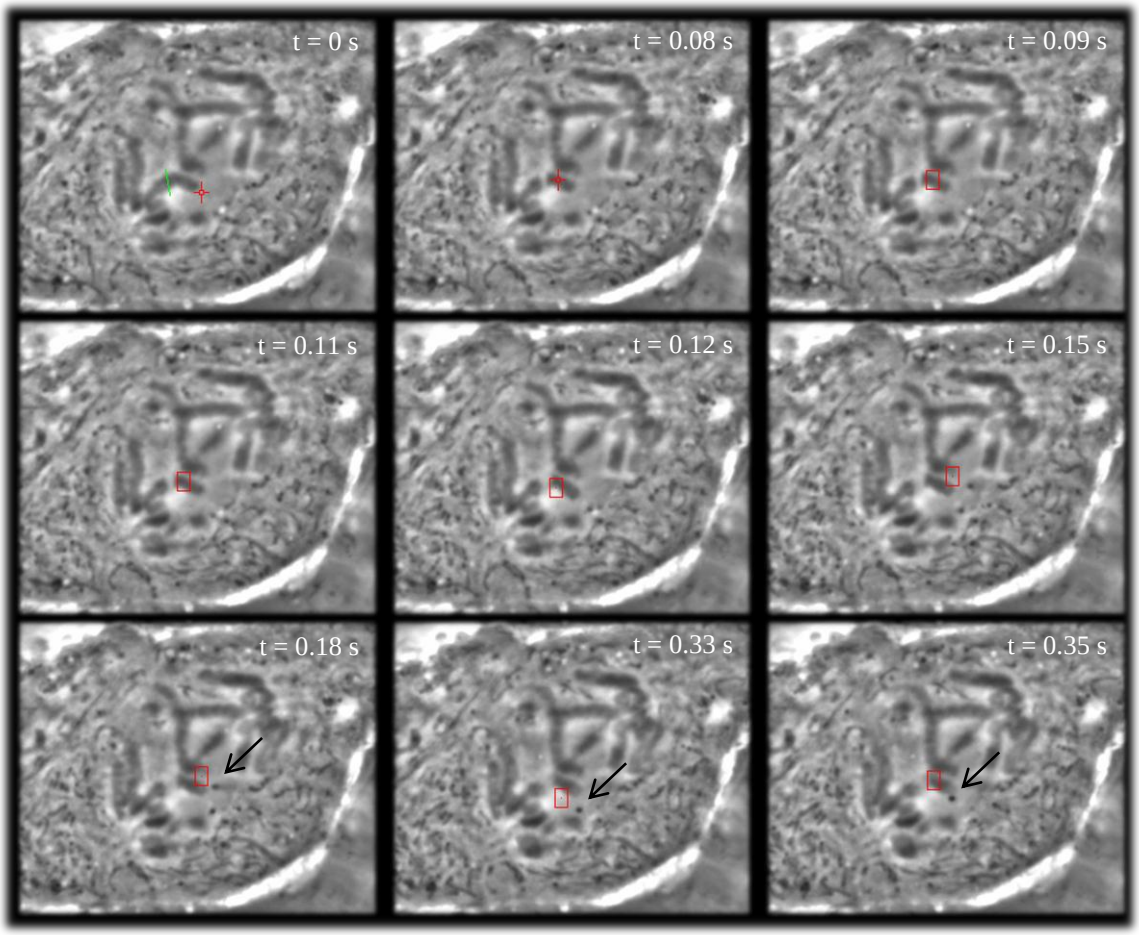

Figure 3.8. Unsuccessful attempt at moving chromosomes in a PtK2 cell treated with nocodazole. The green line represents where the chromosome was cut, while the red rectangle and crosshair represent the optical tweezers.

The cutting power during this experiment was also 18.4 mW (irradiance of 5.53 x 10^6 W/cm^2 at the focal spot), and only one cut was used in frame 1. The damaged caused by the cut is shown in frame 2, where a white line where the green line used to be separates the new fragment from the rest of the chromosome. The trap is turned on in frame 3 with a power of 0.512 W (irradiance of 7.24 x 10^7 W/cm^2 at the focal spot). Although difficult to see in these images, the trap does seem to exert some influence through frames 4-6. However, the trap is not able to freely move the chromosome, even though microtubules have been depolymerized by the effects of nocodazole. Frame 7 actually shows the trap visibly pulling on a small black object, indicated by the arrow, which shows that the trap itself is working and creating forces, but unable to freely manipulate the chromosome fragment. Frames 8 and 9 also show another small object being influenced (arrows) and moved upwards by the forces created at the edge of the trap.

When using the redesigned system with the laser entering the objective directly, the optical tweezers were capable of reaching a power of 4.2 W (irradiance of 5.94 x 10^8 W/cm^2 at the focal spot), roughly eight times what was available in previous experiments. The result was that manipulation of chromosomes using optical tweezers at this power was possible even in a PtK2 control cell that was not treated with a nocodazole. Figure 3.9 below shows a series of images that illustrates this remarkable capability.

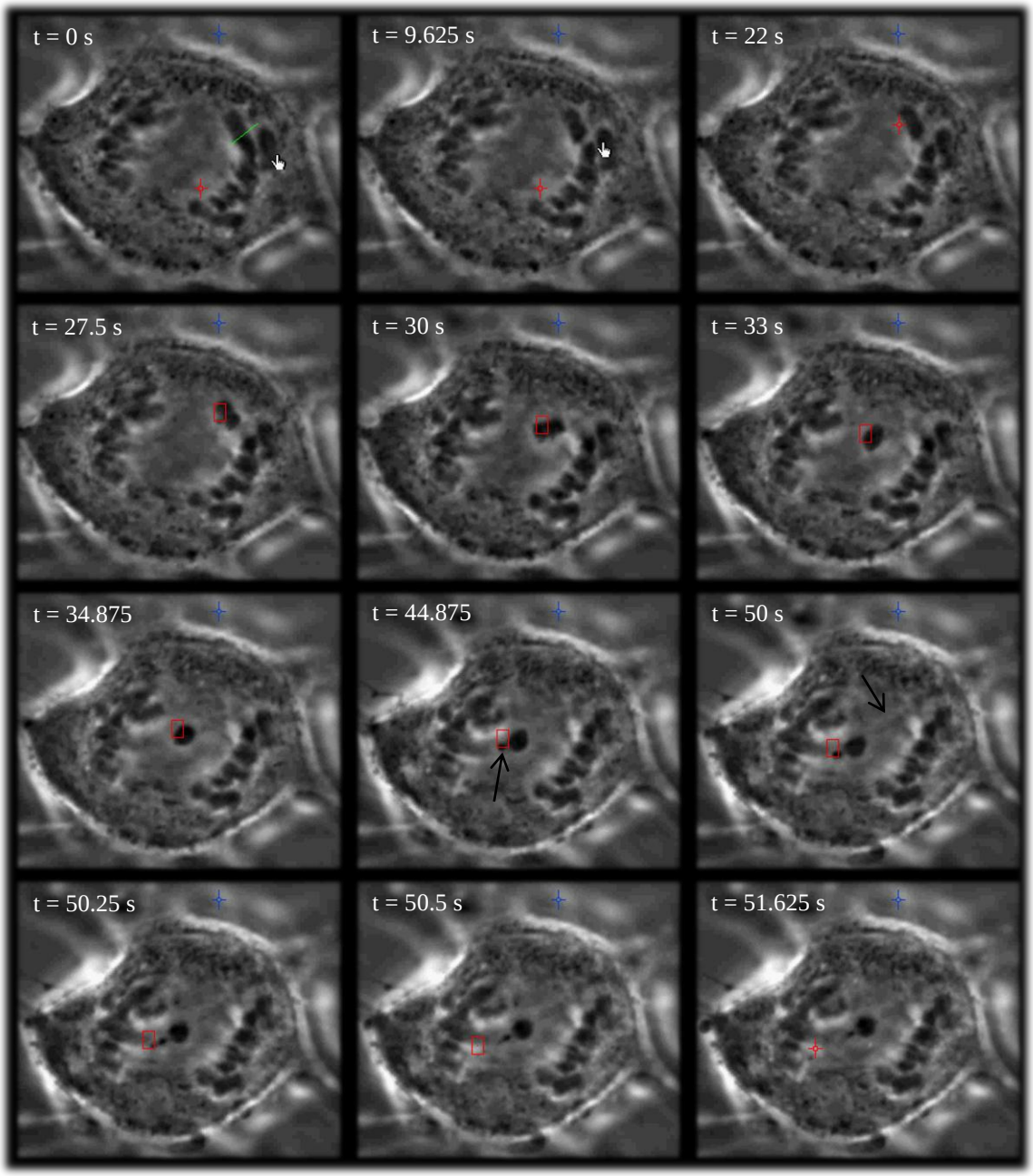

Figure 3.9. Successful manipulation of chromosomes in a PtK2 cell without treatment with nocodazole, using a very strong trap. The green line represents where the chromosome was cut, while the red rectangle and crosshair represent the optical tweezers.

At a power of 26 mW (irradiance of 7.81 x 10^6 W/cm^2 at the focal spot), the chromosome was cut using the laser scissors in frame 1, and the damage caused is shown in frame 2. The trap is moved towards the new fragment in frame 3, and then turned on in frame 4. From frames 5-7, the fragment is slowly moved towards the center of the cell. During frame 8, we attempt to move the fragment further, but

there seems to be an opposing force which pulls the fragment back to its original position. Because the fragment is being pulled back by another force while the trap is pulling the fragment forward, the strength of the trap actually tears part of the chromosome, indicated by a new small black object that appears in frame 8 but not in frame 7 previously (indicated by the arrow in frame 8, partially blocked by the red rectangle). In frame 9, we can see that there is a small strand of partially de-condensed chromosome material still attaching the fragment from the rest of the original chromosome (arrow). As the trap attempts to pull the fragment further (frame 9) it appears to resist additional movement, and in frame 10 the fragment actually bounces or is pulled back towards its original position (see frames 10-12). This result might be due to the "re-coiling" of the chromatin in the highly condensed mitotic chromosome.

Unfortunately, this cell started to die during the experiment, likely a result of the high laser trapping power which caused excessive heating ultimately causing the cell to die.

3.4. Summary of Results

The results from the experiments with PtK2 and Indian Muntjac cells are summarized in Table 3.1 below, which shows (1) the number of cells in which free movement of chromosomes using optical tweezers was possible (Movement), (2) not possible (No Movement), or (3) if the optical tweezers exerted a clear influence (e.g. bending, nudging, or slightly pulling) but free movement was not fully possible (Influence). The rows correspond with the different types of experiments outlined in sections 3.2.1 – 3.2.5.

Table 3.1. Summary of Results.

Type of Experiment	Movement	No Movement	Influence
Isolated Chromosomes	2	0	0
Control	0	16	2
Nocodazole	1	29	6
Box Cuts with Nocodazole	0	23	6
Stronger Trap	5	0	0

P values were determined for Fisher exact tests between the control group and the nocodazole group (P_{noc}), between the control group and the box cut group (P_{box}), and between the control group and the stronger trap group (P_{trap}). The contingency tables used for these calculations can be found in Appendix E. P_{noc} was determined to be 0.77, while P_{box} was 1 and P_{trap} was 0.0005.

Since the first two values are above 0.05, we can conclude for the nocodazole and box cuts that there was no significant difference and thus that it was not possible to move chromosomes in any of the groups. Just from looking at the table, it is clear that free movement of the chromosomes in vivo was not possible when using nocodazole or box cuts. However, the table shows that moving isolated chromosomes outside the cell was possible. Thus, the inability to freely move chromosomes in vivo suggests that either our methods are not working as theoretically expected, or that there are possibly forces other than those due to microtubules acting on chromosomes or obstacles blocking chromosomes, preventing their subsequent movement using optical tweezers.

However, it was possible to move chromosomes using the stronger trap. The *P* value calculated for this group in comparison with the control was 0.0005, indicating that there is a significant difference between these two groups. Thus, using the stronger trap does in fact make it possible to move chromosomes in vivo, even without the use of nocodazole. This does not, however, disprove the theory that there may be other forces other than those due to microtubules that act on chromosomes. It may simply suggest that the higher trapping forces possible after the optical redesign were sufficient to overcome all the resistant forces whether from microtubules or from other parts of the cell.

References

Alberts, Bruce. *Molecular Biology of the Cell*. 5th ed. New York: Garland Science, 2008. 988-89. Print.

Baker, Norman M., Samantha G. Zeitlin, Linda Z. Shi, Jagesh Shah, and Michael W. Berns. "Chromosome Tips Damaged in Anaphase Inhibit Cytokinesis." *PLoS ONE* 5(8): e12398 (2010). doi: 10.1371/journal.pone.0012398. Web.

Derry, W. Brent, Leslie Wilson, and Mary Ann Jordan. "Substoichiometric Binding of Taxol Suppresses Microtubule Dynamics." *Biochemistry* 34.7 (1995): 2203-211. Print.

Forer, A., and J. Pickettheaps. "Fibrin Clots Keep Non-adhering Living Cells in Place on Glass for Perfusion or Fixation." Cell Biology International 29.9 (2005): 721-30. Print.

Green, Richard J., and Gunter F. Bahr. "Comparison of G-, Q-, and EM-banding Patterns Exhibited by the Chromosome Complement of the Indian Muntjac, Muntiacus Muntjak, with Reference to Nuclear DNA Content and Chromatin Ultrastructure." *Chromosoma* 50.1 (1975): 53-67. Print.

Jordan, Mary Ann, and Leslie Wilson. "The Use and Action of Drugs in Analyzing Mitosis."*Methods in Cell Biology*. Ed. H. William. Detrich, Leonard I. Zon, and Monte Westerfield. San Diego, CA: Academic, 1999. 267-95. Print.

Jordan, Mary Ann, Douglas Thrower, and Leslie Wilson. "Effects of Vinblastine, Podophyllotoxin and Nocodazole on Mitotic Spindles Implications for the Role of Microtubule Dynamics in Mitosis." *Journal of Cell Science* 102 (1992): 401-16. Print.

Jordan, M. A., Robert J. Toso, Doug Thrower, and Leslie Wilson. "Mechanism of Mitotic Block and Inhibition of Cell Proliferation by Taxol at Low Concentrations." *Proceedings of the National Academy of Sciences* 90.20 (1993): 9552-556. Print.

Lee, James C., Deborah J. Field, and Lucy L. Y. Lee. "Effects of Nocodazole on Structures of Calf Brain Tubulin." *Biochemistry* 19.26 (1980): 6209-215. Print.

Rogakou, Emmy P., Chye Boon, Christophe Redon, and William M. Bonner. "Megabase Chromatin Domains Involved in DNA Double-Strand Breaks in Vivo." *Journal of Cell Biology* 146.5 (1999): 905-16. Print

Vasquez, Robert J., Bonnie Howell, Anne-Marie C. Yvon, Patricia Wadsworth, and Lynne Cassimeris. "Nanomolar Concentrations of Nocodazole Alter Microtubule Dynamic Instability In Vivo and In Vitro." Molecular Biology of the Cell 8.6 (1997): 973-85. Print.

IV. Discussion

4.1. Discussion: Development of the Joystick User Interface

With the development of the final control scheme, the Onboard/Simultaneous control scheme, the joystick user interface has become a more-than-sufficient solution to the original engineering design problem. The flexible, responsive, and easy-to-use joystick user interface serves as an alternative to the cumbersome point-and-click interface when manual dexterity is necessary to manipulate microscopic objects. The point-and-click method also remains functional, however, as there are also times when robotic precision is necessary, especially when using the optical scissors, where laser dosage is extremely important.

The joystick user interface can also be evaluated against the design goals used to select the best solution in Chapter 2: ease-of-use, performance, customizability, cost, and ease-of-design. The joystick user interface is definitely easy to use with the Onboard/Simultaneous control scheme, since this control scheme allows the joysticks to control the movement of the traps rather than position, a control method with which even new users would be familiar. The system also remains very customizable, since all the connections made were through a solderless breadboard instead of a more permanent solution. Thus, modifying the system (e.g. developing a fifth control scheme) would only require rewiring of this breadboard and the development of new LabVIEW programs. With respect to the speed of the system and the response of the traps and scissors upon movement of the joysticks, the joystick user interface performs very well, with the help of a separately running program independent of Robolase IV to provide the control system that relates joystick movement to trap movement.

However, the problem formulation stated in the beginning of Chapter 2 has not technically been fulfilled: to develop a responsive, intuitive, and user-friendly method to simultaneously control two optical traps and one optical scissors. Thus, the joystick user interface developed does not perform as well as it should, since the system can simultaneously control only two of the three optical tools. This problem will be discussed in the Future Directions section.

Although the design goals of cost and ease-of-design were not fulfilled, these design goals were less important, so it was not necessary to redevelop of a new solution or new control scheme

because of this. Cost was not fulfilled because, although the joysticks themselves were relatively inexpensive, about $400 each, the other hardware—such as the NI DAQ board and the NI Motion Controller and the LabVIEW development suite itself, all of which are necessary for the joystick user interface—is very expensive relative to the joystick, costing several thousand dollars when considered together. Also, the final control scheme, such as how the hardware is configured and the programs required to run the joystick user interface, is quite complicated with respect to its design.

Despite these less important issues however, the joystick user interface is a major improvement over the point-and-click user interface with respect to its potential for optical micro-manipulation. Even though the joysticks themselves are not able to control all three optical tools at once, the entire Robolase IV system with the joystick user interface is now capable of this, using the point-and-click interface for the scissors (CutROI) and the joystick user interface to control the two sets of tweezers. Since cutting needs to be precise such that laser dosage can be easily monitored, using the system in joystick trapping mode and using the point-and-click interface for cutting is suitable for most experiments.

Thus, the Robolase IV system provides the ideal combination of responsiveness and real-time control of the optical tools without sacrificing the capability for precision control of these same optical tools using the point-and-click interface. The ability to simultaneously use these two very different but equally useful user interfaces makes this system even more unique. Indeed, with the addition of the joystick user interface, the Robolase IV system becomes the perfect tool for optical micro-manipulation, allowing users to employ microscopic hands and scissors to interact firsthand with a constantly-changing microscopic world which requires that control of these tools is both fast and dynamic as well as precise.

4.2. Discussion: Experimental Studies

The experimental studies, however, have yielded mixed results. Although it was possible to move isolated chromosomes, initially it was not possible to move chromosomes in vivo even after treating the cells with nocodazole to break down the microtubule cytoskeleton/mitotic spindle or using

laser ablation. However, using the stronger trap which was made possible after a system redesign, it was possible to move chromosomes even in control cells not treated with nocodazole.

The fact that it was possible to move isolated chromosomes in a suspension medium removed from the cell demonstrates that the optical tweezers do indeed create sufficiently strong forces outside of the cell to move chromosomes. However, based on previous preliminary experiments of others, it was expected that the optical tweezers should not be able to move chromosomes inside cells (controls), where microtubules are firmly attached to chromosomes, thus preventing them from being easily moved.

Surprisingly, upon depolymerizing microtubules using nocodazole or laser ablation, it was still impossible to move chromosomes. There could be several reasons for the inability to move the chromosomes freely. One reason may be that the methods we used to destroy the attached microtubules—treatment with drugs and laser ablation—were not sufficient to break down all the microtubules or did not produce the desired effects. Although it is known that nocodazole prevents microtubule polymerization, it is difficult to determine at what concentration the microtubules have depolymerized sufficiently such that the chromosomes are no longer bound to them. Thus, even though the cells are treated with nocodazole at concentrations in accordance with published values, chromosomes may still have residual attachments to microtubules that may not be strong enough to produce the dynamic reorganizing forces that occur during normal mitosis, but still sufficiently strong to prevent free movement when optical tweezers are applied with the amount of force used in the initial studies (i.e. before the system design when it was possible to move chromosomes even without nocodazole treatment) .

The potential problem with using the optical scissors to perform box cuts around the chromosome to destroy these attachments is related to the noninvasive nature of the damage created. The laser ablations may fail to destroy all the remaining attachments because the damage from the laser ablation occurs only at the focal plane. Thus, microtubules or other cytoskeletal elements attached to the chromosome above or below the focal plane would remain attached. In addition, the cells can only sustain so much laser irradiation, which makes more frequent laser ablation (to perform box cuts for

example) difficult to perform without fatally harming the cell, either by heating, creating plasmas, or damage by other mechanisms.

This noninvasiveness presents another problem during the cutting of the chromosomes themselves. Although it is clear in one focal plane that a chromosome has been cut and appears to be severed, it may be true that above and below the focal plane the chromosome fragment remains attached to the rest of the chromosome, which may be another reason why it was impossible to move the chromosome freely even after what appeared to be a clean cut in one focal plane. The experiment shown in Figure 3.9 illustrates this problem. Despite the fact that we were able to move the chromosome fragment, it seemed to resist being pulled by the trap and actually recoiled once it was released from the trap. From the images it is clear that a small strand of material, likely de-condensed chromatin or DNA, is what causes the fragment to resist pulling by the trap and to subsequently recoil. Thus, even though it seemed as if a clean cut was made using laser scissors, residual attachments between the fragment and its chromosome remained.

The strength and interaction of the trapping laser in the cell may also be a factor to consider. The optical tweezers have been shown to work outside of cell (e.g. with beads on a dish or isolated chromosomes), but trying to trap objects within a cell may produce different, unknown, interactions that might contribute to a weaker trapping force within the cell. Although PtK2 cells are relatively flat, they do still have some depth and the incident laser light passing through the cell and its various organelles may weaken the trapping force at the image plane. Even though from certain experiments very small objects such as particles or bacteria within the cell are easily trapped, the trapping force may not be sufficient to counter whatever forces or obstacles are preventing the manipulation of chromosomes using the tweezers. With respect to laser light, however, the contents of most cells under normal illumination can be treated as transparent material, and should only very slightly weaken the trapping strength, possibly by slight scattering forces.

Thus, if in fact the treatment with nocodazole and laser ablation and trapping were both successful and were able to realize their theoretical capabilities—that is, if nocodazole really did depolymerize all of microtubules, the laser ablation removed all cytoskeletal attachments to

chromosomes, and the optical tweezers created a sufficiently strong force—then it may be possible that there are other "forces" acting on the chromosomes during mitosis which are currently unknown. It is questionable whether these unknown forces are cytoskeletal in origin, since theoretically the laser ablation should eliminate any of these attachments.

If these unknown forces are cytoskeletal, it is possible that these cytoskeletal elements are not attached directly to chromosomes as microtubules are but may exert forces on them indirectly. Mori et al have proposed evidence for an F-actin meshwork that seems to support this claim (Mori et al, 2011). Their experiments indicated that it is not probable that transport of chromosomes during mitosis by this actin meshwork relies on physical attachments of actin onto chromosomes, as microtubules are attached specifically to kinetochores or along chromosome arms. Instead, movement of chromosomes by this actin meshwork is due to steric trapping, i.e. chromosomes are large enough to get caught in what may be an actin net, and the movement of this net due to dynamic instability of actin filaments exerts forces on chromosomes. Thus, the actin meshwork acts indirectly as an obstacle preventing movement of chromosomes using optical tweezers. Using laser scissors to perform box cuts may destroy part of this actin meshwork that are close to the chromosome, but outside of this nearby region the remaining, intact actin meshwork would prevent free chromosome movement using optical tweezers.

It may also be possible that this unknown force preventing chromosome movement may be due to the viscosity of the cytosol in the vicinity of the chromosomes. It has been proposed by Johansen et al that there exists an elastic, hydrogel-like spindle matrix consisting of nuclear-derived proteins and whose viscous properties may differ from that of the cytosol (Johansen, 2011). Thus, while it may be expected that movement of chromosomes should theoretically be possible in the cytosol which has a viscosity similar to water, the same phenomena may not be possible in this much more viscous, hydrogel-like spindle matrix where forces due to the viscosity of the surrounding medium counter trapping forces (Parsa, 2010). In addition, there may be other proteins in this spindle matrix that exert forces on chromosomes. (However, experiments presented in this thesis with the higher laser trapping forces would indicate that the laser trap is able to overcome resistance due to viscosity, as discussed later.)

Another possibility may be that the other chromosomes themselves within the cell act as obstacles to movement of a certain chromosome or chromosome fragment. Since some of the cells that were tested were in prophase, the chromosomes have not yet had a chance to reorganize and sometimes appear as a tangled and intertwined mesh of chromosomes. Thus, other chromosomes in this tangled mesh may physically trap this fragment in place, resulting in enough physical constraints and friction that produce sufficient reaction forces to balance trapping forces and prevent movement of the chromosomes using optical tweezers. In addition, in prophase sister chromatids would still be connected by cohesin proteins along chromosome arms (Alberts, 2008). Thus, even when fragments are cut using laser scissors, these fragments may still be attached to their sister chromatid, which would inhibit their movement by an external force such as a laser trap.

In some cases it was also noticeable that pulling on a fragment using the trap seemed to influence nearby chromosomes, as in Figures D.7 in Appendix D, which contains raw experimental images from some of the experiments. Thus, in addition to being tangled in a mesh of chromosomes, there may even be inter-chromosome attachments at this phase of mitosis that result in inter-chromosome forces. LaFountain et al have shown evidence indicating that an elastic tether connects chromatids after their separation during anaphase, and Fabian et al have performed experiments showing evidence that this tether may be composed of titin (LaFountain et al, 2002; Fabian et al, 2007). Thus, these inter-chromosome attachments could also contribute to preventing chromosome movement by optical tweezers.

After the system was redesigned resulting in an eightfold increase in laser trapping power, movement of chromosomes was possible even in cells that were not treated with nocodazole. The fact that chromosome movement was possible without nocodazole suggests that the forces created by the trap were strong enough to overcome even intact microtubules. Thus, if there are any other unknown forces other than those due to microtubules, it is likely that the forces produced by the trap are strong enough to overcome the reaction forces that prevent chromosome movement. The results from this specific experiment do not help to verify whether or not other forces exist, since movement was possible even when microtubules were intact. However, the ability to move chromosomes allows for the

possibility to conduct new experiments that would help to clarify the forces that act on chromosomes during mitosis.

4.3. Conclusion

In conclusion, we have drastically improved the Robolase IV system's user interface with respect to controlling its two optical tweezers and one optical scissors. Using two joysticks to control these optical tools, the user interface has unlocked this system's capabilities for optical micro-manipulation, providing as much responsiveness and dexterity in controlling microscopic objects as our hands provide with macroscopic objects. In trapping mode, each joystick acts as a hand that can "grab" objects when the trap shutters are opened, while in cutting mode, one joystick holds objects while the other cuts them. These capabilities and the flexible, real-time, hands-on feel of the user interface have set a new precedent for how fast, simple, and intuitive it is to manipulate microscopic objects.

With these micro-manipulation capabilities, this system becomes a natural tool for verifying whether or not there are forces other than those due to microtubules acting on chromosomes during mitosis. Initial results before the system redesign suggested that there were in fact other unknown forces, since movement of isolated chromosomes using optical tweezers was possible outside the cell, but not in vivo even when microtubules were depolymerized using nocodazole or destroyed using laser ablation. But using a much stronger trap, chromosome movement using optical tweezers was possible even without the help of nocodazole, which suggests that the forces produced by this stronger trap overcome even the forces due to microtubules. While the ability to move chromosomes using the strong trap does not help to verify what these other forces are or how they originate, it does further the capabilities of the system, upon which new experiments can be designed in order to elucidate any unknown forces. Thus, the inability to move chromosomes after depolymerizing microtubules have raised a new set of questions about other forces acting on chromosomes during mitosis, while the new capability to actually move chromosomes even without drugs have provided a working tool that will help to answer those questions. Hopefully, the conclusions from these experiments will lead to more research about the specific interactions occurring during mitosis, which in turn would lead to important

knowledge about mitosis and possibly new methods for arresting mitosis in cells that multiply and divide uncontrollably.

4.4. Future Directions

4.4.1. Development of the Joystick User Interface

Although the current joystick user interface performs very well, it still is incapable of simultaneously controlling all three optical tools. One solution would be to purchase another joystick and integrate it into the system in a similar fashion as the other two. Thus, there would be three joysticks each dedicated to an optical tool. Although the three may never be used at the same time by one user (although two users can easily use all three), having a third joystick would eliminate the need to switch between two modes, and thus avoid the complex design and connections involving relays. However, the motion controller only has enough analog inputs and outputs for two joysticks (thus four inputs and four outputs, each for one axis of each joystick).

With the development of the Onboard/Simultaneous control scheme, however, the motion controller is not absolutely necessary as it was only introduced into the system in order to use onboard programming to speed up the performance of the joysticks. Since a new solution that does not require an onboard program has been developed, the system could theoretically revert to using the DAQ board as the main medium through which all analog signals are communicated (to the computer, from the Joystick Hub, etc.). Even without a third joystick, the system could be modified to use the DAQ board again, and switching would again become as simple as specifying in LabVIEW which channel to output to. Thus, whether or not a third joystick is added, this modification would serve to simplify the hardware setup and software governing the joystick user interface.

Another option for simultaneous control of the three optical tools would be to go with the touchscreen interface design alternative. However, this would be an entirely new solution that would have to be developed from the ground up, either to replace the joysticks or to serve as another alternative for control. Furthermore, using a touchscreen may not give the same degree of hands-on, real-time, responsive control as with the joystick user interface.

Lastly, another worthwhile modification would be to perfect the control method of the joysticks. Currently, the joysticks are controlled using a simple open-loop, proportional control system. A better control system would result in much more natural movement of the traps in response to the joysticks, and prevent large "jumps" that may cause the trap to lose whatever object it holds. For example, a new control method would be based on acceleration, such that when the joysticks are first moved the trap moves slowly, and then faster as the joysticks continue to be used. Compensating for the lag between the update of the crosshairs on the computer image and actual movement of the fast-steering mirror would also help to perfect the control method.

4.4.2. Future Experimental Studies

With respect to future experiments for studying and verifying the forces on chromosomes during mitosis, two general directions can be taken. The first would seek to improve and verify that the methods used in the previous experiments do in fact work, while the second direction proposes new experiments using the new stronger trap and its capability to move chromosomes to quantify the forces acting on chromosomes as well as other chromosome-related experiments.

Since problems arise due to the noninvasive nature of the laser ablations using the optical scissors, a method for performing laser ablations in the z-direction should be developed in order to create damage above and below the focal plane. The simplest solution for cutting in the z-direction would be to use a motorized focus knob in conjunction with a LabVIEW program that automates the z-cutting. With a motorized focus knob, a program can be written such that a cut using CutROI is performed at the current focal plane, the focus is moved up or down a user-specified step, and the same cut is again performed in the new focal plane. This can be repeated for as many steps and for any size z-step in order to specifically create damage in the z-direction. With the ability to use the optical scissors to perform z-cutting, it would be very easy to destroy any remaining microtubules or other cytoskeletal elements attached to chromosomes, as well as to completely sever chromosomes themselves.

However, this solution may be limited to spatial resolution of the z-steps. If the steps are not small enough, then we may only be creating a perforation that may not completely sever a chromosome

or destroy residual cytoskeletal attachments. A more complicated solution would be to automate the adjustment of the laser in the z-plane itself. The scissors (and tweezers) beam can already be adjusted in the x- and y-directions using the joystick-controlled fast-steering mirror. To be able to control the beam in the z-direction would require another optical element, possibly a lens on a motorized axis that can move back and forth, that could change the plane at which the laser is focused. Thus, cutting could be performed above or below the field of view without moving the actual focus knob. By oscillating this motor at a high frequency and thus changing the cutting laser's focus rapidly, a semi-invasive laser ablation can be performed which would create damage for a certain range in the z-direction, depending on the distance between which the lens oscillates. Motors such as these are commonly used in CD/DVD players, which use a laser that moves along the radius of the CD or DVD very quickly. With some customization, such a motor could also be used in this application. Another option is to use a spatial light modulator which can also adjust the cutting laser's focal point. Using the same strategy of oscillating the focal point would again make it possible to perform semi-invasive laser ablation.

With the capability of z-cutting, we can be sure that chromosome fragments are fully severed, and that any inability to move fragments after cutting are due to possible other unknown forces. Thus, we can then design new experiments, some using the stronger trap, in order to verify some of the possible unknown forces acting on chromosomes. The first set of experiments would be to determine the threshold power necessary for moving chromosomes using optical tweezers. In Figure 3.9, the trap was used at 4.2 W but the cell died after the experiment. Thus, experiments should be performed in order to determine the minimum trapping power necessary to move chromosomes in a control cell without killing the cell itself. Once this threshold power is found, we can treat cells with drugs such as nocodazole and again determine the threshold power for moving chromosomes. Without microtubules exerting forces on the chromosomes, this threshold power should be lower, i.e. it should take less power and be easier to move chromosomes when there are no microtubules. Different threshold powers can also be determined as a function of nocodazole concentration. This would help to verify what minimum concentration of nocodazole is necessary in order to eliminate all microtubule forces and move chromosomes freely using optical tweezers. Such an experiment would also serve to measure

quantitatively the effects of nocodazole, using chromosome movement as an indicator of their strength and the forces they are capable of exerting.

In addition to using nocodazole, we can also use other drugs such as latrunculin, which depolymerizes actin filaments (Alberts, 2008). Using this drug would help to test the theory of whether or not the actin meshwork exerts forces on chromosomes by attempting to move chromosomes using optical tweezers after treatment of cells with this drug. Again, threshold powers can be determined as a function of drug concentration in order to verify the effects of the drug. Determining a threshold power with latrunculin and nocodazole used in conjunction—such that both microtubules and the actin meshwork are depolymerized—would indicate indirectly how much force, if any, the actin meshwork exerts on chromosomes. If the actin meshwork does in fact exert forces on chromosomes, then upon its depolymerization with latrunculin (and in the absence of microtubules), the threshold trapping power for moving chromosomes should be lower than with only nocodazole. If the threshold power does not change significantly, then that may suggest the actin meshwork is not the source of the other unknown forces preventing movement of chromosomes with optical tweezers.

Experiments should also be done to characterize the cytosolic environment of cells during mitosis, since this may give a clue as to why the chromosomes cannot be freely manipulated using optical tweezers. Most importantly, the actual in vivo viscosity should first be measured in order to determine whether or not viscous forces are sufficient to counter trapping forces. Again, one approach would be to determine threshold power as a function of the viscosity of the medium. Isolated chromosomes could again be prepared and placed in media of different viscosity, and we could then determine the threshold power necessary to trap and move chromosomes freely as a function of viscosity. These threshold power measurements can then be compared to those in vivo, which may help to indicate the actual viscosity in vivo during mitosis. It is likely that in vivo, although the actual viscosity of cytosol may be similar to water, the apparent viscosity with respect to moving chromosomes may be higher due to unknown forces. If the viscosity during mitosis is higher than published values for cytosol viscosity (and thus threshold power necessary to move chromosomes is

higher), this may support the existence of an elastic, gel-like spindle matrix that makes chromosome movement using optical tweezers more difficult.

Electron microscopy could also be performed in order to verify the contents of the cytosol during mitosis, as certain organelles, protein complexes, or other parts of the cytoskeleton may act as obstacles that restrict chromosome movement upon depolymerization and destruction of microtubules using nocodazole and laser ablation, respectively. This could be done with cells untreated and treated with nocodazole and other drugs in order to further verify different drugs' effects. Electron micrographs of the chromosomes during mitosis may also give clues as to what forces or obstacles exactly are preventing the manipulation of chromosomes using optical tweezers.

We can also test the possibility that titin or cohesin may be preventing chromosome movement, by interfering with the actions of these proteins as well and measuring threshold power. Again, if we see significant differences in threshold power after interfering with these proteins, it may be possible that these proteins do in fact exert reaction forces that prevent chromosome movement using optical tweezers.

Using the stronger trap, we can also quantify these forces as well. For example, we can trap chromosomes using the optical tweezers during mitosis in a control cell with excessive (but not fatal) powers. At this power, intact microtubules would be not able to produce enough force to counter the trapping forces, and normal reorganization of the chromosomes during mitosis would not occur. We could then gradually decrease the trapping power until we see chromosome movement and reorganization. From this escape power, we can then quantify the actual amount of force with which microtubules pull on chromosomes, using the formula below:

$$F = \frac{QP}{c}$$

where P is the trapping power, c is the speed of light, and Q is a parameter representing dimensionless trapping efficiency that depends on the sample and beam properties (Nascimento et al, 2008).

References

Alberts, Bruce. *Molecular Biology of the Cell*. 5th ed. New York: Garland Science, 2008. 988-89. Print.

Fabian, Lacramioara, Xuequin Xia, Deepa V. Venkitaramani, Kristen M. Johansen, Jorgen Johansen, Deborah J. Andrew, and Arthur Forer. "Titin in Insect Spermatocyte Spindle Fibers Associates with Microtubules, Actin, Myosin and the Matrix Proteins Skeletor, Megator and Chromator." Journal of Cell Science 120 (2007): 2190-204. Print.

Johansen, Kristen M., Arthur Forer, Changfu Yao, Jack Girton, and Jorgen Johansen. "Do Nuclear Envelope and Intranuclear Proteins Reorganize during Mitosis to Form an Elastic, Hydrogel-like Spindle Matrix?" Chromosome Research 19.3 (2011): 345-65. Print.

LaFountain Jr., James R., Richard W. Cole, and Conly L. Rieder. "Partner Telomeres during Anaphase in Crane-fly Spermatocytes Are Connected by an Elastic Tether That Exerts a Backward Force and Resists Poleward Motion." Journal of Cell Science 115 (2002): 1541-549. Print.

Mori, Masashi, Nilah Monnier, Nathalie Daigle, Mark Bathe, Jan Ellenberg, and Peter Lenart. "Intracellular Transport by an Anchored Homogeneously Contracting F-Actin Meshwork." Current Biology 21.7 (2011): 606-11. Print.

Nascimento, Jaclyn M., Linda Z. Shi, Stuart Meyers, Pascal Gagneux, Naida M. Loskutoff, Elliot L. Botvinick, and Michael W. Berns. "The Use of Optical Tweezers to Study Sperm Competition and Motility in Primates." Journal of The Royal Society Interface 5.20 (2008): 297-302. Print.

Parsa, Shahab. *A Double Tweezers and Laser Scissors Microscope for Biological Studies*. Thesis. University of California, San Diego, 2010. Print.

Appendix A. Detailed Explanation of Robolase IV Program Controls

A.1. Main Image Control

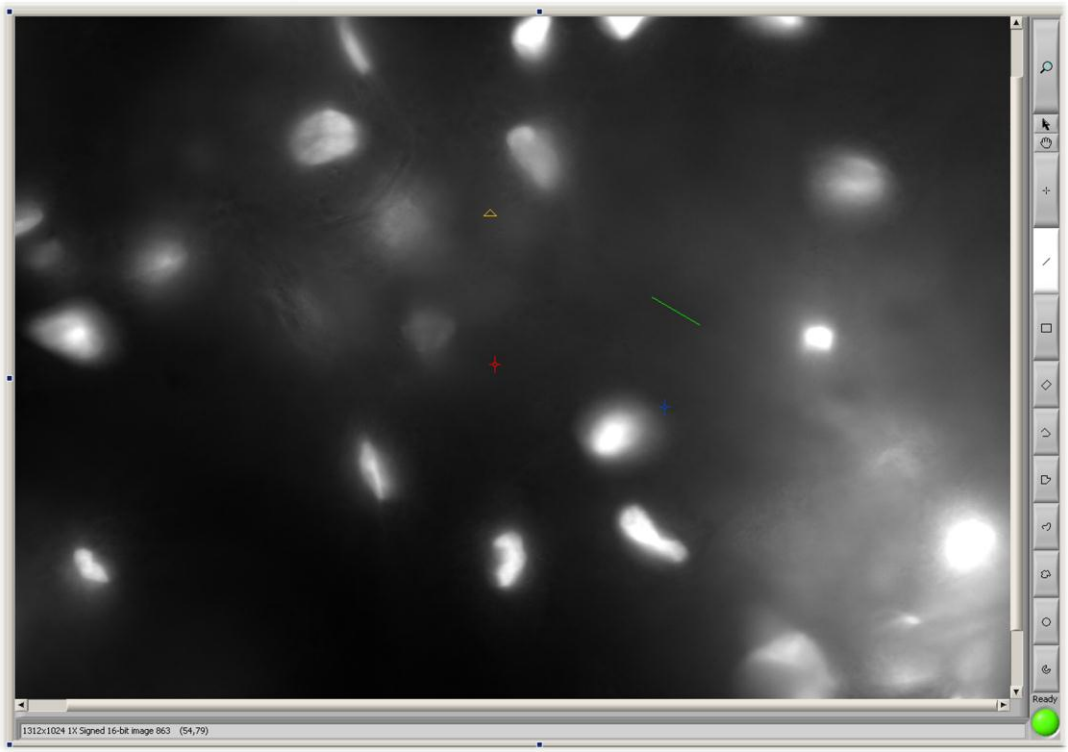

Figure A.1. Main Image Control. Images acquired by the camera are shown here. ROI overlaid onto the image represent trapping and cutting beam positions (red and blue crosshairs and yellow triangle). The user also draws green ROI to designate shapes for cutting using CutROI.

The Main Image Control above consists only of a LabVIEW NI Vision image control which is an indicator of image data. In other words, images acquired by the Hamamatsu camera are shown here in this rectangle. The red and blue crosshairs overlaid on the image represent, respectively, the S and P closed trap positions (which turn into rectangles when open), while the yellow triangle represents the optical scissors position (used only during joystick cutting). To the right of the image there is small column of buttons built into the image control that allow zooming, selecting, or drawing of green regions of interest (ROI). Various ROIs can be drawn, such as lines, rectangles, ellipses, or free shapes, the coordinates of which can be extracted from the image control in the block diagram and used to direct the laser beam to cut those various shapes on the sample by rotating the fast-steering mirror. Below the image there is a text indicator that shows information on the image, such as the resolution

and type of the image, and the gray level and x, y pixel coordinates of where the mouse cursor hovers over, as well as information about ROI when they are drawn (e.g., the length and angle of a line). There is also an indicator Boolean at the bottom right corner that shows when the system is ready after initially running the program.

A.2. Image Acquisition Control

Figure A.2 below shows one of the controls in the tabs on the right side of the Robolase IV front panel shown in Figure 1.9, the Image Acquisition Control:

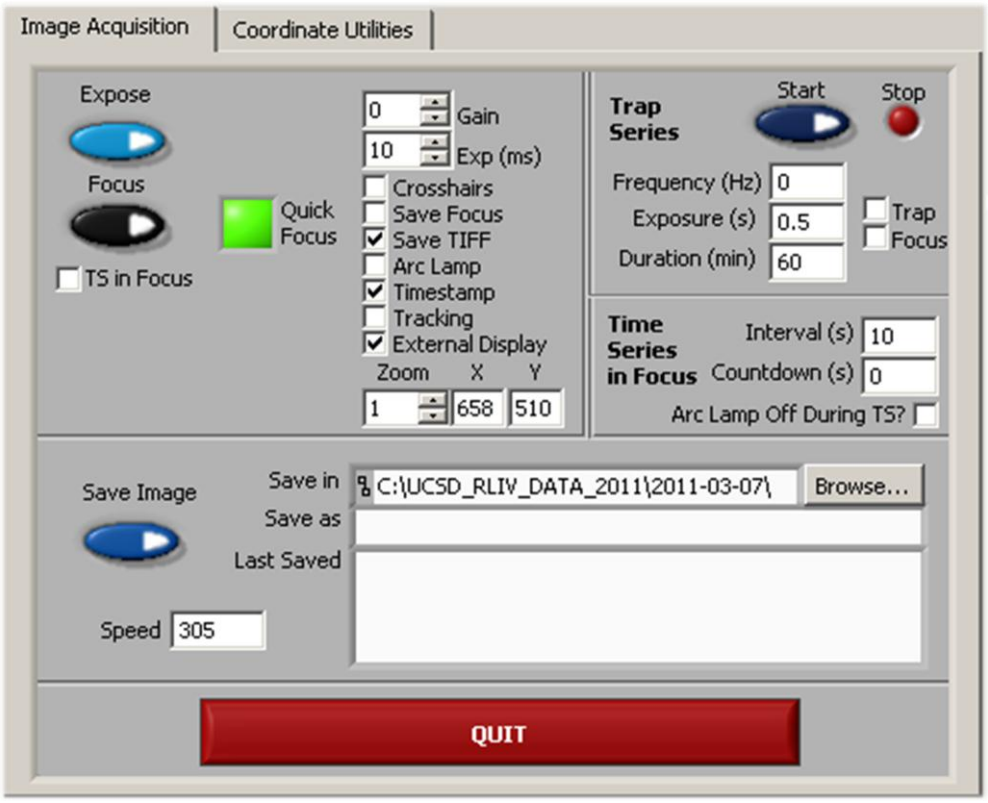

Figure A.2. Image Acquisition Control. The controls on this tab are used to acquire images and save them to the hard drive.

In the upper left rectangle of this control, we have a set of buttons, checkboxes, and some numeric controls. Expose will acquire a single frame using the camera based on the Gain and Exposure controls above the checkboxes. Focus will acquire a continuous sequence of frames. If Quick Focus is on, the programming uses a different, double while-loop architecture that separates the acquisition of images

during Focus mode from all other events and increases the frequency of while-loop iterations (represented by Speed) and thus the responsiveness of the program. If External Display is checked, then the Main Image will be shown on a secondary monitor covering the entire resolution. The Save Image button saves the image currently shown on the main image control to the hard drive in a folder automatically created by the program and automatically named with date and time information. Using Time Series, or TS, a sequence of images can be acquired at regular intervals set by the user.

A.3. Laser Trapping Control

Figure A.3 below shows the Laser Trapping Control, another one of the controls on the right side above the Image Acquisition Control.

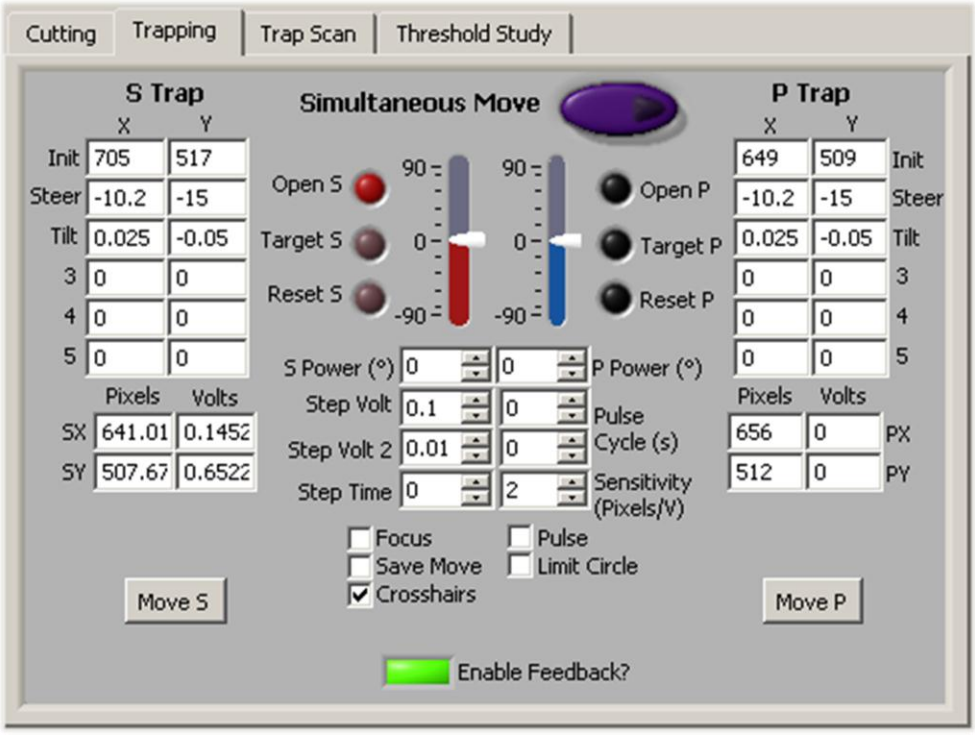

Figure A.3. Laser Trapping Control. Controls on this tab are mostly alignment parameters and buttons used to control the two, P and S polarized laser traps.

The column of numeric controls in the upper half of the control are alignment parameters used to make sure the crosshairs representing the optical traps on the main image are exactly lined up with where the

traps actually are as seen through the camera. The array of numeric controls in the bottom half indicate where the traps are in pixel coordinates of the main image and voltages of the fast-steering mirrors which control each trap. The Move controls move the trap by step sizes specified by Step Volt 1 and Step Volt 2 to where the point ROI is drawn on the main image, whereas the Target controls move the trap to that point directly without steps. The Open buttons open the shutter blocking the laser, and the Reset controls bring the controls back to the position when zero voltages are applied to both axes of the fast-steering mirrors. The sliders controls in the center control polarizers that adjust the power of each trap. The Crosshairs checkbox toggles the crosshairs on and off on the main image.

Controls related to the joystick user interface include the Sensitivity control, which adjusts how sensitive the movement of the traps is in response to movement of the joysticks, used in the Velocity, Onboard Program, and Simultaneous program control schemes for the joystick interface discussed in Chapter 2. The Enable Feedback? control essentially "turns on" the ability to use the joysticks, although exactly what is enabled differs between control schemes. All of these controls will be explained in more detail in Appendix C, User Manual.

A.4. Laser Cutting Control

Figure A.4 below shows the Laser Cutting Control, one of the other tabs behind the Laser Trapping control:

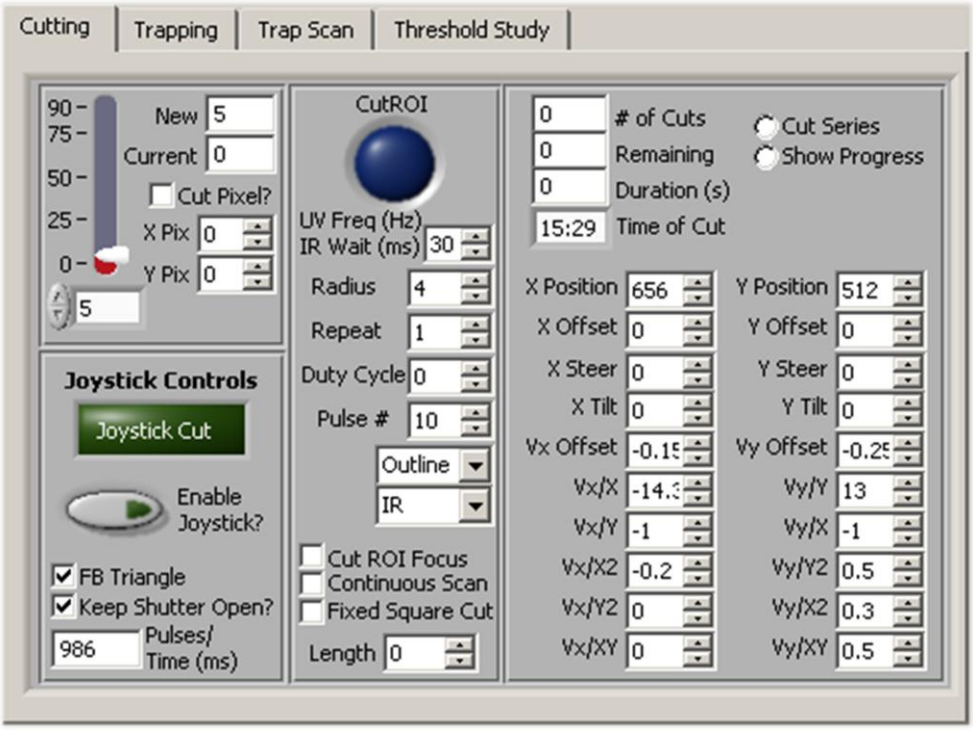

Figure A.4. Laser Cutting Control. Controls on this tab are mostly alignment parameters and buttons used to control the optical scissors.

The large blue CutROI control initiates the event to cut whatever ROI is drawn on the main image. The parameters below are used to define how the ROI is cut (e.g. the Radius determines the distance between each single point cut in a line). The numeric controls on the right represent alignment parameters again to align the ROI on the image with the voltages of the fast-steering mirror that directs the cutting beam. The slider on the left controls another polarizer that adjusts the power of the cutting laser. The controls under "Joystick Controls" are used for joystick cutting, which will also be explained in more detail in Appendix C. Briefly, the Enable Joystick? switches the system to joystick cutting mode used in several control schemes, while the large green rectangular button indicates whether the system is in this cutting mode. The FB Triangle checkbox toggles a triangle ROI in the main image that shows the position of the cutting beam. The Keep Shutter Open? checkbox toggles how cutting occurs in cutting mode, and the numeric control below is used to measure the laser dosage.

Appendix B. Detailed Descriptions of Earlier Control Schemes

B.1. Positional Control Scheme

B.1.1 Hardware Setup

The Positional control also makes use of the relays as described in Chapter 2. Again, two of these relays are needed since this switching between joystick control and computer control is done for each trap. In this case, however, each relay works separately, connecting for one trap the fast-steering mirror voltage input to the output voltages of the computer (via the NI DAQ board) in the off position. In the on position, the relay electrically connects the fast-steering mirror voltage input to the output voltages of the joystick. This is schematically represented in Figures B.1 and B.2 below:

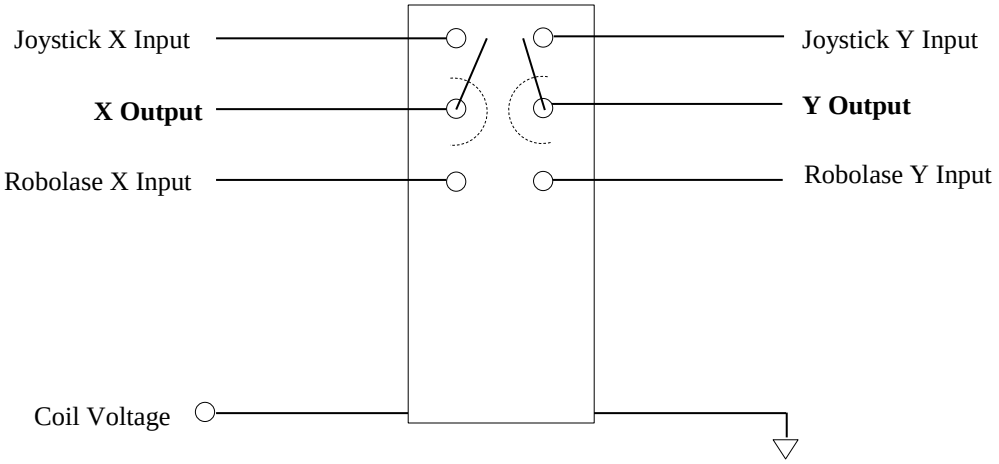

Figure B.1. Schematic showing electrical connections for the switching relay. The dotted arcs show how the switch rotates between the two positions.

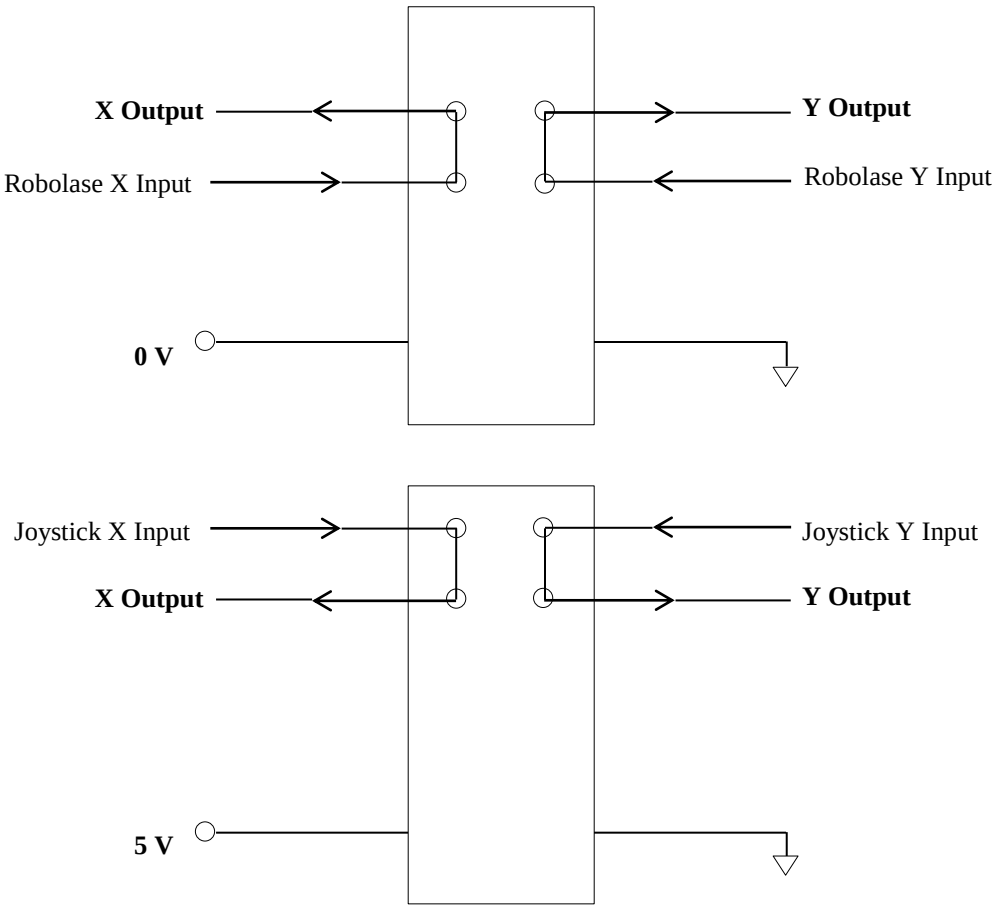

Figure B.2. Electrical connections during the on (5 V coil) and off (0 V coil) positions of the relay.

For the sake of organization, simplicity and customizability as in Onboard/Simultaneous control, the Positional control scheme also uses a Joystick Hub, although it is wired very differently than in the Onboard/Simultaneous control scheme, as shown in the circuit diagram in Figure B.3 below.

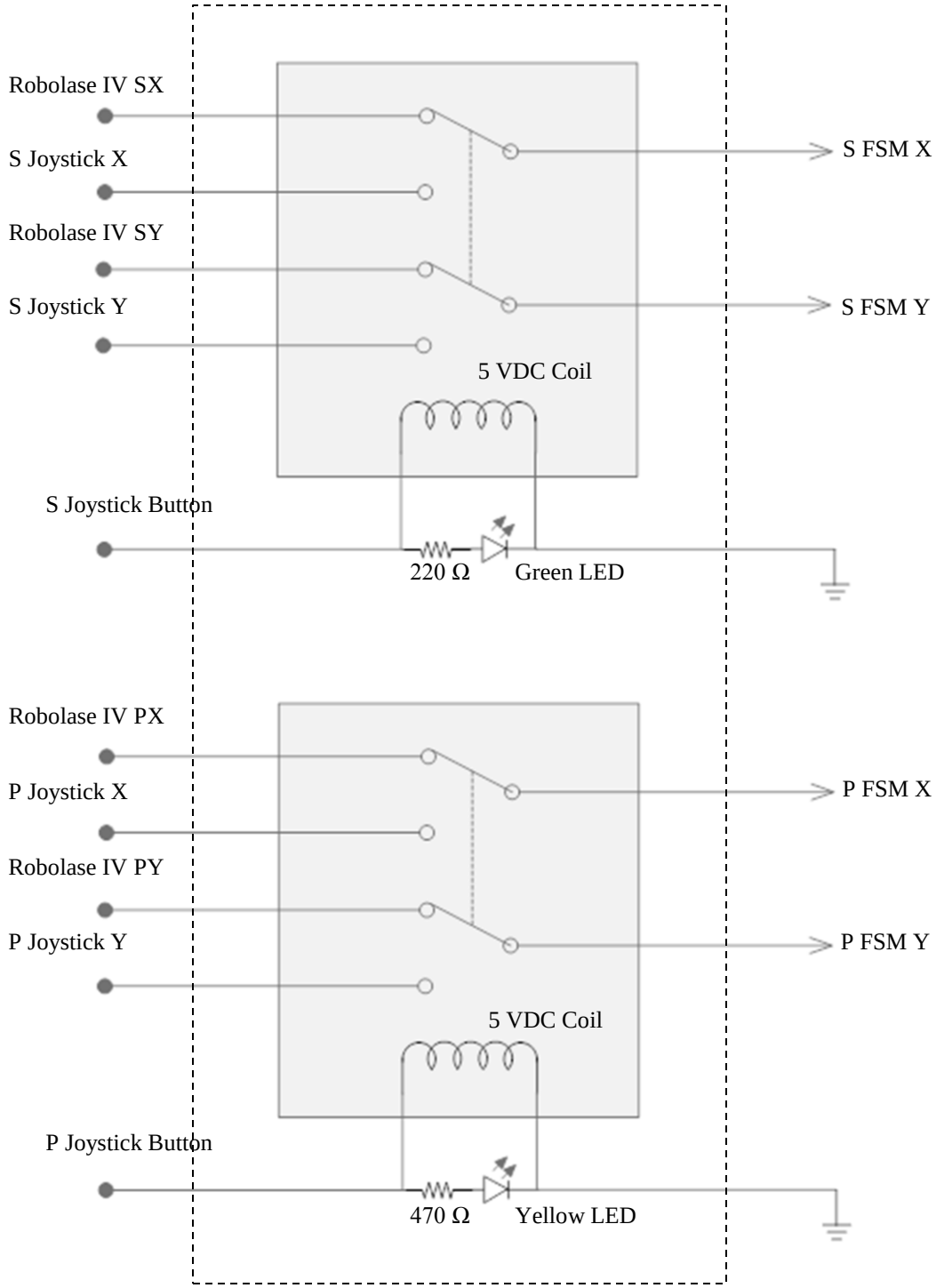

Figure B.3. Circuit Diagram of the Joystick Hub for Positional Control. The x- and y-axes of the joysticks go through the above relays (gray shaded area) and are outputted to the fast-steering mirrors (FSM). The outer dashed rectangle represents the Joystick Hub. Not shown are the joystick z-axes which are inputted directly to Robolase IV via the DAQ board. The analog voltages are with respect to a common ground, also omitted in the figure for simplification.

Each of the analog x- and y-voltages is with respect to ground, but this is omitted from the diagram. The outer dashed rectangle represents the Joystick Hub, while the gray dashed rectangles within are the relays (top for S trap and bottom for P trap). The LEDs in parallel are designed to turn on whenever the relay is turned on, using the same voltage that triggers the coil. Thus, it serves as a visual indicator that the relays have been turned on. In the normally off configuration, the relays electrically connect the fast-steering mirror input voltages to the computer. Thus, turning on the relay switches control to the joysticks. The coil voltage (+5 V) comes from the DAQ board and is triggered by one of the joystick buttons on each of the joysticks, that status of which is read using the LabVIEW program on the computer (discussed in the software section, section B.1.2). The z-voltages are directly passed to the computer via the DAQ board and never directly control any fast-steering mirrors. The Joystick Hub also supplies +12 V power to the joysticks' axes and +5 V power to the pushbuttons and also directs incoming digital signals from the pushbuttons to the DAQ board, as shown in Figure B.4 below.

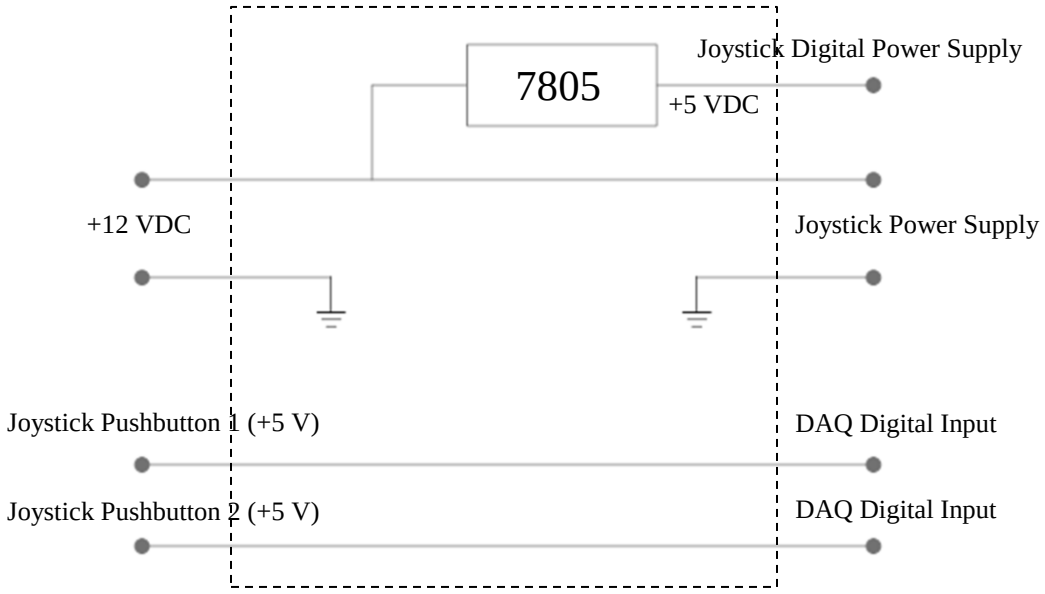

Figure B.4. Power supply and digital signals in Joystick Hub for Positional Control. The 7805 is a 5 VDC regulator. The digital signals are also with respect to ground, which is omitted in this diagram. The dashed outer rectangle represents the Joystick Hub. This circuit is for one joystick, so there are actually two of these within the Joystick Hub.

As mentioned earlier in Chapter 2, because the joysticks will always revert back to a neutral, zero voltage position, the positional control scheme must be able to switch between joystick control and

computer control of the positions of the optical traps and scissors—controlled directly by the fast-steering mirrors corresponding to each. This physical switching is performed by the relays in the Joystick Hub. Thus, x- and y-output voltages from both the joysticks and the computer are inputted into the Joystick Hub for both traps. The Joystick Hub then outputs the correct set of x- and y-voltages—depending on whether the system is in joystick control mode or computer control mode—to the optical trap fast-steering mirrors. The computer also outputs digital input and output (I/O) signals to the Joystick Hub to activate the relays that determine which control mode the system is currently in. The complete hardware setup is shown in Figure B.5 below.

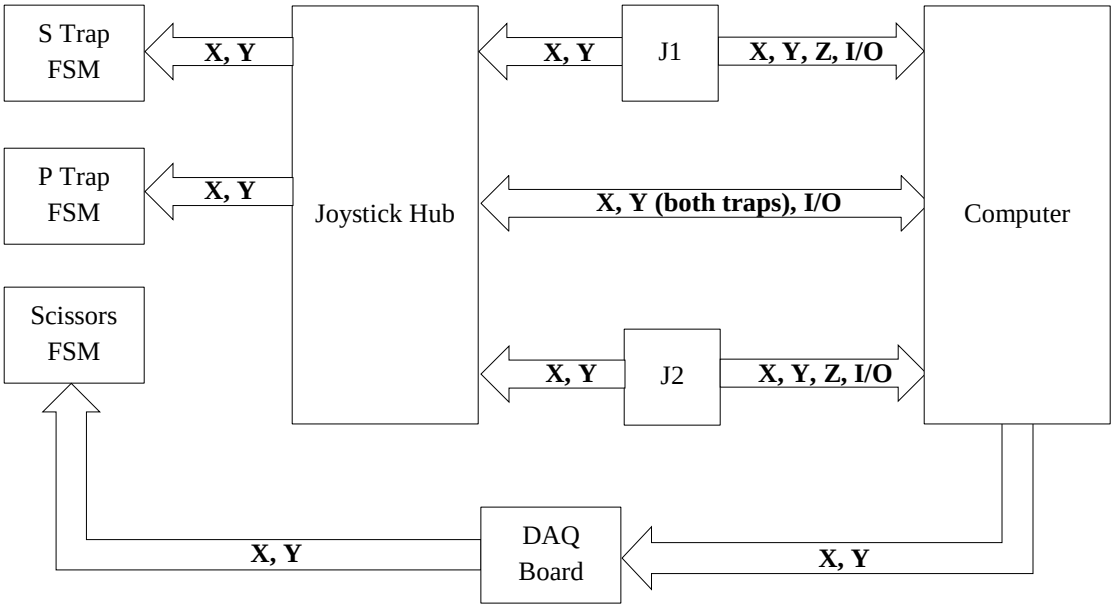

Figure B.5. Hardware setup for Positional Control scheme. J1 and J2 represent Joystick 1 and Joystick 2, respectively, and FSM is the abbreviation for fast-steering mirror. Arrows represent signals communicated between each device, including x-, y- and z-voltage signals as well as digital I/O signals.

The x- and y-output voltages of the joysticks are also inputted into the computer, so Robolase can track the locations of the optical traps (and move their corresponding crosshairs on the image accordingly) while in joystick control mode. In addition, the joysticks also output z-voltage signals and digital I/O to the computer. The z-voltage signals from each joystick are used to control cutting using the optical scissors, while the digital I/O signals communicate the state of the buttons on the joysticks.

The z-voltages do not directly control the cutting fast-steering mirror as the x- and y-voltages do with the traps. Instead, Robolase IV reads the z-voltages, determines the cutting ROI and outputs x- and y-voltages via the DAQ board to the scissors fast-steering mirror. How cutting works and the functions of the buttons are both explained more in the software section later in the appendix.

Figure B.6 below illustrates the difference between joystick control mode and computer control mode.

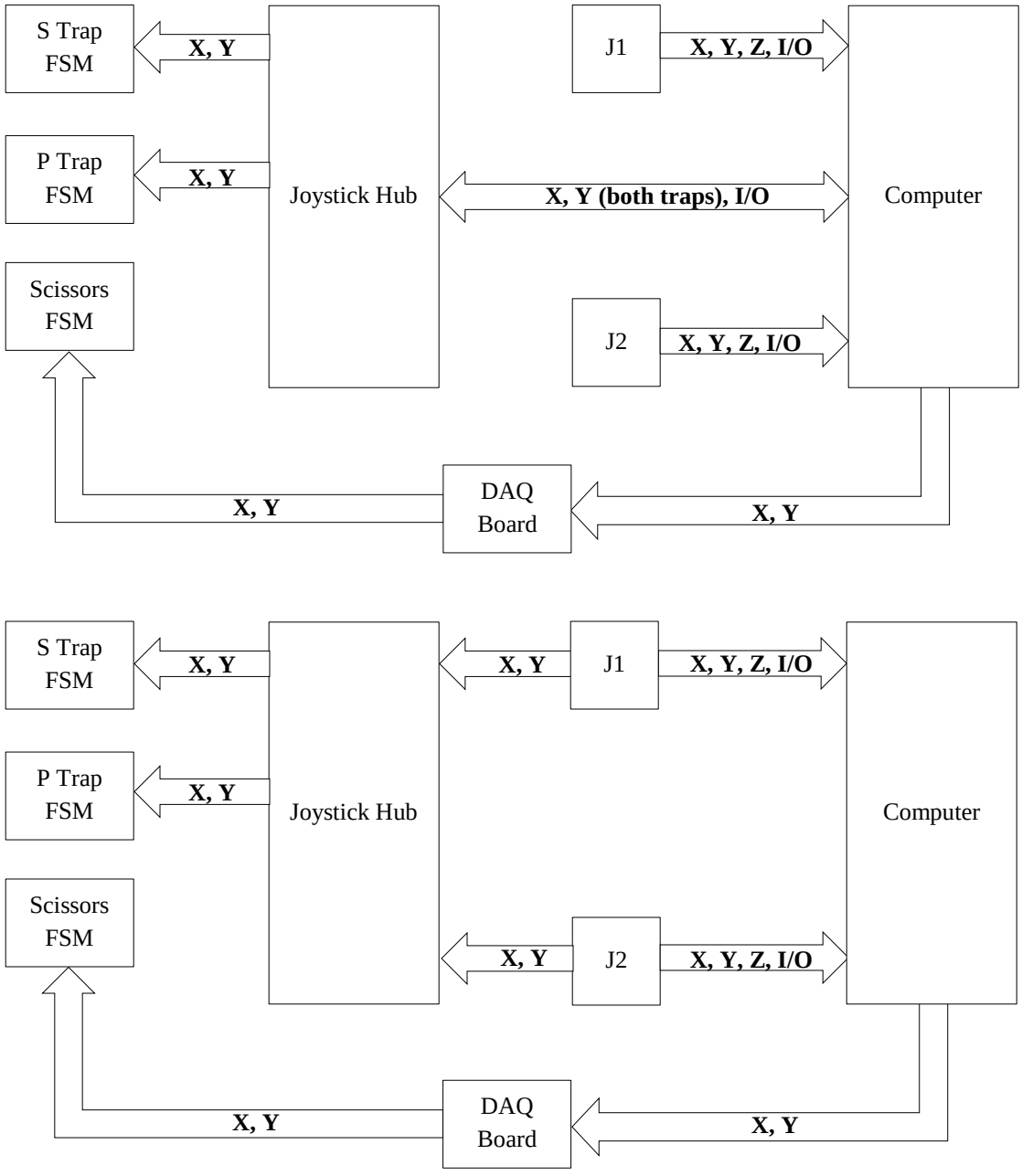

Figure B.6. Joystick control mode (bottom) and computer control mode (top). This figure illustrates the conceptual difference between the two control modes.

In joystick control mode, the relays in the joystick hub pass the output voltages of the joysticks to the inputs of the fast-steering mirrors for the optical traps, and thus the positions of the traps depend on the positions of the joysticks. These voltages are also outputted to the computer, where Robolase IV

continuously monitors the joysticks and moves the crosshairs on the image for each trap accordingly. In computer control mode, the joysticks have no influence over the positions of the traps since the relays are switched off and the joysticks' output voltages are not electrically connected to the fast-steering mirror. Instead, the computer outputs voltages via the DAQ board which determines the position of the traps (but can still read the positions of the joysticks). Note in both cases the cutting fast-steering mirror is always controlled by the computer.

Figure B.7 below shows the hardware diagram from Figure 1.7 previously now including the Joystick Hub and the joysticks for Positional Control.

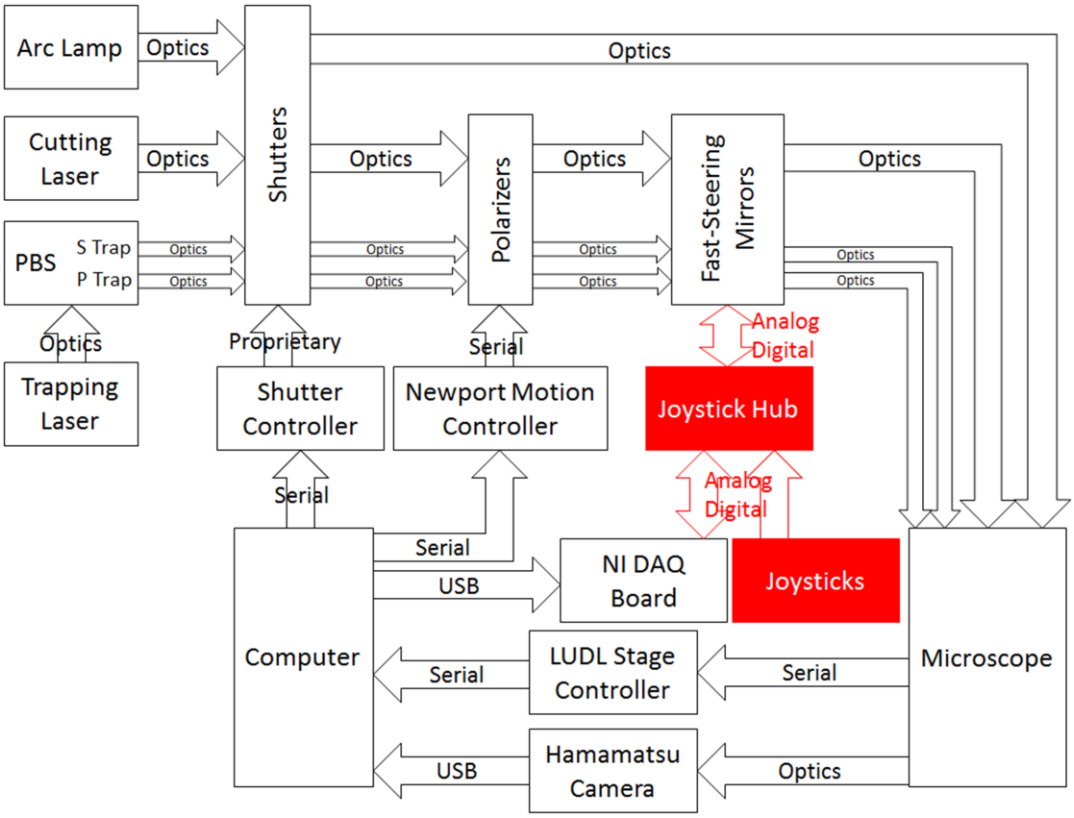

Figure B.7. Hardware diagram including the joysticks and Joystick Hub for Positional Control.

B.1.2. Software

B.1.2.1. Control by User

Because this control scheme was based on positional control, the user would have to go through a certain process to move the optical traps and manipulate microscopic objects using the joysticks. This process can be summarized in the following steps:

1. Prepare sample and run Robolase (PC Control)
2. Enable Feedback and turn on FB Circles
3. Switch to Joystick Control (pushbutton)
4. Trap object by moving joysticks
5. Switch to PC Control (pushbutton)
6. PC Control using Robolase resumes with saved trap positions from Joystick Control

Each step will be explained in more detail and with figures below. The following legend in Figure B.8 below for the different types of crosshairs used in Robolase IV is also useful for the explanation.

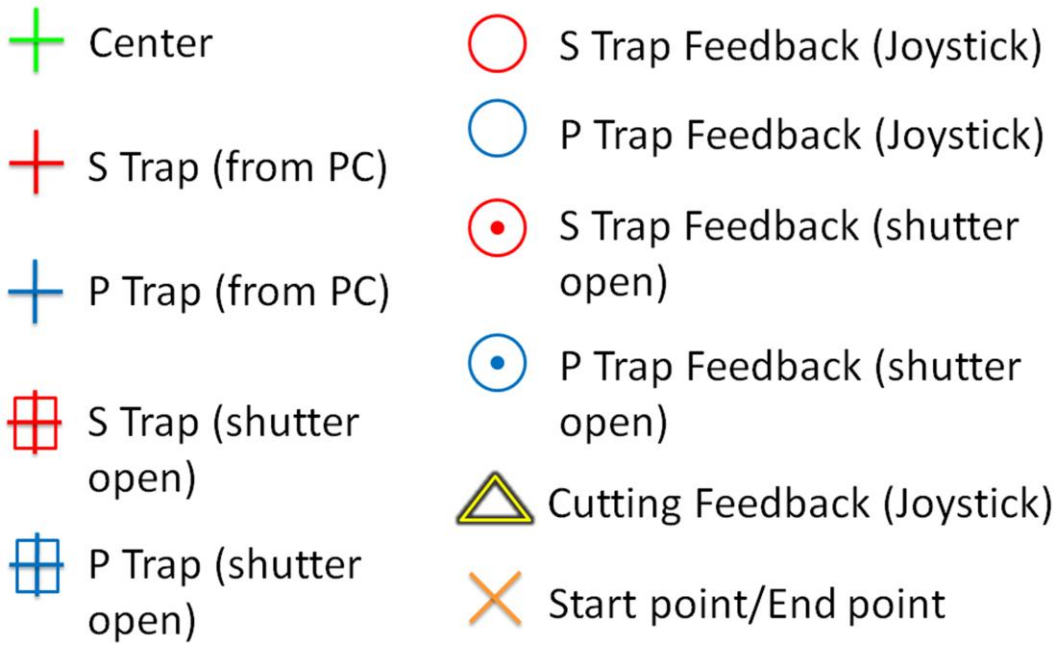

Figure B.8. Different types of crosshairs for Robolase IV. Each of these crosshairs is overlaid onto the main image (which shows the image from the camera) on Robolase IV.

Figure B.9 below represents the main image area of Robolase IV, and shows a sample of beads, which will be used for the purposes of explaining the process for trapping using the joysticks.

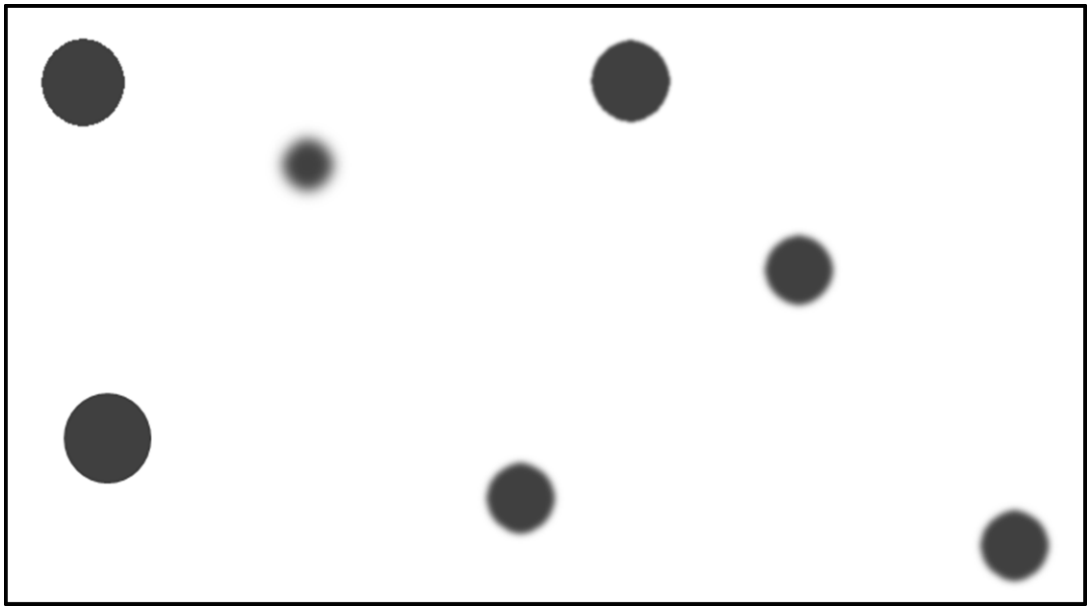

Figure B.9. (Step 1) Prepare sample and run Robolase (PC Control). The image above represents the main image of Robolase IV. The gray circles represent beads in and out of focus.

Robolase IV runs in PC Control by default. Thus, the joysticks are electrically connected to the computer via the DAQ board, as shown in the top figure of Figure B.2 and Figure B.6, and can only be controlled using the point-and-click method. The next step is shown in Figure B.10 below.

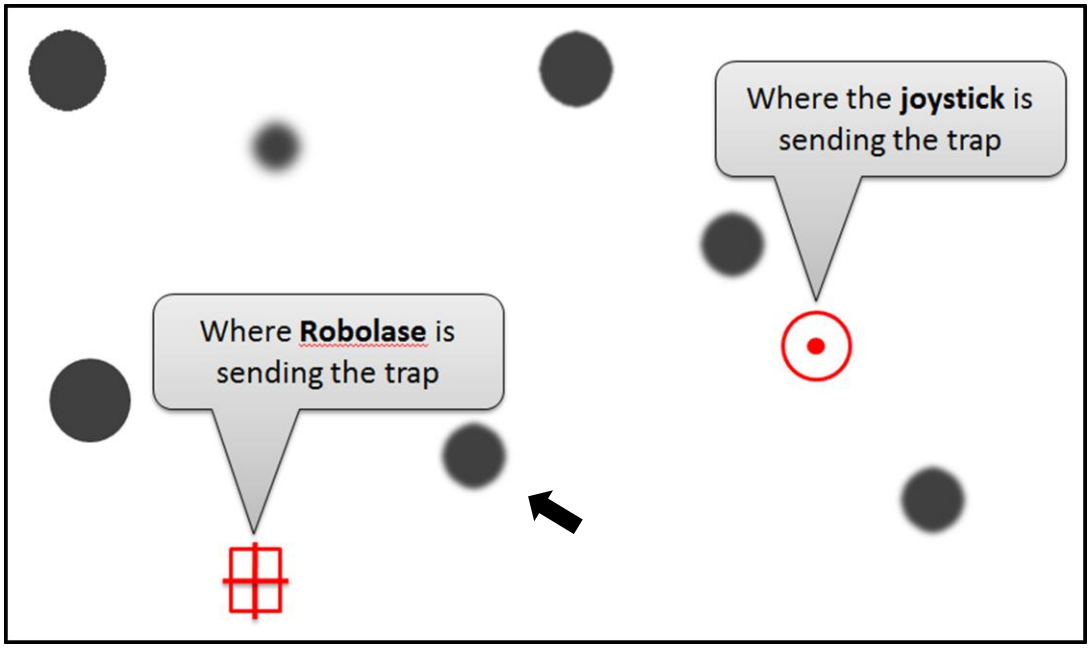

Figure B.10. (Step 2) Enable Feedback and turn on FB Circles. The crosshair legend is shown in Figure B.8. The shutter is already open in this case. The arrow shows the "bead" that will be moved later.

Turning on the crosshairs and feedback circles (for S trap only in this case) by checking the "Crosshairs" and "FB Circles" checkboxes in the Trapping tab of Robolase IV overlays these figures on the image. In this case the shutter is already open and the box around the crosshairs and the dot within the circle indicate this (see Figure B.8 for legend). Feedback is enabled by pressing the "Enable Feedback" button in the same tab. The Trapping tab and these controls can be seen in Figure A.3 (although "FB Circles" has been removed in the most updated version). Because the system is in PC control, moving the crosshairs using the point-and-click method moves the traps. Moving the joysticks will move the feedback circles, since Robolase IV is still reading the position of the joysticks; however, this will not move the trap itself because the system is in PC control mode. In step 3, the system is switched from PC control to joystick control by pressing the pushbutton on the joystick. This changes the configuration of the system from the top diagram in Figures B.2 and B.6 to the bottom diagram. Moving the joystick now will result in moving the trap itself, which is shown below in Figure B.11, where the trap has been moved to the location of the bead indicated by the arrow in the above figure, and then moved upwards with the bead in the trap.

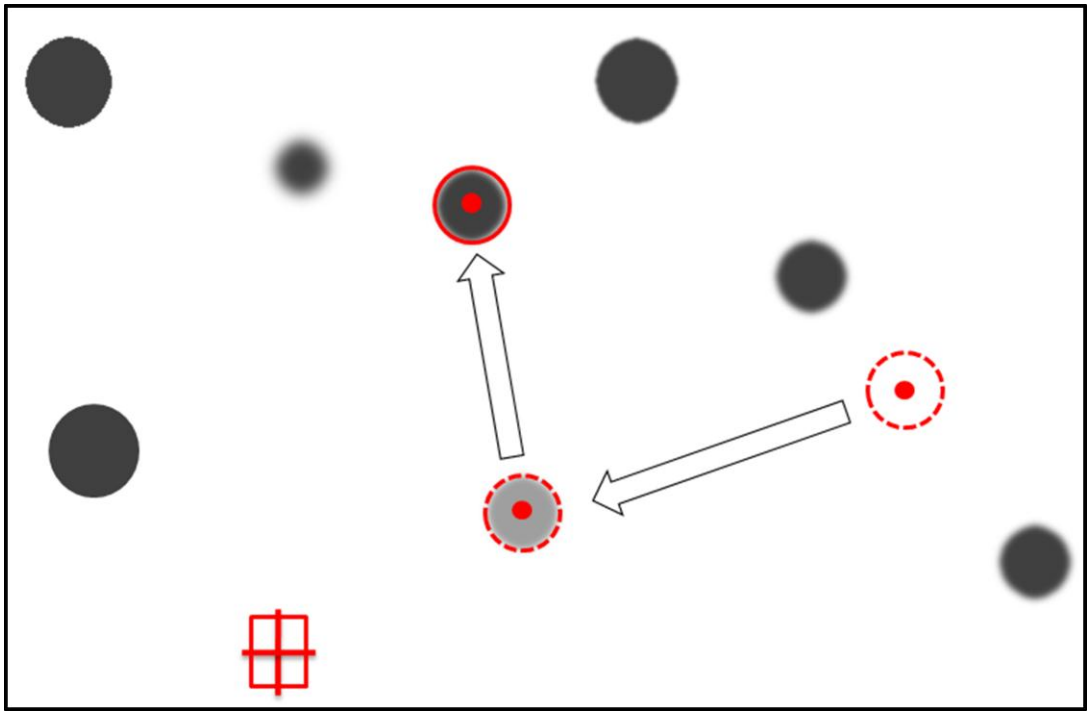

Figure B.11. (Step 4) Trap object by moving joysticks. In this figure the bead has been moved using the joysticks. Arrows show direction of movement. The dotted circles represent where the trap used to be.

To maintain the position of the trap in the figure above while in Joystick control mode, the user must maintain the joystick in whatever position it is in, since letting go will cause the trap to move back to its original position. This problem is solved by using the relays and the hardware configuration specifically developed to resolve this issue. Thus, step 5 is to use the pushbutton on the joystick to switch back to PC control mode, so the trap positions can be maintained without the user having to hold the joysticks in the same position. This changes the hardware configuration back to the top figure in Figures B.2 and B.6. Once control modes have switched, Figure B.12 represents what the main image will look like, with the crosshairs at the position where the trap has been moved to by the joysticks, and the feedback circles returning to their original position.

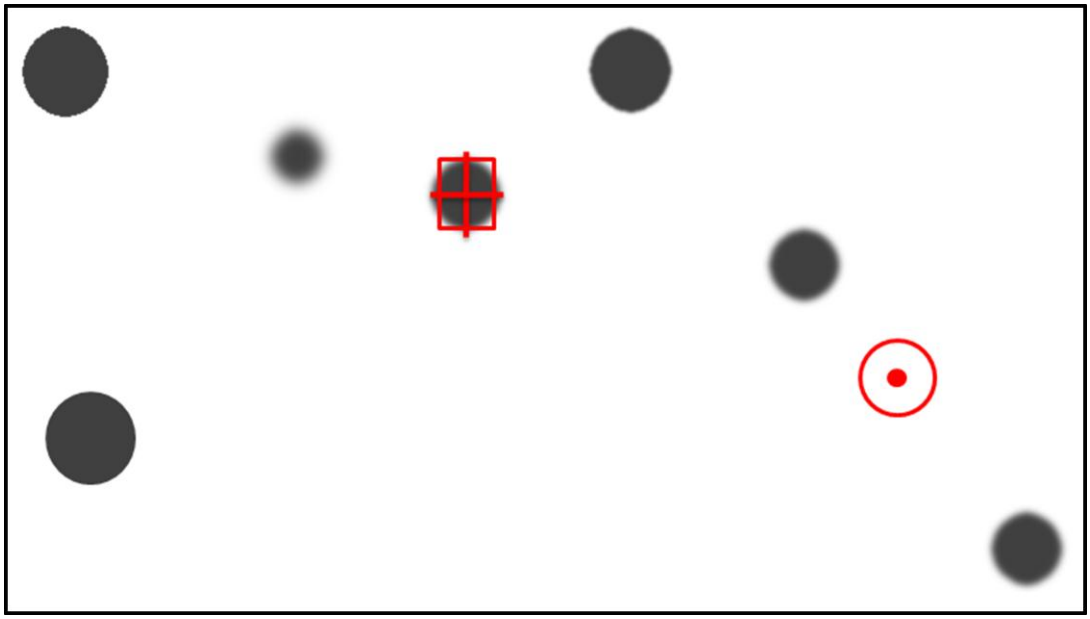

Figure B.12. (Step 6) PC control using Robolase resumes with saved trap positions from Joystick control. The crosshairs has now moved to where the trap was moved using the joystick, while the feedback circle has moved back to its original position.

There is also a process to manipulate the optical scissors using the joysticks. The steps for this process are summarized below and explained in detail again afterwards:

1. Check “FB Triangle” to see the joystick z-axes’ positions
2. Rotate joysticks to move yellow triangle to desired start point
3. Push button to save start point
4. Rotate joysticks to determine end point
5. Select cutting style: Line, Rectangle, Ellipse
6. Push button to select end point and initiate cutting

Using the same “sample” of beads as before, we will illustrate each step of joystick cutting. The first step is to check the “FB Triangle” checkbox to see the positions of the joysticks’ z-axes (their rotational position). Rotating each joystick will then move the feedback triangle on the main image of Robolase IV in an “Etch-a-Sketch” manner as previously described. Just like for the x- and y-axis, the rotation of the joysticks also reverts back to the default position after the user releases the joystick. In Figure B.13 below, step 2 is shown, where the feedback triangle has been turned on and moved to a different position shown by the arrow.

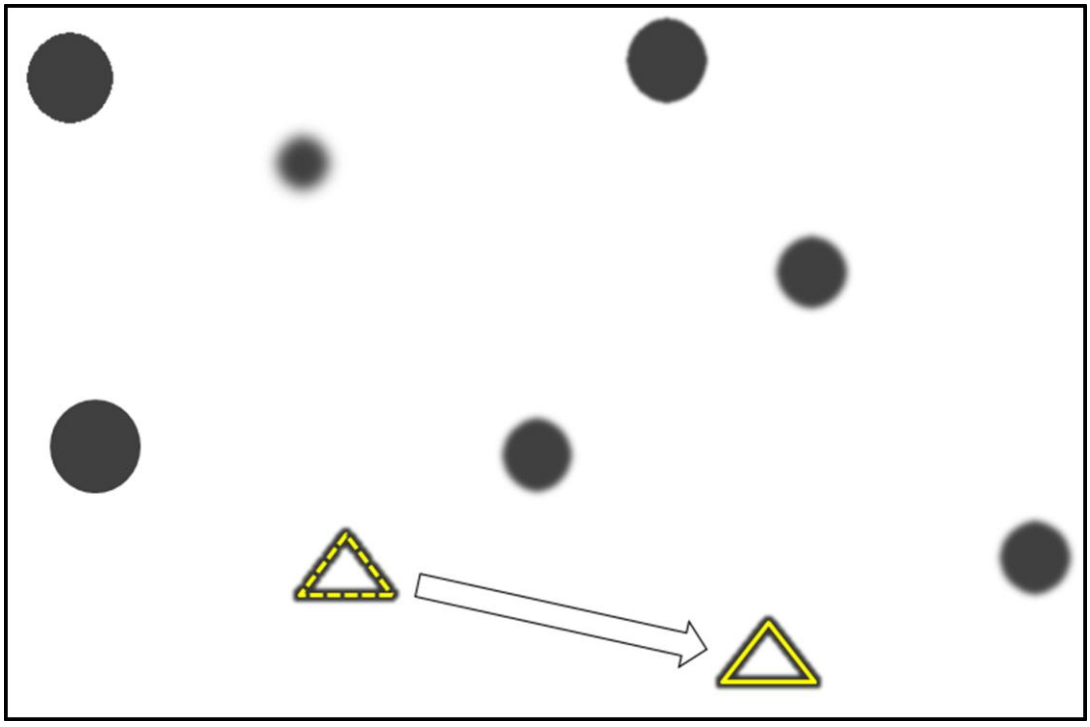

Figure B.13. (Step 2) Rotate joysticks to move yellow triangle to desired start point. The feedback triangle has been moved by rotating the joysticks according to the arrow shown. The dotted triangle is the previous position.

This position represents the start point for the cut. This coordinate is designated as the start point in step 3 by pressing another of the pushbuttons on the joystick, which overlays an orange "X" on this position. The joysticks can then be rotated again in step 4 to change the position of the feedback triangle, moving it towards the end point of the cut. A line is automatically drawn between the start point and end point as the joysticks are rotated. Figure B.14 below shows steps 3 and 4.

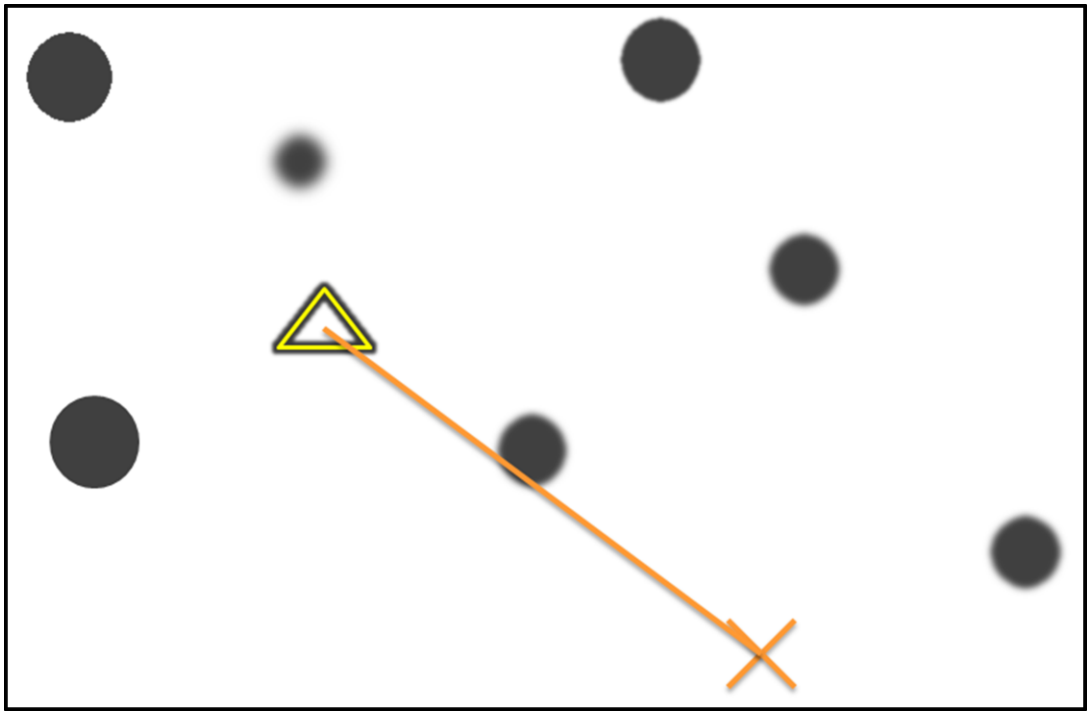

Figure B.14. (Steps 3 and 4) Push button to save start point and rotate joysticks to determine end point. A line, ellipse, or rectangle is automatically drawn between the saved points.

In step 5, the user determines the cutting style, which determines the shape of the cut and can be line, rectangle, or ellipse. A line is simply the line drawn between the start point and end point. The rectangle is defined by the top left and bottom right coordinates. Thus, the start point and end point will determine the top left and bottom right of the rectangle. An ellipse is defined by a bounding rectangle which is defined in the same way as the rectangle. These shapes are shown in Figure B.15 below.

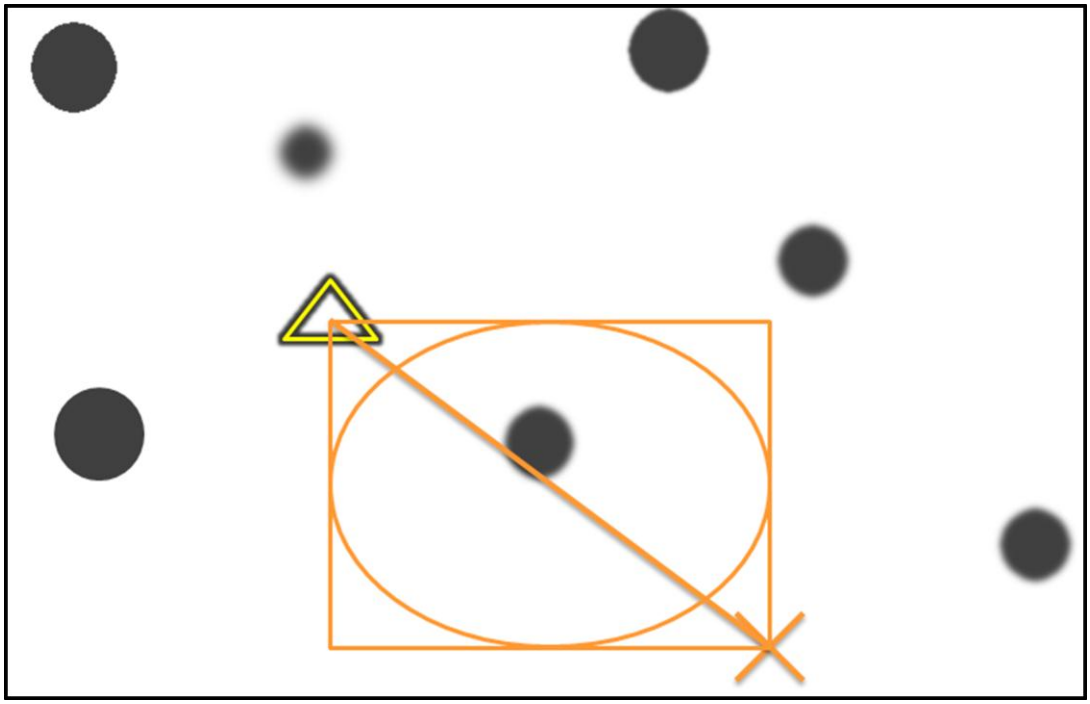

Figure B.15. (Step 5) Select cutting style: Line, Rectangle, Ellipse. The different shapes are overlaid on the image (only one is shown at a time, but here all are shown to show how they are defined by the coordinates.

The last step is to push the same pushbutton used to save the start point to designate the end point, which cuts whatever shape has been selected between the saved points. Note that during the entire process the rotation of the joysticks and the voltages from their z-axes are never sent directly to the fast-steering mirror for cutting. Instead, these z-voltages are read by Robolase IV via the DAQ board and displayed on the main image. Once the start point and end point have been chosen, this information is sent to the VI for cutting already programmed into Robolase IV. Thus, the computer controls the cutting at all times in this case, unlike for trapping.

B.1.2.2. LabVIEW VI

Figure B.16 below shows a pseudo-code flow chart of the LabVIEW VI used to control joystick trapping in Robolase IV.

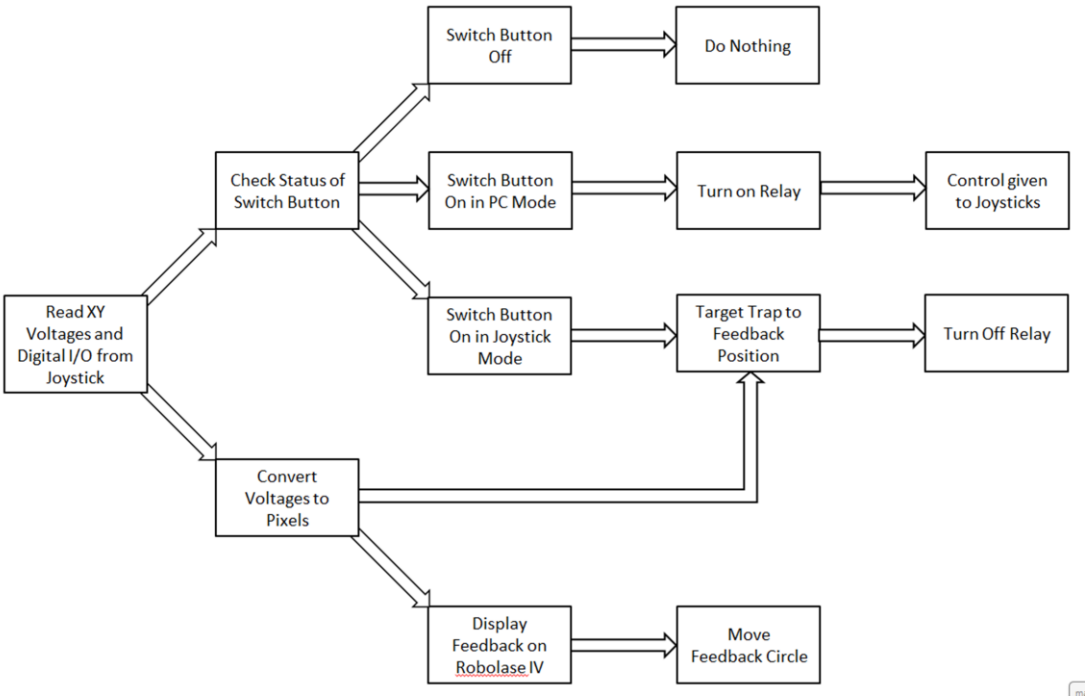

Figure B.16. Flow chart diagram representing pseudo-code of the LabVIEW VI used to control joystick trapping.

This code runs repeatedly in a while-loop as Robolase IV runs in order to update, assuming feedback is enabled in Robolase IV. Also, since there is one joystick for each trap, two instances of this code run simultaneously. The code first reads the feedback voltages (x and y) and digital signals from the buttons coming from the joystick via the DAQ board's analog input channels. Following the bottom path, the code then back-calculates the position of the joystick in pixels from the voltages, displays the voltages in indicators in the Trapping tab of Robolase IV, and overlays the feedback circle in the correct position on the main image. Thus, in either joystick control mode or PC control mode, moving the joystick moves these feedback circles on the main image, although in PC control mode the traps themselves (the fast-steering mirrors) do not move.

Following the top path, after reading the voltages, the code checks the status of one of the pushbuttons on the joystick designated for switching control from PC to joystick and vice-versa. If the switch button is off, then nothing happens and the code iterates again. If the switch button is turned on and the program is currently in PC control (middle path), then the relay is turned on, and control of the

fast-steering mirror controlling the trap is given to the joystick. This is equivalent to step 3 in the trapping process outlined in the previous section, section B.1.2.1. If the switch button is turned on and the system is in joystick control, then the code first targets the trap in Robolase IV to the current position of the joysticks. Thus, the crosshairs move to the feedback circle (between steps 5 and 6). Note that control has not yet switched back to the computer. Once the correct voltages are sent out through the DAQ board from Robolase IV, then the relays are turned off and control goes back to the PC. The actual delay between these two steps is too short for users to notice (thus the user would not let go before the switch has occurred), but it ensures that the fast-steering mirror does not move during the transition. If the voltages were not sent out before the relay was turned off, then whatever may be trapped during an experiment may be lost during the switch.

The code for joystick cutting is similarly structured, although different actions occur with regard to initiating a CutROI sequence. The pseudo-code flow chart is shown below in Figure B.17.

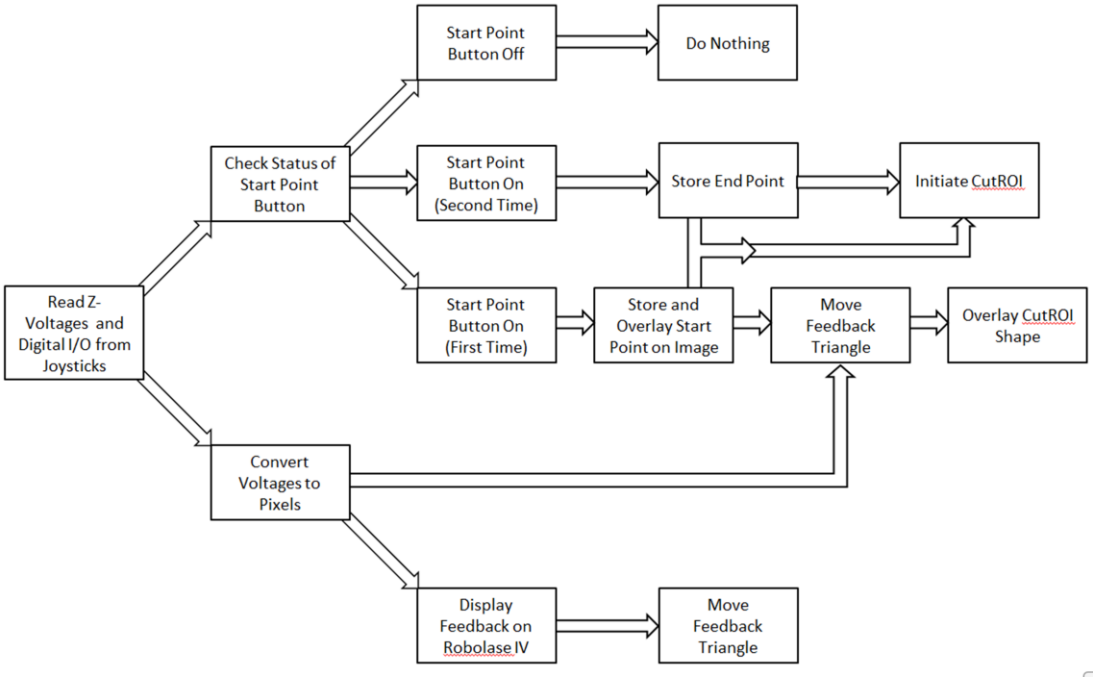

Figure B.17. Flow chart diagram representing pseudo-code of the LabVIEW VI used to control joystick cutting.

Once again, this code runs repeatedly in Robolase IV if feedback is enabled. In this VI, the code checks the z-voltages and digital signals of both joysticks instead of the x- and y-voltages from one joystick.

The bottom path again shows the voltage being converted back to pixels, displayed on Robolase IV, and overlaid on the main image, this time as a feedback triangle (see legend above). In the top path, this VI checks for the status of the start point button, which is a different pushbutton than the switch button. If the start point button is off, then nothing happens. If the start point button is turned on for the first time (bottom path)—meaning no start point has been chosen yet—then the current position of the z-voltages (the location of the feedback triangle) is stored as the start point and this coordinate is overlaid with an orange "X" on the main image. Then, the user can rotate the joysticks to move the feedback triangle again, using the voltages read from the DAQ board. The feedback triangle moves according to these voltages and between the two points the cutting shape is drawn, depending on whether line, rectangle, or ellipse is chosen.

When the user presses the start point button for the second time, after the start point has already been stored, then the code takes the middle path in the top portion. The current position of the feedback triangle is stored as the end point and CutROI is initiated in Robolase IV using the stored start and end points. After this, the program uses the original CutROI algorithm programmed into Robolase IV. Thus, the z-voltages are never used to directly control the cutting fast-steering mirror.

B.2. Velocity Control Scheme

B.2.1. Hardware Setup

The hardware setup for velocity control is much simpler because the output voltages of the joystick go directly to the computer and all the "switching" is done using software. Thus, the relays were not necessary in this control scheme. Figure B.18 below shows the simple circuit within the Joystick Hub for the velocity control scheme:

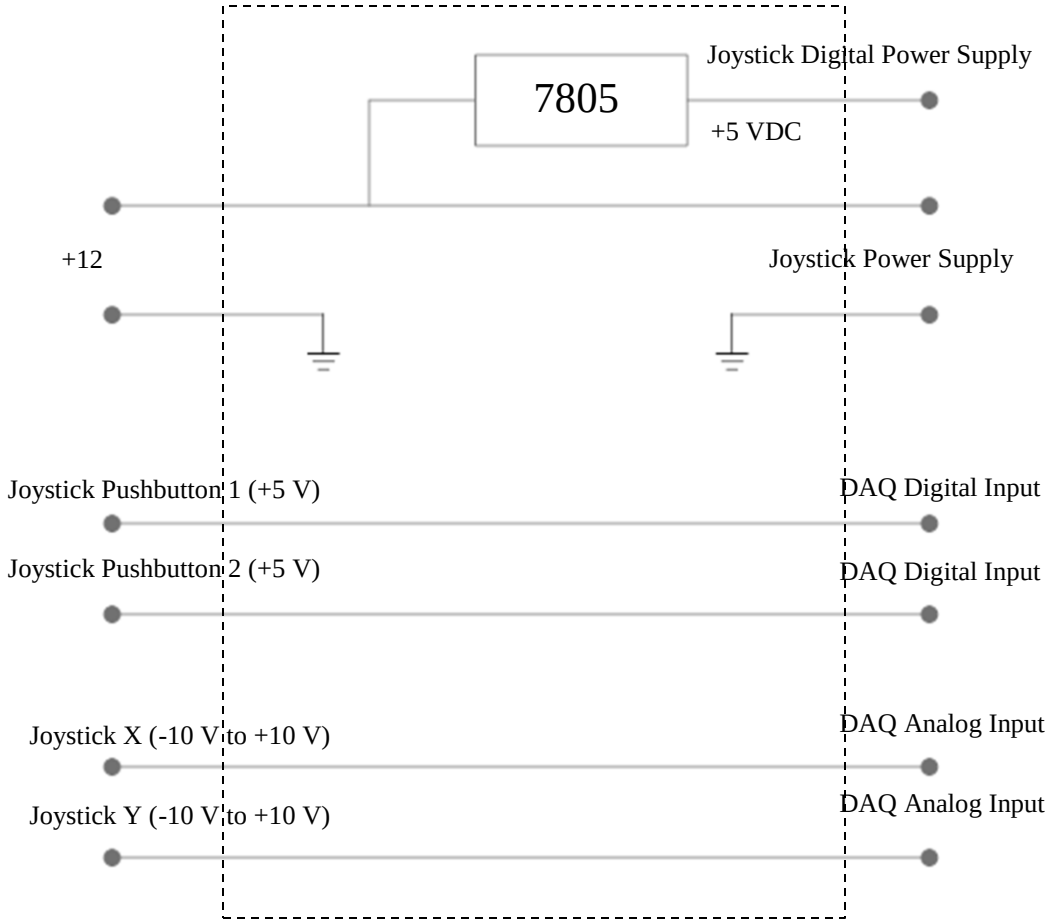

Figure B.18. Circuit diagram of Joystick Hub for Velocity Control. The 7805 is a 5 VDC regulator. The analog and digital signals are also with respect to ground, which is omitted in this diagram. The dashed outer rectangle represents the Joystick Hub. This circuit is for one joystick, so there are actually two sets of the digital and analog inputs and outputs within the Joystick Hub.

The circuit is very simple in that the incoming x- and y-voltages are passed straight to the computer via the DAQ board's analog inputs, and the rest of the circuit is actually the same as Figure B.4, which showed how the power supply and digital signals are handled in the Joystick Hub. Once again, the grounds are omitted in order to avoid complicating the circuit, and there are actually two of these circuits within the Joystick Hub, one for each joystick. The figure below shows the hardware setup pertaining to only the joysticks, Joystick Hub, and the computer.

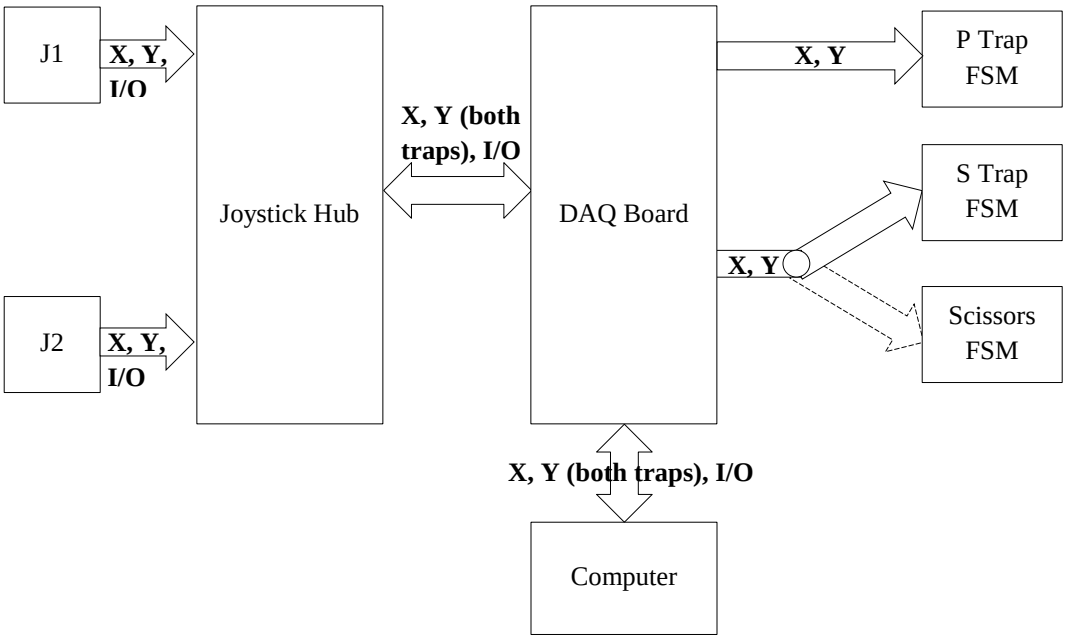

Figure B.19. Hardware setup for Velocity Control scheme. The computer both acquires signals from the Joystick Hub and outputs signals to the fast-steering mirrors via the DAQ Board. The splitting arrow connecting the DAQ board and the S Trap and Scissors fast-steering mirrors represents how the target for the S joystick can be switched to enable joystick cutting mode.

Similar to the circuit, the hardware setup for the Velocity control scheme is much simpler as well, which is an added bonus. The joysticks communicate only with the computer via the Joystick Hub and the DAQ board. The computer then translates the voltages read from the joysticks into displacements for trap movement, which it sends to the appropriate fast-steering mirrors, again via the DAQ board. The splitting arrow connecting the DAQ board to the S Trap and Scissors fast-steering mirrors represents the fact that the target for the S joystick can be switched in order to control the scissors fast-steering mirror using the joystick. Otherwise, the scissors—as well as the optical traps—may still be controlled using Robolase IV. The figure below shows the entire hardware diagram once again, this time for velocity control.

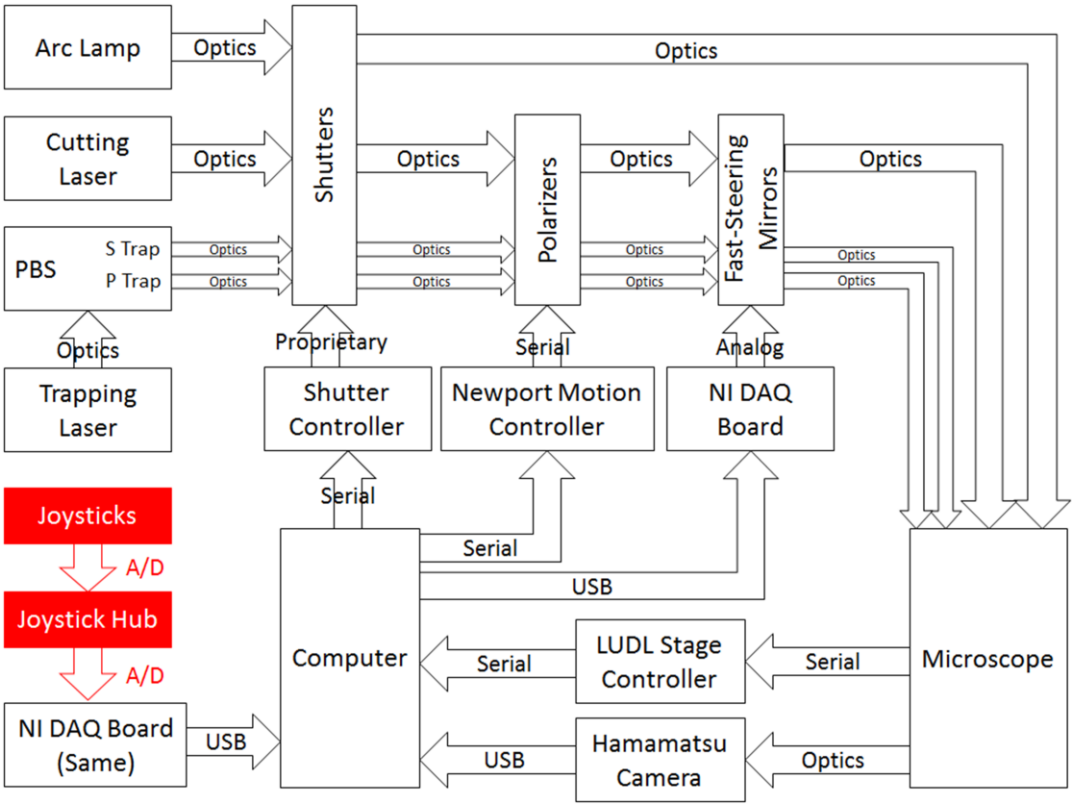

Figure B.20. Hardware diagram including the joysticks and Joystick Hub for Velocity Control. A/D is an abbreviation for Analog/Digital.

This hardware diagram is much more similar to the original, which emphasizes how much simpler this configuration is with respect to the hardware setup. Note that there is only one NI DAQ board (the one in the bottom right corner is the same as the one in the middle-right area).

B.2.2. Software

B.2.2.1. Control by User

Controlling the joysticks for trapping and cutting is essentially the same in this control scheme as in the Onboard/Simultaneous control scheme. That is, the movement of the two traps can be controlled using the two joysticks in trapping mode, or the P trap and the cutting beam can be controlled when the appropriate pushbutton is pressed and the system switches to cutting mode. Each of the shutters for the two traps or the scissors can be opened using one of the joystick buttons as well (the scissors shutter only stays open as long as the button is pressed).

B.2.2.2. LabVIEW VI

Figure B.21 below shows the pseudo-code flow chart of the LabVIEW VI used to monitor the joysticks in the Velocity control configuration.

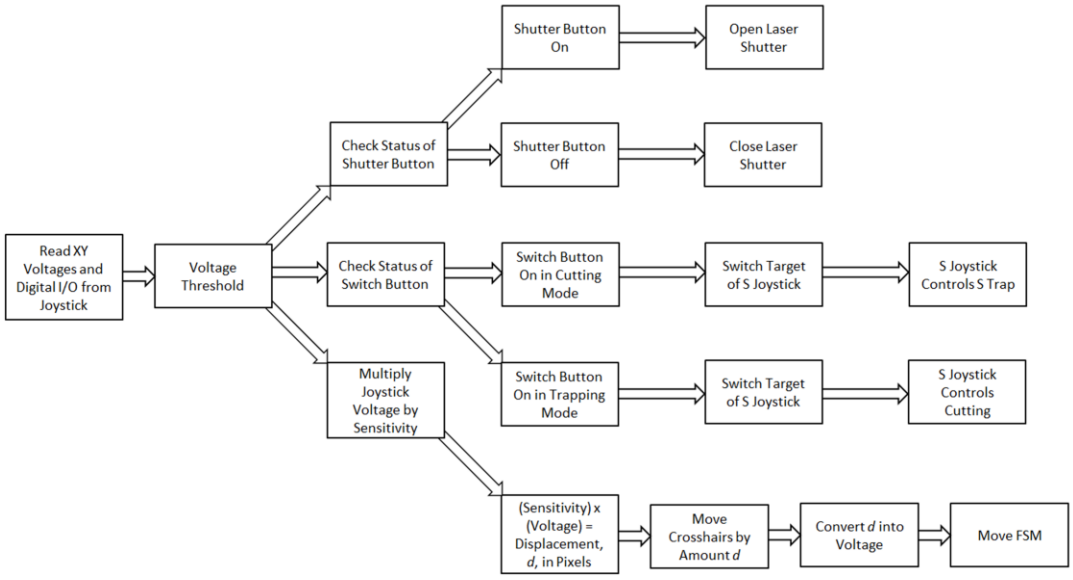

Figure B.21. Flow chart of pseudo-code for LabVIEW VI used in Velocity Control.

Like in Position control, this VI starts by reading the x- and y-voltages and the digital signals from the joystick. The voltage threshold represents a software check to prevent idle drifting; that is, when the joystick outputs very small, millivolt or tens of millivolt signals due to random noise, the program ignores these to prevent the fast-steering mirrors from moving small amounts in random directions. Instead, the code only passes through the voltage threshold if the voltages read from the joystick are greater than 0.5 V in magnitude (increased to 0.7 V in Onboard/Simultaneous control for reasons stated in Appendix C). Following the bottom path first, the code then multiplies the voltage of the joystick by a sensitivity value that is adjustable in Robolase IV and uses this as a displacement in pixels for the crosshairs representing the optical trap in the main image. Thus, if the user moves the joystick left and the joystick sends out a 5 V signal, assuming the sensitivity was 0.2 pixels/volt, then the crosshairs on the main image in Robolase would move by 1 pixel to the left. The new coordinate is then converted into voltage and the fast-steering mirror moves according to this displacement. As the code iterates

within a while loop, the program continues to displace the trap by some displacement depending on the degree to which the user has moved the joystick in a certain direction. Thus, over continuous iterations this displacement resembles a movement of the trap, and the trap is thus controlled by its velocity when using the joysticks. Since there are actually two directions the joystick and trap can move in, x or y, the code does this for both axes, reading the voltage from the joystick sequentially for each axis and then sending voltages sequentially to the fast-steering mirror sequentially (since the DAQ board cannot send multiple signals simultaneously). However, there is never a jerky motion in which the trap moves in one axis then the other because the program is slow in iterating to check the voltages and thus sees changes in both axes before sending voltages to the fast-steering mirror.

Taking the middle path from the voltage threshold box, the program checks the status of the switch button, similar to Position control. However, this switch button does not switch between computer and joystick control. Instead, it switches between trapping mode and cutting mode for the S joystick. When the button is pushed and the system is in trapping mode, the program switches the target of control of the S joystick to the cutting fast-steering mirror. Since Robolase communicates with all three of the fast-steering mirrors via the DAQ board, this "switch" is as simple as changing which analog output channels with which the S joystick voltages are paired. Thus, when the pushbutton is pressed during trapping mode, the analog output channels—to which the new, displaced voltages calculated from the joystick voltages are sent—are switched to the channels that control the cutting fast-steering mirror. Now, moving the S joystick will move the fast-steering mirror for cutting. On the Robolase IV main image, this is indicated by movement of the yellow feedback triangle, representing the location of the cutting beam, instead of the red crosshairs, which represents the location of the S trap. When the button is pushed during cutting mode, these channels are switched back, such that the S joystick controls the S trap fast-steering mirror. Note that during cutting mode, the P joystick still controls the P trap, so that one trap and one scissors can be manipulated using the traps during cutting mode.

The top path controls the opening and closing of the cutting laser shutter. During cutting mode, the user can press one of the pushbuttons in order to open the laser shutter while moving the joystick to

move the cutting beam, which allows the user to cut virtually any shape or curve desired. Unlike the switch button, the laser shutter is only activated for as long as the button is pressed. This prevents the user from neglectfully opening the cutting laser and leaving the system unattended—which could be harmful to other people in the lab or disastrous for samples—since the user's hand must be on the joystick and actively pressing the button for the laser shutter to be open. An option in Robolase IV allows the user to decide between keeping the shutter open for as long as the button is pressed, or opening the shutter in short, timed (usually 30 ms) bursts while the button is pressed.

Pseudo-code for opening the trap shutters is not shown, but works similar to the switching status button. That is, pressing the button while the shutter is closed opens the shutter, and vice-versa. The trap shutter remains open even if the button is released, and is only closed when the button is pushed again, unlike the cutting beam shutter.

Appendix C. Joystick UI User Manual and Developer References

This appendix represents a user manual instructing how to use the joystick user interface, some references for developers, as well as a troubleshooting section for possible problems that may occur.

C.1. Joystick Button Layout

The figure below shows the physical joystick button layout.

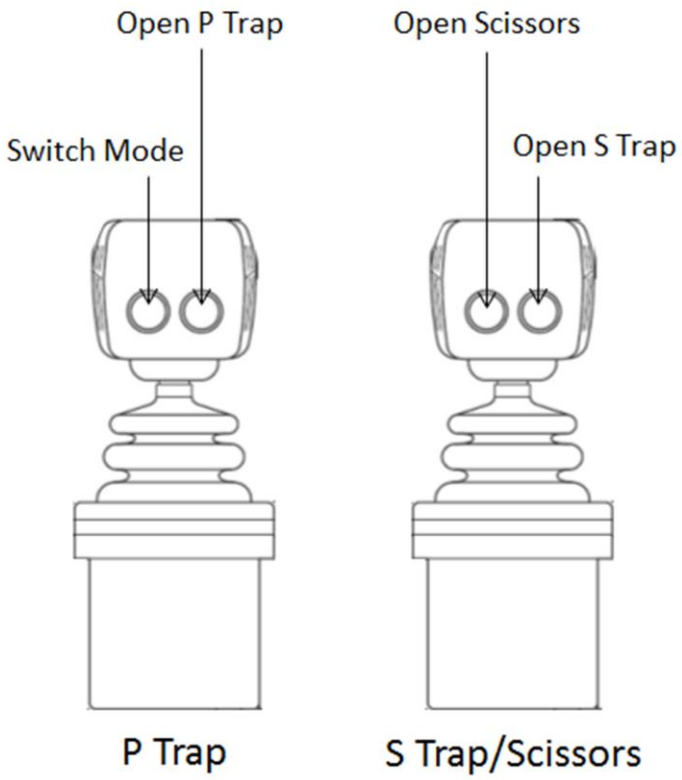

Figure C.1. Physical button layout for each joystick.

As shown above, the left joystick is for the P Trap, while the right joystick switches between the S Trap and the optical scissors. The left button on the P Trap joystick switches the system between joystick cutting mode—where the P Trap and scissors can be controlled—and joystick trapping mode—where both traps can be controlled. Thus, pushing this button once will switch the joystick mode, and pushing it again will switch it back to the original mode. This button press is sensed virtually immediately; thus,

it must be pressed and unpressed very quickly, or the system will quickly switch the mode and then switch back (although this can be avoided by adding a wait time, doing so may slow the feedback of the LabVIEW program which runs within Robolase IV). When this button is pushed, the "Joystick Cut" green rectangular indicator is lit in the Cutting tab of the Robolase IV front panel (explained in the next section), and the LEDs in the Joystick Hub are also lit to visually indicate the mode of the system.

The right button on the P Trap joystick opens the P Trap shutter. This shutter remains open until the next time this button is pressed (or closed from Robolase IV). The right button on the S Trap joystick functions the same way. The left button on the S Trap joystick controls the shutter for the scissors. Unlike the buttons that control the S and P trap shutters, the shutter remains open only as long as this button is held down. The mode of this button, whether the shutter opens and closes repeatedly for user-specified times (as in CutROI) or stays open, can be changed in Robolase IV in the Cutting tab.

C.2. LabVIEW Controls

This section will explain the joystick-related controls in the front panel of Robolase IV, mainly in the Cutting and Trapping tabs which are shown again below for convenience. All functions are explained with respect to the current Onboard/Simultaneous control scheme.

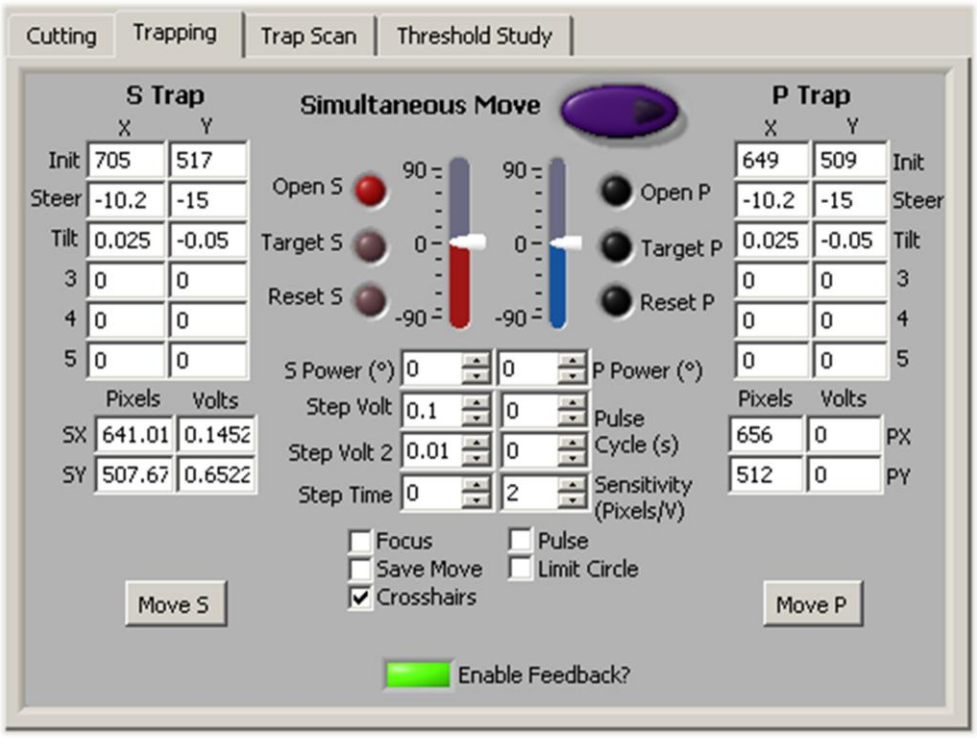

Figure C.2. Laser Trapping Control. Controls on this tab are mostly alignment parameters and buttons used to control the two, P and S polarized laser traps.

Joystick-related controls on the trapping tab include “Enable Feedback?” control. This button must be on for Robolase IV to detect joystick button presses and open shutters or switch the joystick mode. However, this button does not have to be on for the trapping crosshairs to move with joystick movement for the Onboard/Simultaneous control scheme.

The “Sensitivity (Pixels/V)” numeric control adjusts how many pixels the crosshairs move per volt of joystick output voltage. Thus, the greater this control, the further the crosshairs will move for the same amount of movement on the joystick and vice-versa. Too large a value may result in large jumps that might cause the trap to lose whatever object it is holding.

The “Crosshairs” checkbox toggles the red and blue crosshairs on the main image that represent the position of the S (red) and P (blue) traps. When using the traps either with the joysticks or with the computer, this should be on so the user can observe the location of the traps. These crosshairs are saved in images with overlay, but not saved in images without overlay. The positions of these

crosshairs are specified in pixels and volts by the “SX”, “SY”, “PX”, and “PY” controls. These values will change as the traps are moved using the joystick. The alignment parameters (such as Initial, Steer, etc.) will affect whether or not the crosshairs on the image is aligned with the physical location of the trap (both when controlled with the joysticks as well as Robolase IV).

The Cutting tab is shown again below.

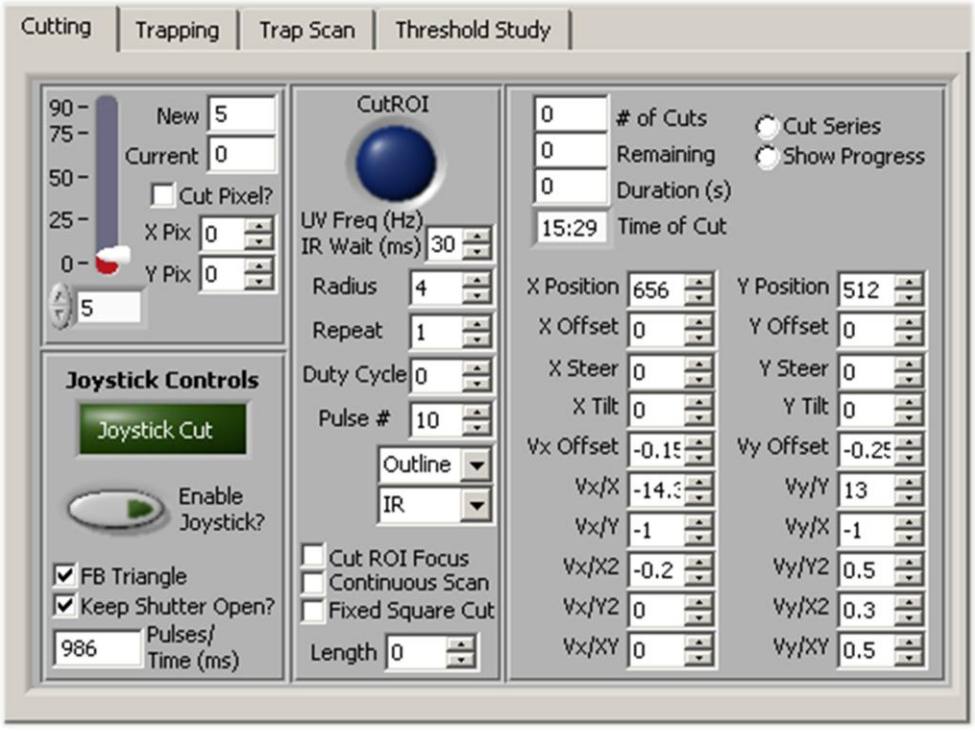

Figure C.3. Laser Cutting Control. The joystick-related controls are under “Joystick Controls”.

The large green, rectangular button labeled “Joystick Cut” is an indicator that shows whether or not the system is in joystick cutting mode (since it is an indicator, pressing it will not do anything). When it is on, the system is in joystick cutting mode, and when off, the system is in joystick trapping mode. The “Enable Joystick?” button switches between these modes, turning the large green indicator and the LEDs in the Joystick Hub on when pressed during joystick trapping mode. Like the physical joystick button, the response of this button is very fast so it should be pressed quickly.

The “FB Triangle” checkbox toggles a yellow triangle on the main image that shows the position of the cutting beam. This triangle will move with the S Trap joystick (the joystick on the right)

when the system is in joystick cutting mode. The “Keep Shutter Open?” control switches how the left button on the S Trap (right) joystick behaves. As mentioned before, this control switches whether the shutter is repeatedly opened and closed or kept open when the button is open. When checked, it keeps the shutter open as long as the button is pressed. The last numeric control, “Pulses/Time (ms)” indicates the time the scissors shutter is opened, depending on the mode. When “Keep Shutter Open?” is not checked, pressing the button results in repeated openings of the shutter and the system counts how many times the shutter is opened, from which the total time can be calculated since the length of time the pulse lasts is specified in this with the “IR Wait (ms)” control. When “Keep Shutter Open?” is checked, the system measures how long this button is pressed, giving the time in milliseconds.

Again, the alignment parameters on the right will affect the alignment of the triangle with the actual beam position (as well as how accurate ROIs are cut when using CutROI on Robolase IV).

C.3. Diagram of Joystick Hub

The figures below show diagrams of the signals going into and coming out of the solderless breadboard within the Joystick Hub, as well as internal connections within the breadboard. The rows are numbered and the columns are labeled using the letters at the top of the breadboard (not the bottom, where the numbers are reversed). The top is considered the side opposite the “Radio Shack” logo. Numbering of the rows in the left side begins at the bottom, while numbering on the right begins at the top. As with all breadboards, the nodes in the same row in the middle area are electrically connected, while nodes in the same column in the left and right side areas are electrically connected (wires were used to electrically connect both the top and bottom halves of the entire column). Since the entire breadboard was not used, only parts of the breadboard are shown.

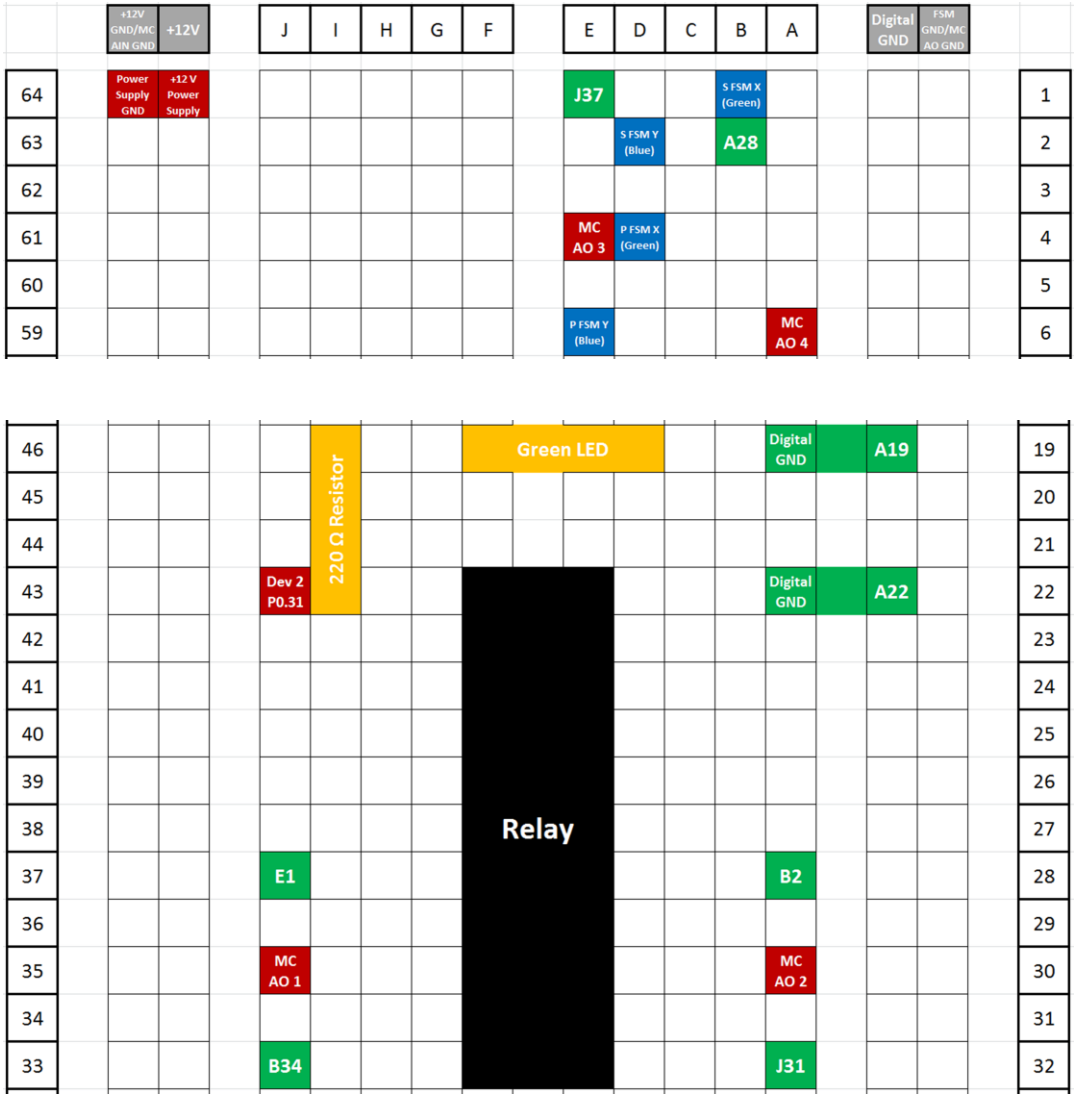

Figure C.4. Diagram of top half of the solderless breadboard within the Joystick Hub (excerpts). The definition of each abbreviation is shown in the Table C.1.

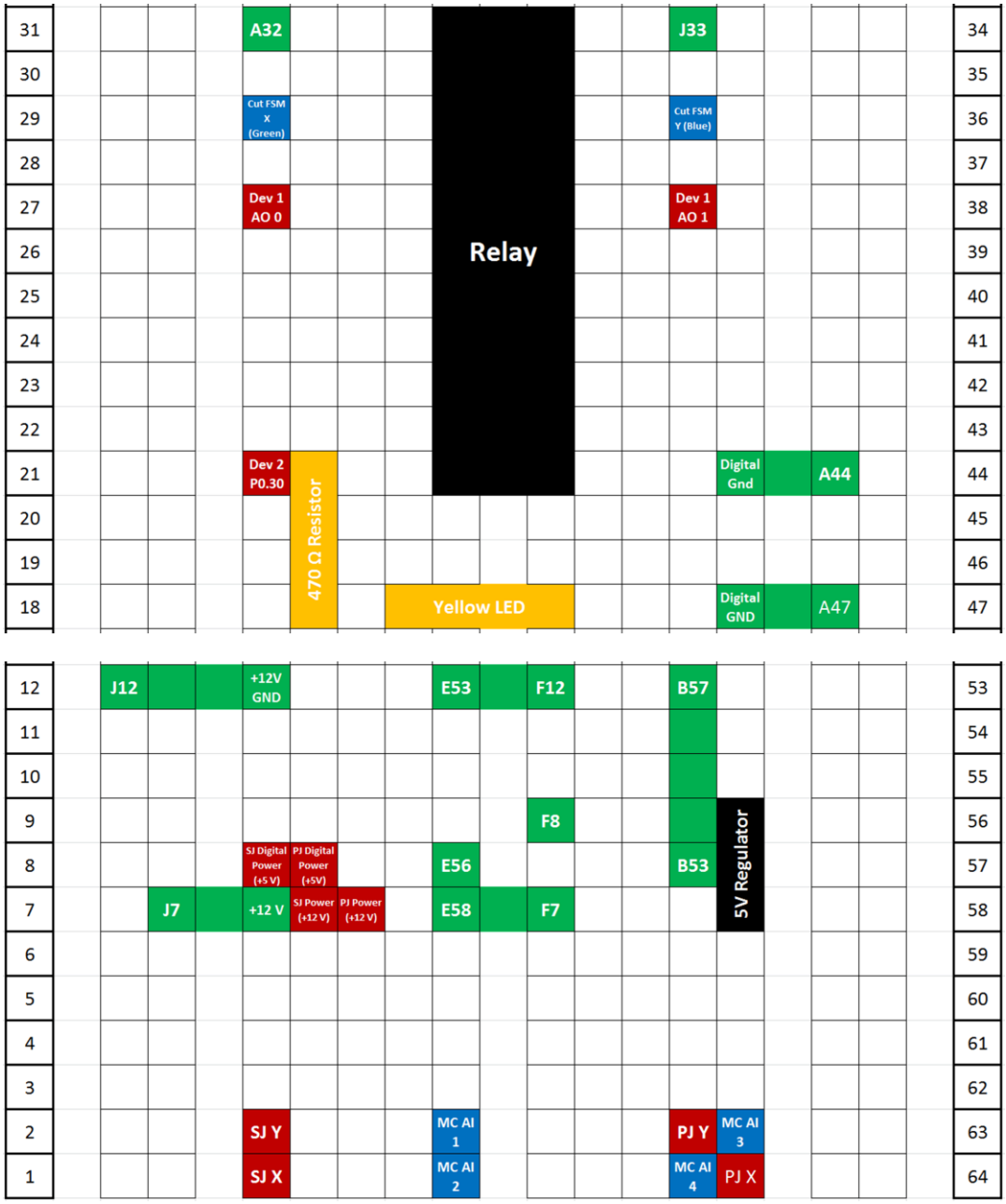

Figure C.5. Diagram of bottom half of the solderless breadboard within the Joystick Hub (excerpts). The definition of each abbreviation is shown in the Table C.1.

Most of the ground connections are omitted in the figure above. All the ground signals coming in from the joystick and going to the analog input channels of the motion controller are grounded with the +12V power supply ground in the leftmost column. All of the ground signals going to the fast-steering mirrors or coming from the analog outputs of the motion controller are grounded with each other in the

rightmost column. In addition, all of the digital grounds for both the buttons and the relay coils are grounded together as well in the column to the immediate right of the rightmost column.

The abbreviations and color codes used in the figures above are listed below:

Table C.1. Table of Abbreviations and Color Codes for Figures C.4 and C.5.

Abbreviation	Description
S	S Trap
SJ	S Joystick
P	P Trap
PJ	P Joystick
FSM	Fast-steering Mirror
X	x-voltage
Y	y-voltage
MC	Motion Controller
AO	Analog Output
AI	Analog Input
GND	Ground
Dev [X]	DAQ Board Reference
P[X].[Y]	Digital Line Reference
[Letter][Number]	Another Location on Breadboard
Red	Input
Blue	Output
Green	Connection to another location on board
Orange	Circuit Element
Black	Circuit Device

The DAQ Board references and digital line references can both be found in Measurement and Automation Explorer. As shown in the table, red squares are inputs and blue squares are outputs. Green squares represent internal connections to another location on the breadboard; this location is stated in the square itself. These connections are explicitly drawn as straight sequences of green squares where possible (where a straight sequence can be drawn). Sequences of orange squares represent the area over which circuit elements such as resistors or LEDs span. Note that the squares in between the ends of the vertical sequences of orange or green squares are not electrically connected to each other, but the top and bottom squares of those sequences are electrically connected. Black areas represent areas covered by circuit devices such as the relays or the regulator.

C.4. Troubleshooting

C.4.1. P Trap FSM Spontaneous Movement

On occasion the P Trap fast-steering mirror makes a quiet, regular, ticking sound. This was determined to occur because the joysticks output approximately 0.67 V when the joystick power supply is off. Since the threshold was set to 0.5 V previously, Robolase IV would move the fast-steering mirrors even when the joysticks were off. However, the threshold has now been set to 0.7 V in order to avoid this problem.

The problem should be resolved, but in the event that this occurs again, take the following actions in the order listed below:

1. Turn off the P Trap fast-steering mirror
2. End Robolase IV (LabVIEW program).
3. Turn on the joystick power supply if it is not on.
4. Run Robolase IV.
5. Turn on the P Trap FSM.

C.4.2. Joystick Cutting Mode and CutROI

The system cannot do a CutROI when it is in joystick cutting mode. Thus, when performing a CutROI, make sure that the system is in joystick trapping mode (i.e. LEDs in the Joystick Hub are off). If a CutROI is performed while in joystick cutting mode, a dialog box will be shown telling the user to switch joystick modes.

C.4.3. Joystick Buttons Do Not Work

If the joystick buttons are not working, check if the “Enable Feedback?” control on the Trapping tab is on. If it is on, then use Measurement and Automation Explorer to open the Test Panels of the DAQ board (Dev 2) under Devices and Interfaces. In the Test Panels, go to the Digital I/O tab and read Port 0/Line 25-28 (to see which lines correspond to each button, see section C.3, the Diagram of the Joystick Hub). If these do not turn on when the buttons are pressed, it may be possible that the

digital power supply, which comes from the 5VDC regulator in the Joystick Hub, is not working or that the power supply for the joysticks itself is not working. If these are working, check the connections involving the joystick buttons (again, see section C.3).

C.4.4. Moving the Traps with the Joysticks and with Move S/P

The Move S/P controls on the Trapping tab take priority over joystick movement. Thus, trying to move the joystick during a Move will not work. Instead, if you attempt to move the joystick during a Move, the crosshairs will move one step but then return to its original path. Please cancel the Move before attempting to move the trap using the joysticks.

C.4.5. Crosshairs or Traps Do Not Move with Joystick

First check whether the SX/SY/PX/PY Voltages are near ±10V. If they are, then the trap cannot be moved further in the axis that is near ±10V. If the voltages are not near these values, check first whether the crosshairs are not moving, the trap itself (the fast-steering mirrors) is not moving, or both are not moving in response to joystick movement.

If the crosshairs do not move with joystick movement, check the Sensitivity value in the Trapping tab. If this value is too low, the trap may not move very fast in response to joystick movement. A value of 1 or 2 pixels/V should be sufficient. If the Sensitivity value is sufficiently high, check if the Simultaneous Joystick Trapping.vi is running (C:\Documents and Settings\Berns lab\Desktop\Testing VIs\Onboard\Simultaneous Joystick Trapping.vi). This VI should be running for the joysticks to work and the crosshairs to update. If this program is running, then probe the voltages for reading the joystick and outputting to the motion controller. If the values are all correct (i.e. the voltages respond to joystick movement), then there might be a hardware problem.

It might also be a hardware problem if the fast-steering mirrors themselves do not move. In the event that this occurs, check the power supplies and physical connections in the Joystick Hub using a multimeter.

C.4.6. Crosshairs are Not Visible

If the crosshairs are not visible for either the S Trap, P Trap, or scissors, check to make sure each of the respective checkboxes are checked (“Crosshairs” in Trapping tab for traps, “FB Triangle” in Cutting tab for scissors).

If these checkboxes are checked, reset the trap or scissors to the default position. For traps, this can be done by using the Reset S/P buttons on the trapping tab. For scissors, this can be done by performing a CutROI with “Origin” chosen for ROI Style.

Appendix D. Supplemental Raw Images for Experimental Studies

The sections below correspond to the different experiments and methods used during the experimental studies, outlined in section 3.2. In each section, images are shown and explained to illustrate each different type of experiment and the results of each as well.

D.1. PtK2 and Indian Muntjac Control

The raw imaging data for a control experiment with PtK2 can be seen below in Figure D.1.

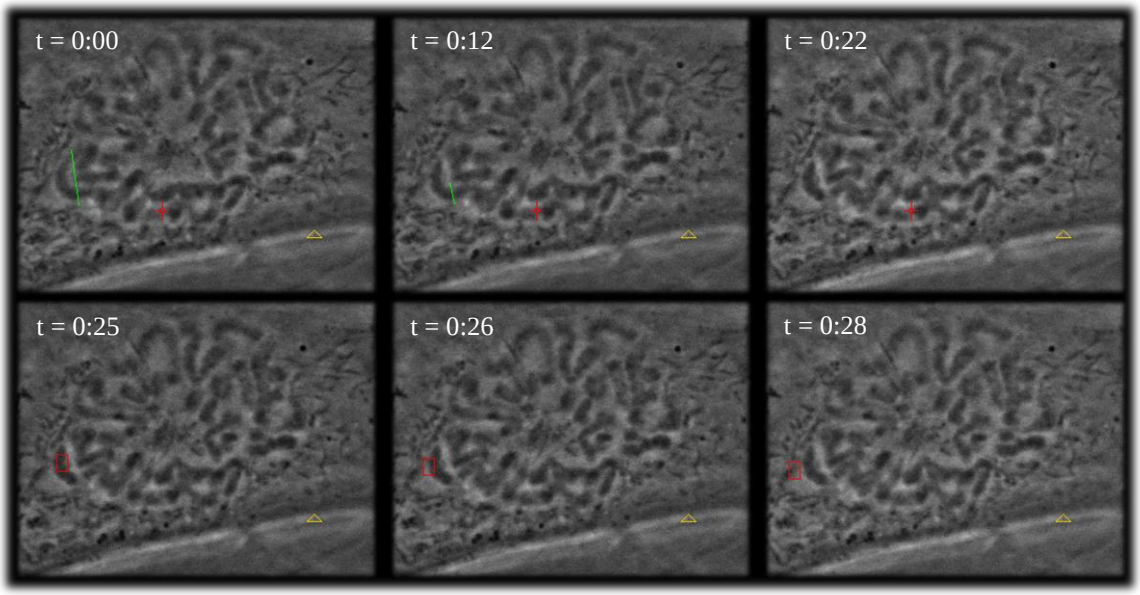

Figure D.1. PtK2 Parental Control. Chromosome is cut and an attempt at moving the resulting fragment is made, but is unsuccessful. The trap does not seem to exert any influence.

The trapping power in the experiment above was 0.2032 W (irradiance of 2.87 x 10^7 W/cm^2 at the focal spot), while the cutting power was approximately 18 mW (irradiance of 5.41 x 10^6 W/cm^2 at the focal spot). Referring to the frames from top left to bottom right, in frame 1, the first cut is performed. A second cut is performed in frame 2 to sever the bottom portion of the fragment. Frame 3 shows that the fragment has clearly been cut. In frame 4, the S Trap is brought onto the fragment. The trap is turned on and moved slightly to the left in frame 5 and further in frame 6, but the fragment does not seem to be influenced at all.

Figure D.2 below shows an experiment with an Indian Muntjac control cell.

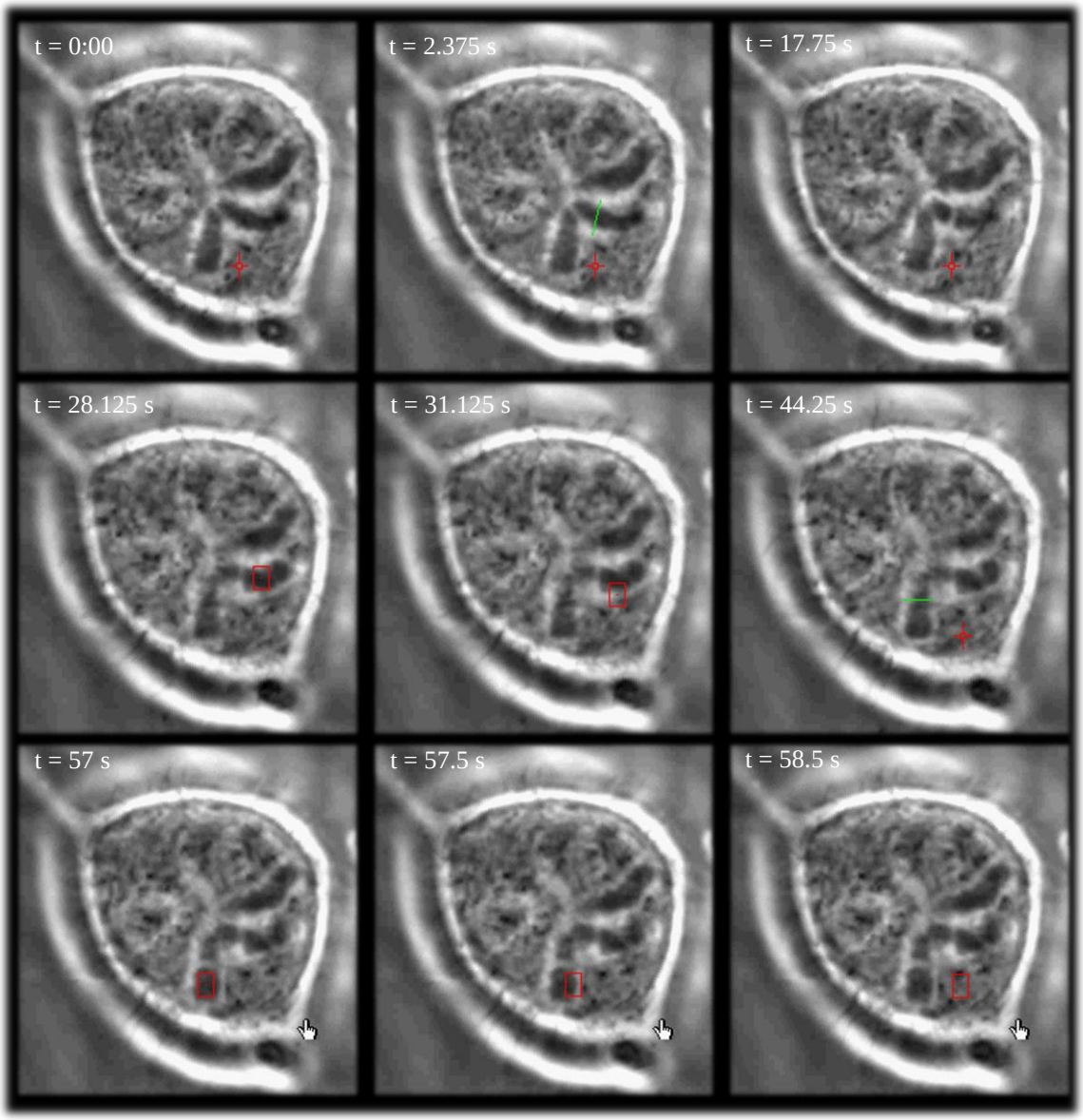

Figure D.2. Indian Muntjac Control. Two attempts are made to cut and trap a chromosome fragment, but both are unsuccessful.

The cuts were performed at 28.3 mW (irradiance of 8.50 x 10^6 W/cm^2 at the focal spot), using two repetitions both in frame 2 and frame 6. The trapping power was 0.472 W (irradiance of 6.67 x 10^7 W/cm^2 at the focal spot). Frame 1 shows the cell before any cutting or trapping. After a cut is performed in frame 2, the damage is clearly seen in frame 3. The trap is moved to the fragment and turned on in frame 4, but attempts to move the fragment are unsuccessful and the trap does not seem to exert any

influence, seen in frame 5. In frame 6 another cut is attempted, but attempts at moving this fragment are again unsuccessful, shown in frames 7-9.

D.2. PtK2 and Indian Muntjac with Nocodazole

Experiments were mostly unsuccessful using nocodazole, which prevents microtubule polymerization. Figure D.3 below shows the inability of the P trap to move a chromosome fragment after it has been cut using 6 µg/mL nocodazole.

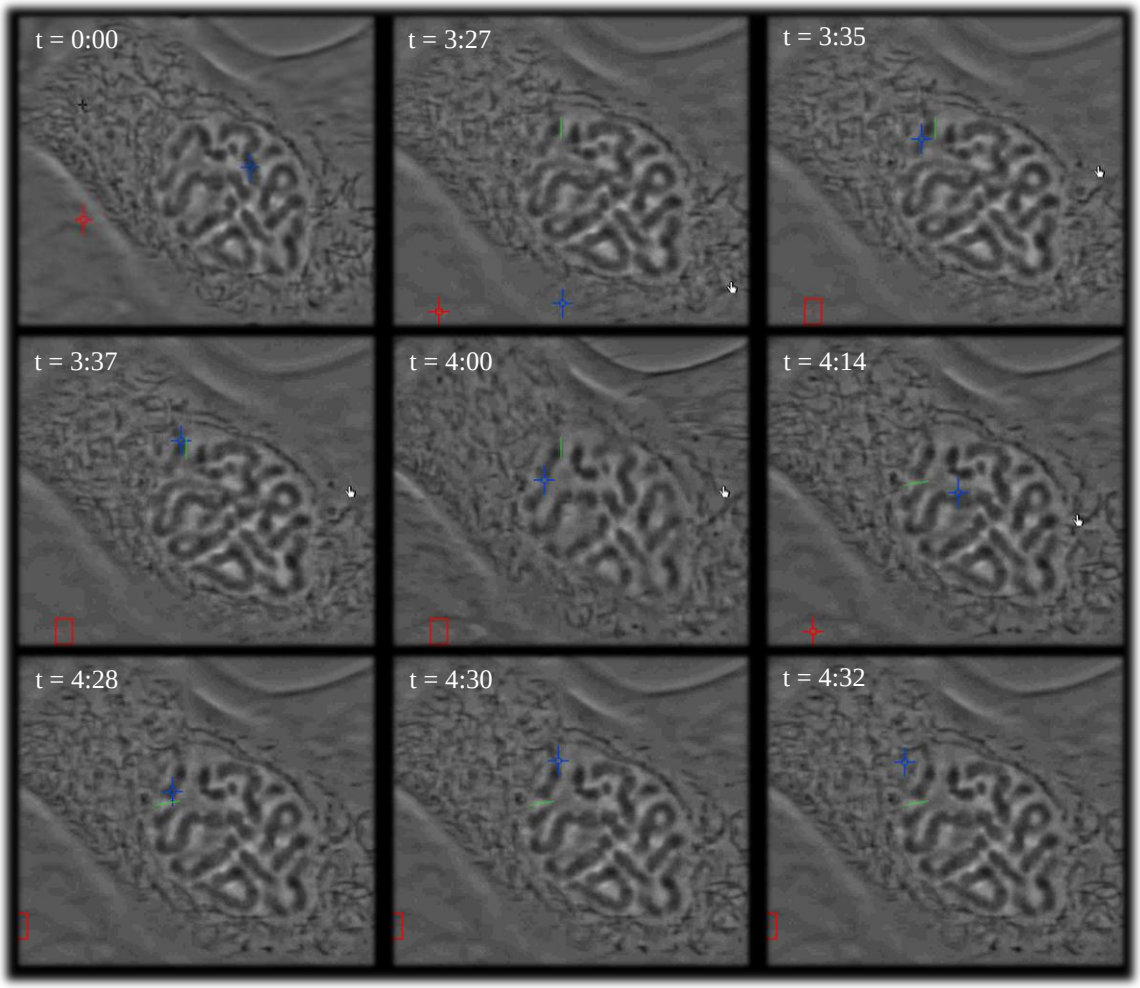

Figure D.3. Unsuccessful attempt at moving chromosome fragment in nocodazole-treated PtK2 mitotic cell. The blue rectangle represents the trap, while the green line represents the cut. Cuts were performed in frames 2 and 6. Time is in minutes and seconds.

Referring to the images from top left to bottom right, the first frame shows the cell before any laser ablations. The green line in frame 2 near the center of the image shows the location of the first cut. In

this frame, the chromosome has already been cut at 48.6 mW (irradiance of 1.46 x 10^7 W/cm^2 at the focal spot), which is indicated by the white region to the right of the chromosome and the green line, which was not apparent in the first frame. In the third frame, the P trap (blue crosshair) is moved to the fragment and moved upward and downward in frames 4 and 5, respectively. However, the trap, at 0.446 W (irradiance of 6.31 x 10^7 W/cm^2 at the focal spot), does not seem to influence the fragment at all. Another cut was made below the fragment in frame 6, and attempts at moving it with the trap were again in the following frames, without success.

The set of images below shows one special case where chromosome cutting and moving was successful. The series of images in Figure D.4 below shows the last two laser ablations that finally freed the chromosome fragment, as well as the subsequent movement of the fragment by one of the traps.

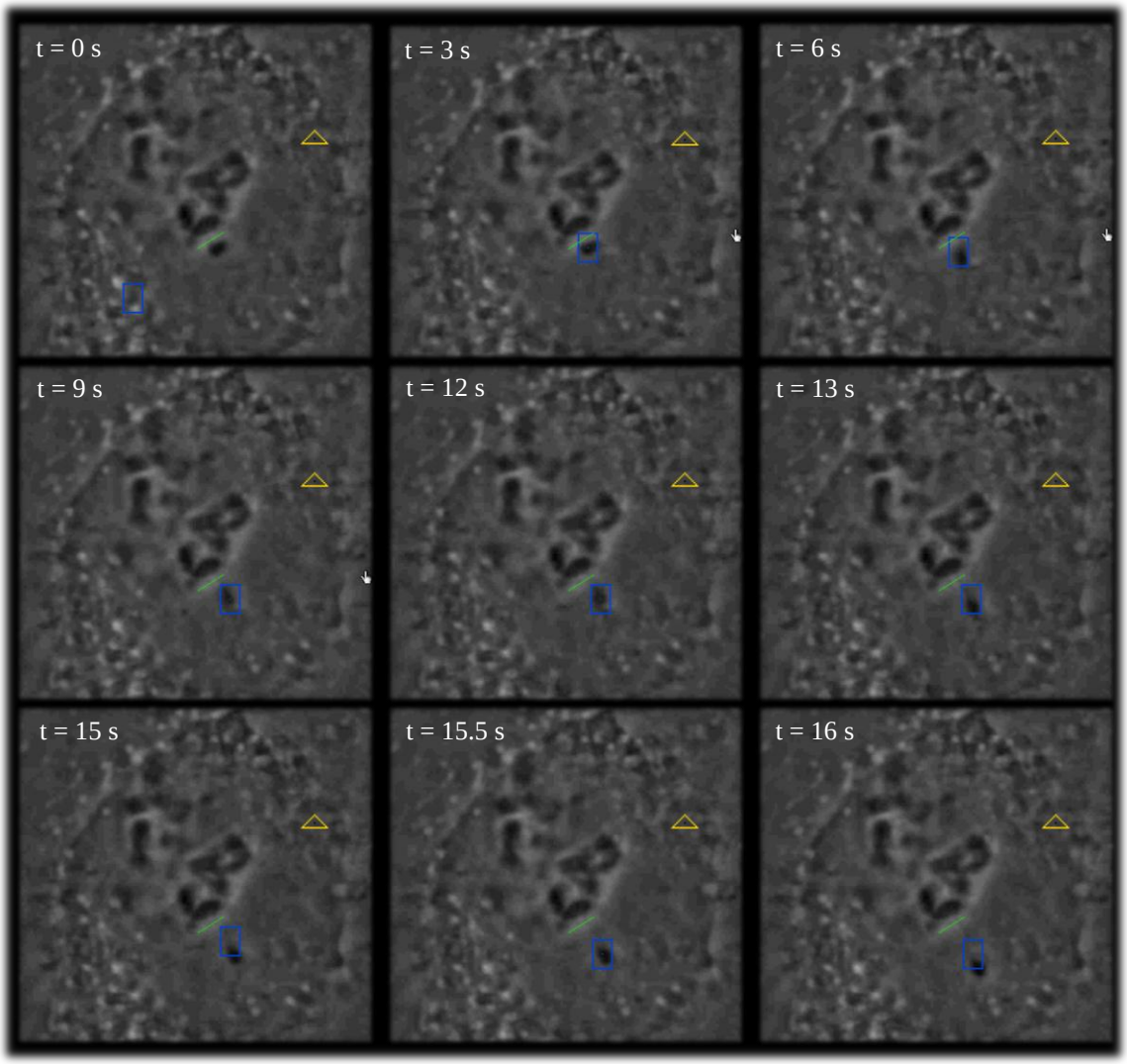

Figure D.4. Time series of chromosome fragment being severed completely and moved using the optical trap. Cuts were performed in frames 1 and 5.

This dish was treated with 0.01 µg/mL of nocodazole. Referring to the images from top left to bottom right, in the first frame the fragment beneath the green line is being cut using the optical scissors at approximately 48.8 mW (irradiance of 1.47 x 10^7 W/cm^2 at the focal spot). In the next three frames, the trap (blue rectangle), at 0.460 W (irradiance of 6.51 x 10^7 W/cm^2 at the focal spot), is moved towards the fragment using the joystick. In frame 3 and 4, the trap pulls the fragment down, but it is not completely cut. In frame 5, another cut is performed along the same green line. Finally, in frames 6 and 7, the fragment is severed from the rest of the chromosome and moves to the center of the trap (the rectangle and the trap were not perfectly aligned at this location of the field of view). In frames 8 and 9,

the fragment is moved slightly down. Images showing further movement of this fragment are shown below.

Despite this ability to move the fragment, however, at this point, the cell was not very healthy since it had already been undergoing intermittent laser ablation for roughly 20 minutes. Thus, it is likely that the slow necrosis of the cell contributed to altering of the normal cytosolic environment, which may have made it easier to move the chromosome fragment.

Figures D.5 and D.6 below follow the images from Figure D.4. In Figure D.5 the freed fragment moved down, left, and then up. In Figure D.6 it is moved down, right and up the right side of the cell.

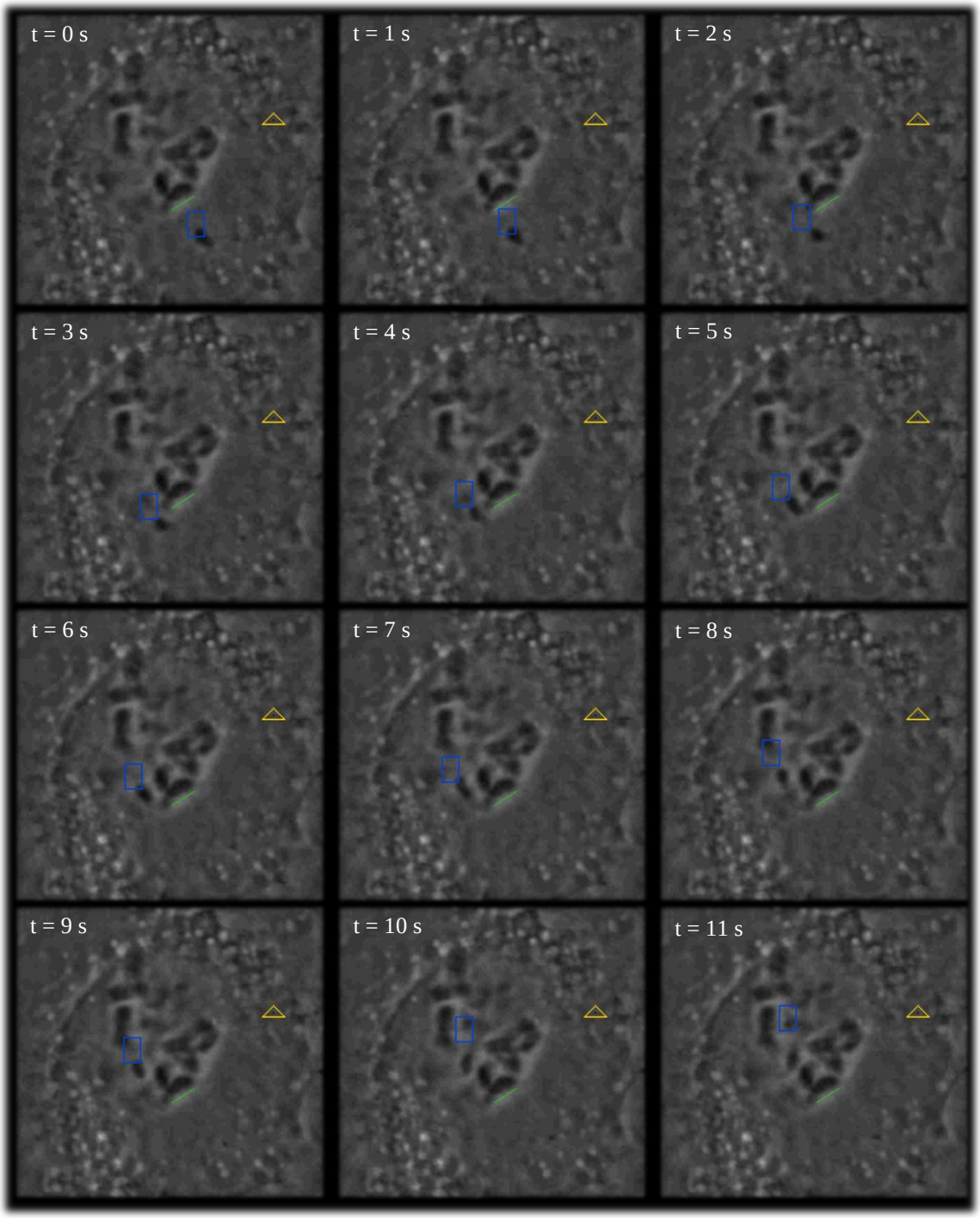

Figure D.5. Time series of chromosome fragment being moved towards the left and up with the optical trap using the joysticks, whose position is indicated by the blue rectangle.

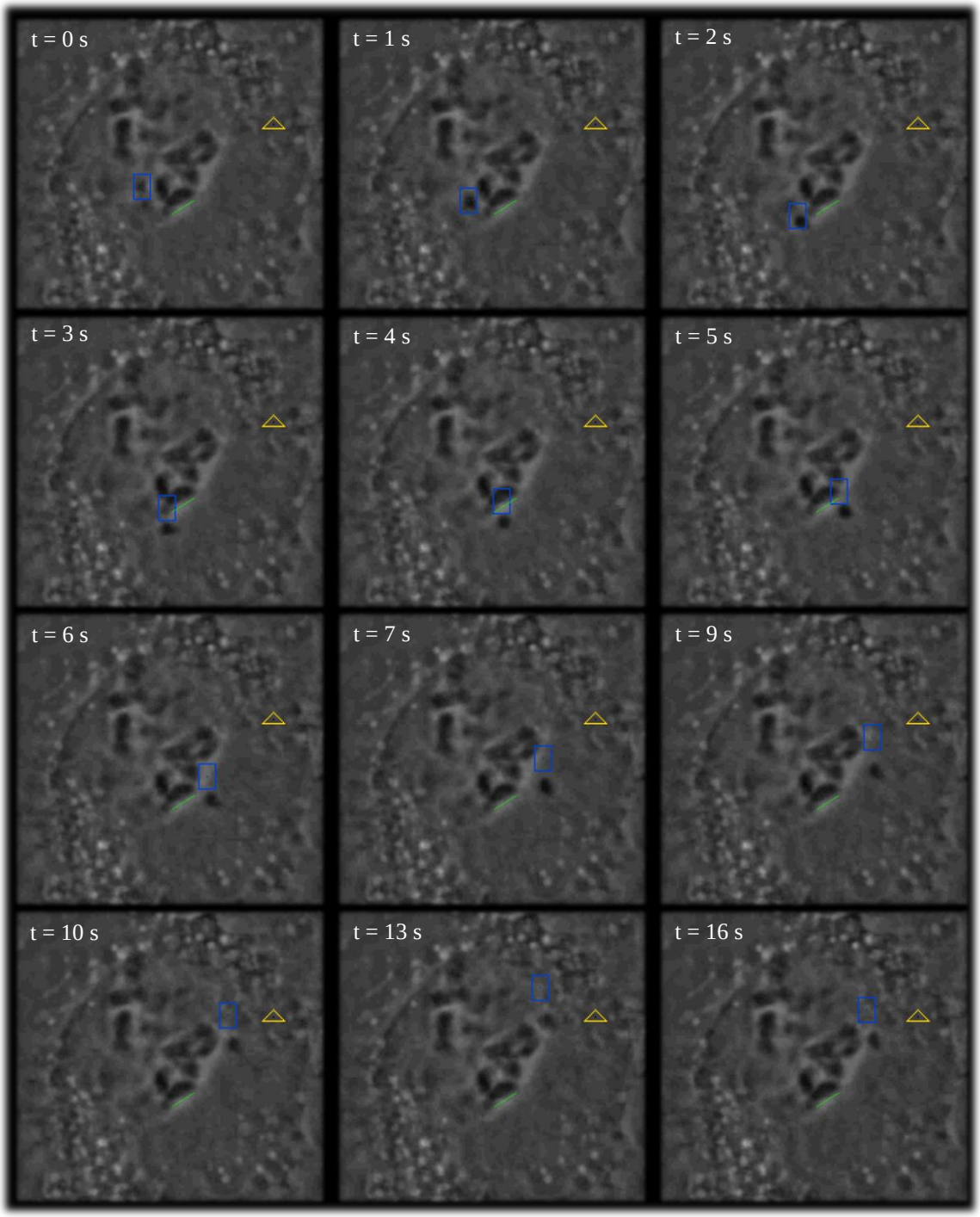

Figure D.6. Time series of chromosome fragment being moved down, towards the right, and up with the optical trap using the joysticks, whose position is indicated by the blue rectangle.

In addition to the inability to move chromosome fragments during most experiments, it is also sometimes difficult to cleanly sever a chromosome fragment, especially in the z-direction. An example is shown in Figure D.7.

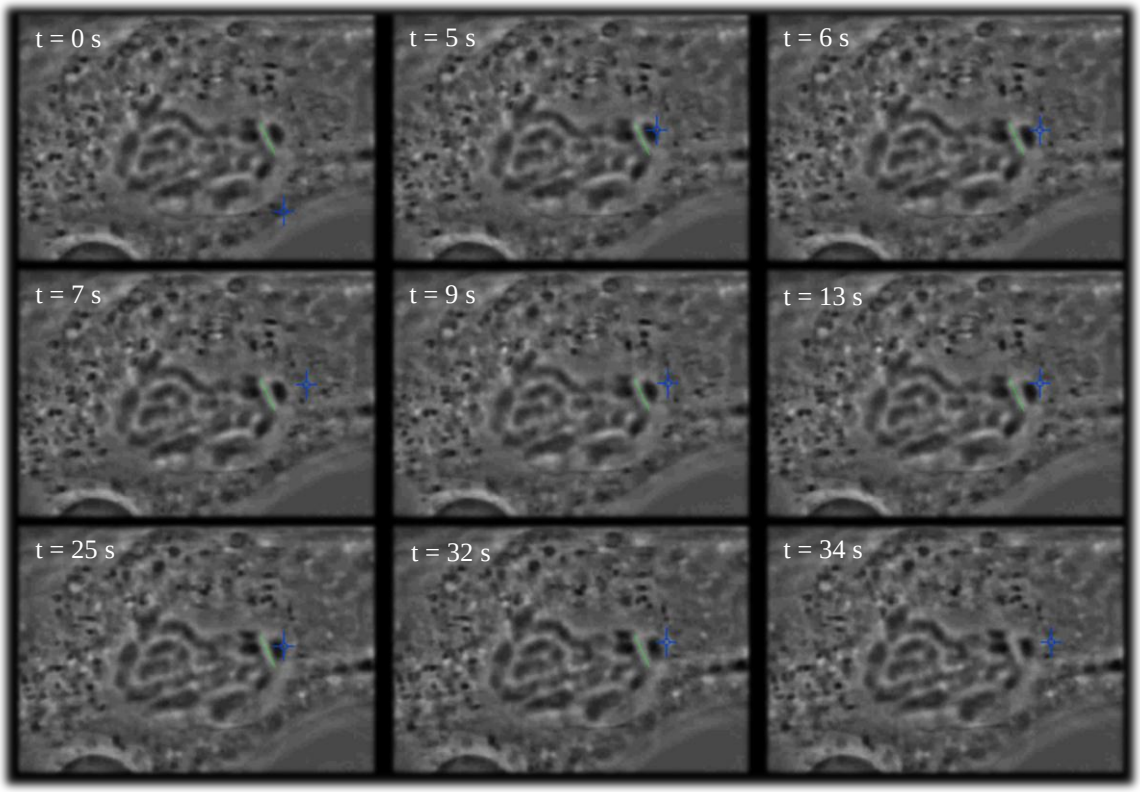

Figure D.7. Time series of chromosome fragment being incompletely cut and then pulled with the optical trap using the joystick in an attempt to free the fragment.

Cutting occurs in frame 1 and 7 at 48 mW (irradiance of 1.44 x 10^7 W/cm^2 at the focal spot). The blue cross represents the trap, at 0.451 W (irradiance of 6.38 x 10^7 W/cm^2 at the focal spot), being moved by one of the joysticks. After trying to cut the fragment free in frame 1, the trap is moved onto the fragment and moved left. The fragment moves very slightly to the left as well. In frame 6 the fragment moves its farthest to the left, but is still not free. The area between the fragment and the rest of the chromosome was cut again in frame 7 and another attempt was made to pull the fragment with the trap, but was again unsuccessful.

Although not as visible, trapping the fragment and pulling it leftward seems to pull nearby chromosomes as well, which may indicate that either the chromosome fragment was not completely

severed and possibly still attached above or below the focus, or other elements, possibly microtubules (not visible), were bound to the fragment and other chromosomes. This residual attachment despite laser ablation may have prevented the chromosome from being moved freely by the trap as in the previous figures.

D.3. PtK2 GFP-Tubulin with Nocodazole and BrdU

Figure D.8 shows a fluorescent image of a field of view of PtK2 cells with GFP-tubulin before and after treating with nocodazole, where its effects are visualized by fluorescence of the microtubules.

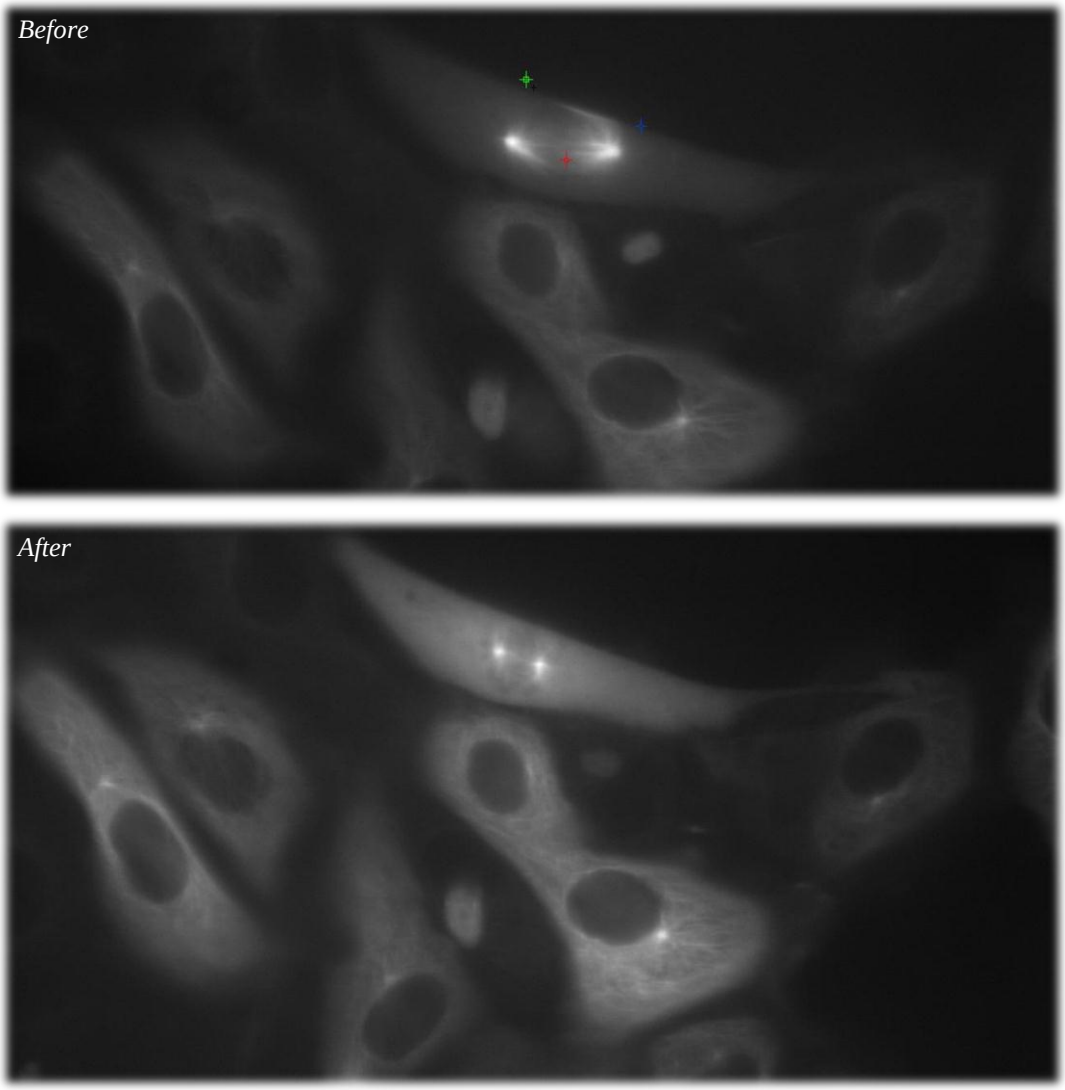

Figure D.8. Fluorescent images of PtK2 P133 (GFP-Tubulin) cells before and after treatment with nocodazole.

The cell in the top and center is mitotic. The mitotic spindle is much more clearly defined before treatment with nocodazole, and becomes blurry and undefined after treatment, indicating the destabilization effect of nocodazole. The microtubules in the non-mitotic cells also seem to become less defined, although the difference is less noticeable in these cells since the microtubules are not organized into a spindle. Fluorescent images such as these were used to confirm the destruction of microtubules when box cuts were performed, as demonstrated in the next figure.

When BrdU was used, cells seemed to be able to withstand more ablations than before and looked healthier for a slightly longer time compared to cells without BrdU on average, but additional cuts or box cuts were still not enough to completely free chromosomes fragments. Figure D.9 shows a series of images for an unsuccessful experiment using box cuts and nocodazole at 0.01 µg/mL, with BrdU added approximately 28 hours prior to the experiment.

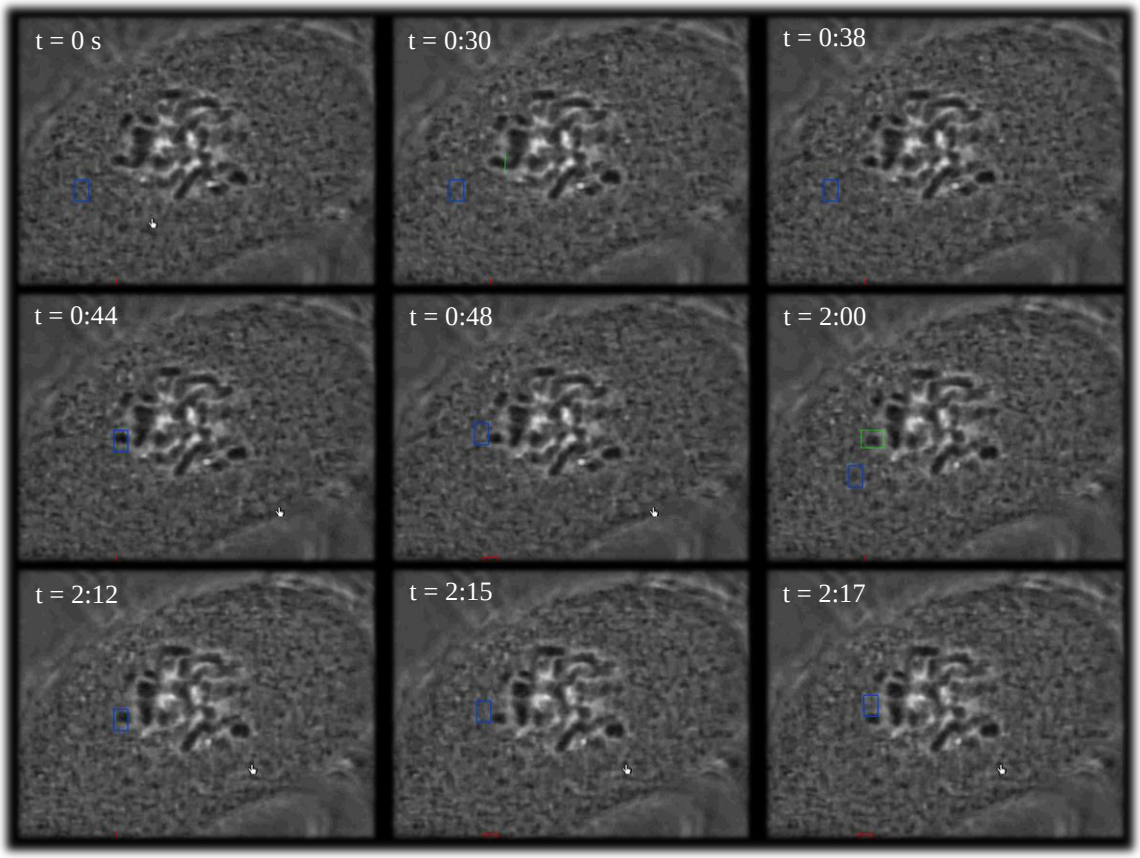

Figure D.9. Time series of PtK2 P133 cell with nocodazole and BrdU. Time is in minutes and seconds.

Trapping power was 1.90 W (irradiance of 2.69 x 10^8 W/cm^2 at the focal spot) and cutting power was 40.3 mW (irradiance of 1.21 x 10^7 W/cm^2 at the focal spot). Frame 1 is the cell before any laser ablation. Frame 2 and 3 show the cut and the cell after the cut. The trap is moved onto the fragment in frame 4 and moved, without success, in frame 5. After more cutting (not shown), a box cut is done on

the fragment in frame 6, but the fragment still cannot be moved in frames 7-9. Figure D.10 below shows fluorescent images before and after the box cut in frame 6.

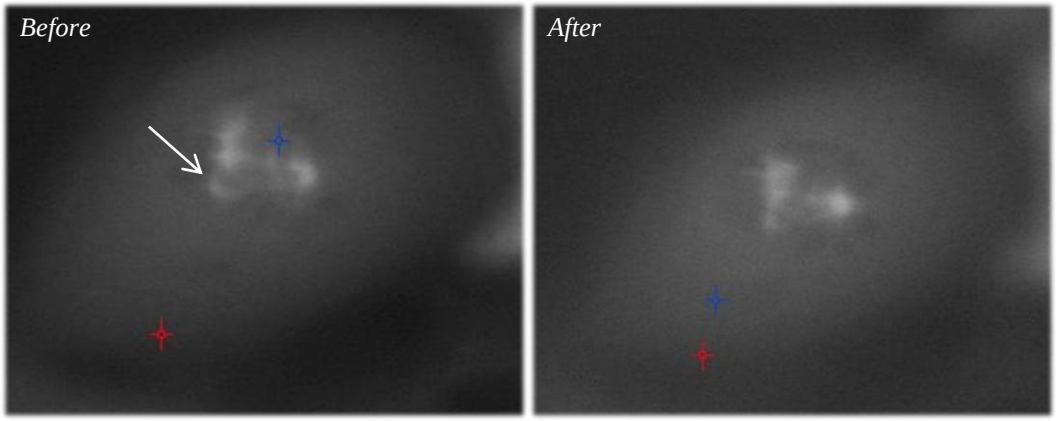

Figure D.10. Fluorescent images of cell in Figure D.9 before and after box cut. The white arrow points to the general region where the box cut occurred.

The difference between the two images above is not very noticeable, but the box cut seems to have pushed microtubules near the area leftward or destroyed microtubules in the rectangle ROI.

Figure D.11 shows another fluorescent image of microtubules after treatment with nocodazole and Figure D.12 shows a series of images of the same cell where a box cut was made but attempts at moving the fragment were still unsuccessful.

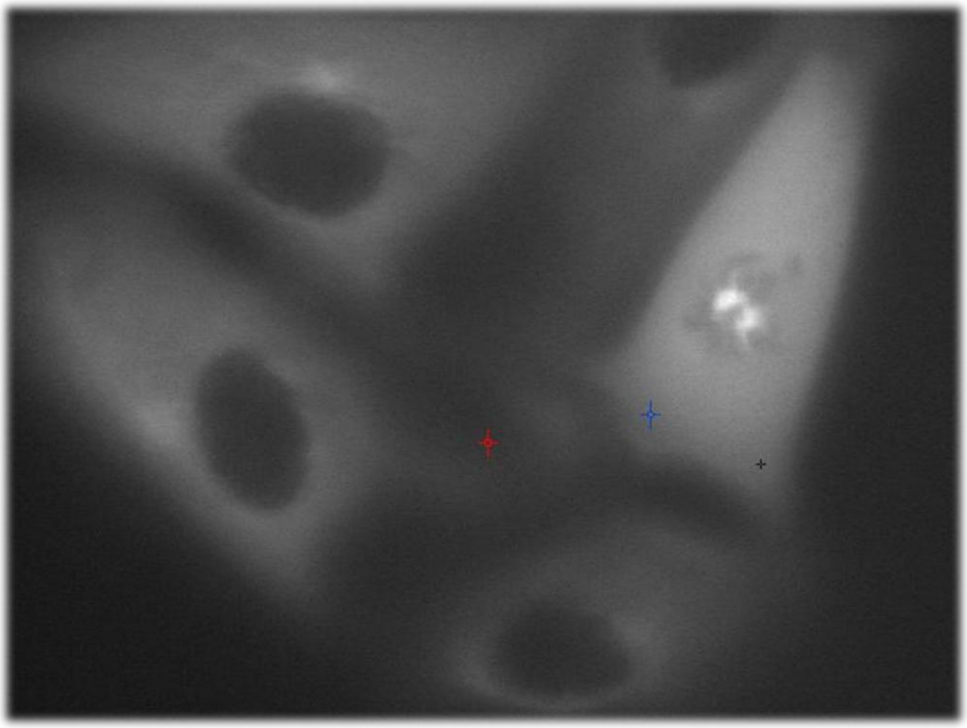

Figure D.11. Fluorescent images of PtK2 P133 (GFP-Tubulin) cells after treatment with nocodazole.

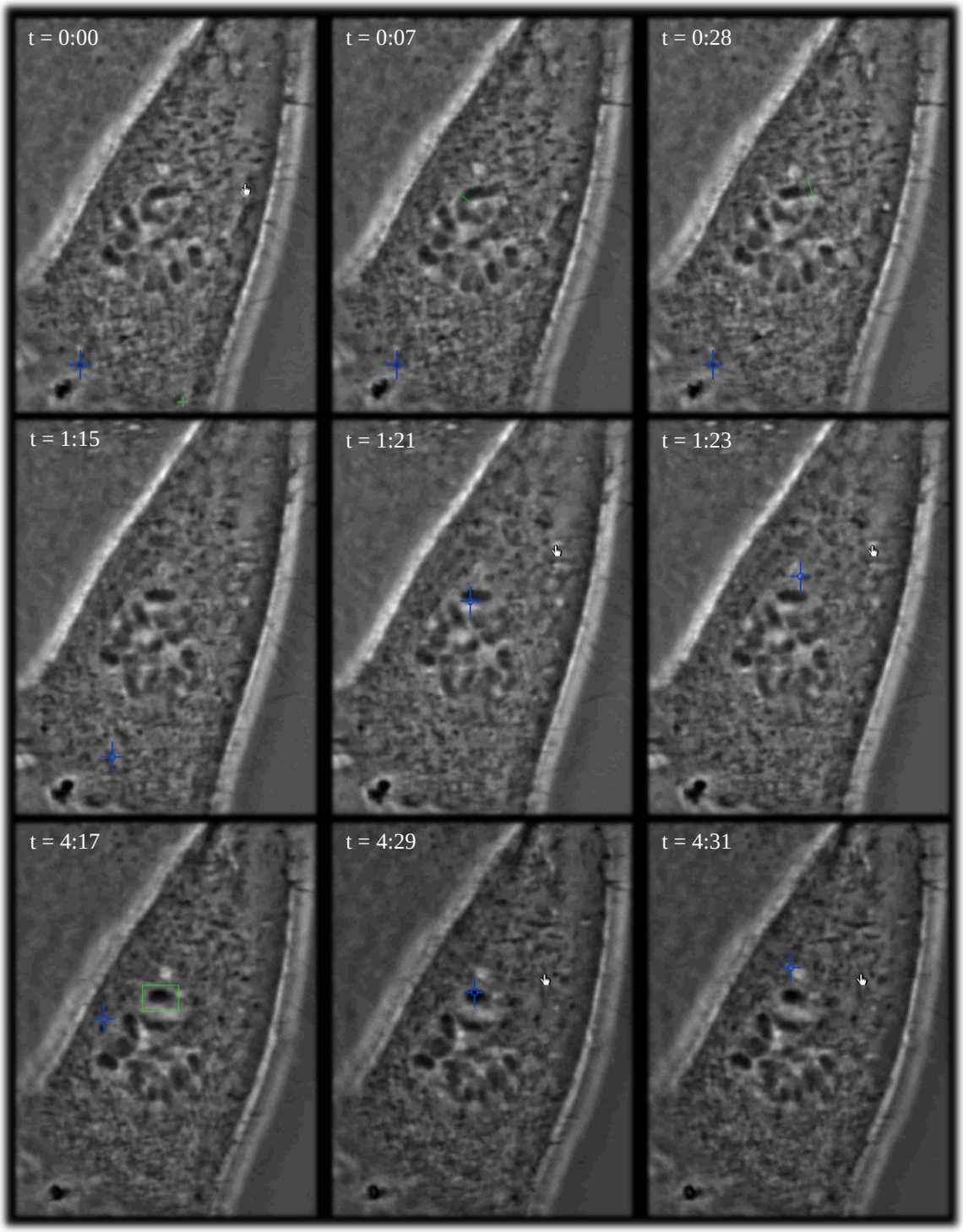

Figure D.12. Time series of same cell. A fragment is first cut off, unsuccessfully trapped, and then cut using a box ROI in order to remove all other attachments. Trapping was still unsuccessful, however.

BrdU was actually not used in this experiment. Trapping power was 0.446 W (irradiance of 6.31 x 10^7 W/cm^2 at the focal spot) and cutting power was 47 mW (irradiance of 1.41 x 10^7 W/cm^2 at the focal spot). The first frame shows a before-cut image. A piece of chromosome is cut in two places in frame 2 and 3. The seemingly severed piece is then trapped in frame 5, but does not move with the trap as shown in frame 6. After many other ablations around the fragment (not shown), a box cut is finally performed in frame 7, after which another attempt to trap the fragment is made in frame 8, but was again unsuccessful as shown in frame 9.

The figure below shows a slightly promising cell, where a fragment cut at 37.07 mW (irradiance of 1.11 x 10^7 W/cm^2 at the focal spot) (the cell is treated with BrdU) can be seen to be influenced just barely by the trap, again at 1.90 W (irradiance of 2.69 x 10^8 W/cm^2 at the focal spot).

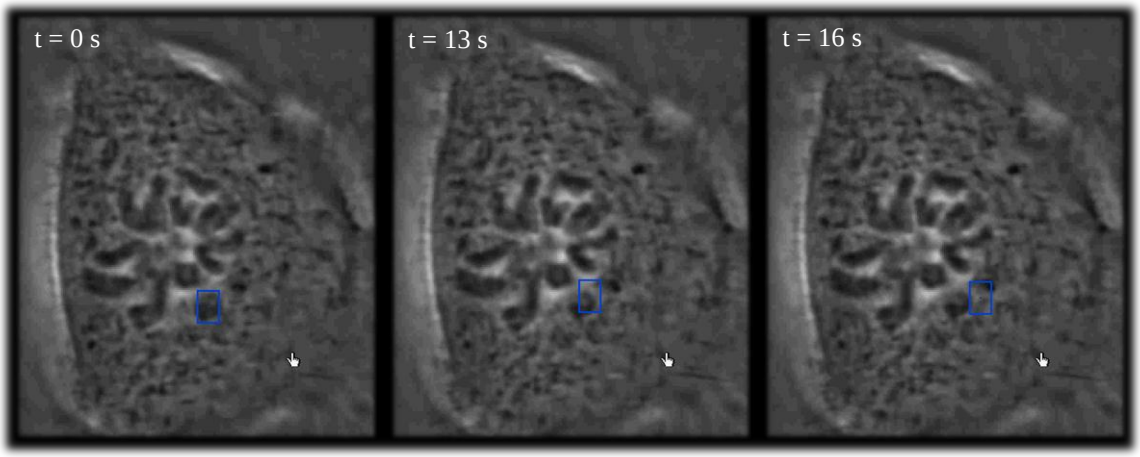

Figure D.13. Fragment is influenced by trap (blue rectangle) very slightly after being cut (not shown).

Although it appears as if the fragment has been completely severed, it only seems to be nudged by the trap and recoils once the trap is far enough such that it loses its influence (frame 3). This behavior suggests that there are still other elements either attached to the fragment and restricting its movement or elements in the cytosol that block movement.

Appendix E. Supplemental Tables for Fisher Exact Tests

E.1. Computing *P* Value Using a Fisher Exact Test

The *P* value from a Fisher exact test is calculated using a 2 x 2 contingency table, such as the one below.

Table E.1. Example of a 2 x 2 contingency table used to calculate a *P* value using a Fisher exact test.

			Row Totals
	O_{11}	O_{12}	R_1
	O_{21}	O_{22}	R_2
Column Totals	C_1	C_2	N

The probability of a particular table is calculated as follows:

$$P = \frac{\frac{R_1!R_2!C_1!C_2!}{N!}}{O_{11}!\,O_{12}!\,O_{21}!\,O_{11}!}$$

The two-tailed *P* value is determined first by computing the probability for the observed data. The cell with the smallest frequency in the table is reduced by 1, and then the other three cells are adjusted such that the row and column totals remain constant. The probability for this new table is then calculated. This process is repeated until the smallest element is zero. These probabilities are added to obtain the first tail of the test.

To obtain the second tail, we identify whether O_{12} or O_{21} is smaller. We then reduce this smaller element by 1 and compute the probability of this particular table. This process is repeated until this smaller element has been reduced to zero. We then identify those tables with probabilities less than the probability associated with the original data and add these probabilities to the first-tail probability calculated earlier to obtain the two-tail *P* value (Glantz, 2005).

E.2. Contingency Tables Based on Experimental Data

The tables below show the contingency tables used to calculate *P* values for control vs. nocodazole, control vs. box cuts, and control vs. taxol. This data is taken from table 3.1, where instances where influence was seen are grouped with the no movement group (i.e. the "influence" column is added to the "no movement" column).

Table E.2. 2 x 2 contingency table used to calculate P_{noc}.

	Control vs. Nocodazole		Row Totals
	0	9	9
	1	29	30
Column Totals	1	38	39

Table E.3. 2 x 2 contingency table used to calculate P_{box}.

	Control vs. Box Cuts		Row Totals
	0	9	9
	0	29	29
Column Totals	0	38	38

Table E.4. 2 x 2 contingency table used to calculate P_{trap}.

	Control vs. Stronger Trap		Row Totals
	0	9	9
	5	0	5
Column Totals	5	9	14

The *P* values that resulted from performing Fisher exact tests on these tables are 0.77, 1, and 0.0005 respectively for nocodazole, box, and trap.

References

Glantz, Stanton A. Primer of Biostatistics. New York: McGraw-Hill Medical Pub., 2005. Print.